ISTANBUL TECHNICAL UNIVERSITY ★ GRADUATE SCHOOL OF SCIENCE ENGINEERING AND TECHNOLOGY

TACTICAL MISSILE GUIDANCE AND HOMING LOOP APPLICATIONS

M.Sc. THESIS

Erdem TURAN

Department of Defence Technologies

Defence Technologies Programme

JUNE 2019

ISTANBUL TECHNICAL UNIVERSITY ★ GRADUATE SCHOOL OF SCIENCE ENGINEERING AND TECHNOLOGY

TACTICAL MISSILE GUIDANCE AND HOMING LOOP APPLICATIONS

M.Sc. THESIS

Erdem TURAN
(514171007)

Department of Defence Technologies

Defence Technologies Programme

Thesis Advisor: Prof. Dr. Cengiz HACIZADE

JUNE 2019

ISTANBUL TEKNİK ÜNİVERSİTESİ ★ FEN BİLİMLERİ ENSTİTÜSÜ

TAKTİKSEL FÜZE GÜDÜMÜ VE HEDEF İZLEME DÖNGÜSÜ UYGULAMALARI

YÜKSEK LİSANS TEZİ

Erdem TURAN
(514171007)

Savunma Teknolojileri Anabilim Dalı

Savunma Teknolojileri Programı

Tez Danışmanı: Prof. Dr. Cengiz HACIZADE

HAZİRAN 2019

Erdem TURAN a M.Sc. student of ITU Graduate School of Science Engineering and Technology student ID 514171007, successfully defended the thesis/dissertation entitled "TACTICAL MISSILE GUIDANCE AND HOMING LOOP APPLICATIONS", which he prepared after fulfilling the requirements specified in the associated legislations, before the jury whose signatures are below.

Thesis Advisor :	**Prof. Dr. Cengiz HACIZADE** Istanbul Technical University	.....
Jury Members :	**Prof. Dr. Fikret ÇALIŞKAN** Istanbul Technical University	.....
	Asst. Prof. Dr. Janset DAŞDEMİR Yildiz Technical University	.....

Date of Submission : 02 May 2019
Date of Defense : 11 June 2019

To my family,

FOREWORD

First of all, I am extremely grateful to my supervisor Prof. Dr. Cengiz HACIZADE for his support, motivation and immense knowledge. His guidance helped me in all the time.

I would like to thank Miray for all her love and infinite support throughout my years of study and through the process of researching and writing of this thesis.

Also, I would like to thank Tunahan for providing me unfailing support and continuous encouragement throughout the entire process.

I would like to express my thanks to Dr. Mohammad M.GOMROKI, Oğuzhan DEMIR, and A.Serkan ALTINOK for their comments and help in this study.

Finally, I take this opportunity to express my gratitude to my family for supporting me spiritually. Without their precious support it would not be possible to conduct this thesis.

June 2019

Erdem TURAN
(Astronautical Engineer)

TABLE OF CONTENTS

Page

ABBREVIATIONS

AAM : Air to Air Missile
AOR : Augmented Optimal Rendezvous Guidance Law
APN : Augmented Proportional Navigation Guidance Law
ASM : Air to Surface Missile
BPN : Biased Proportional Navigation Guidance Law
CLOS : Command to Line of Sight
DG : Differential Game Guidance Law
DME : Distance Measuring Equipment
DOF : Degree of Freedom
EIG : Earliest Intercept Geometry
EO : Electro-Optical
EPN : Extended Proportional Navigation Guidance Law
FCS : Flight Control System
GNC : Guidance Navigation and Control
GPS : Global Positioning System
GTPN : Generalized True Proportional Navigation Guidance Law
ICBM : Inter-Continental Ballistic Missile
IPSOG : Improved Particle Swarm Optimization Guidance
IR : Infrared
IRBM : Intermediate Range Ballistic Missile
KF : Kalman Filter
LOS : Line of Sight
MEL : Minimum Effort Guidance Law
MELN : Minimum Effort Law without Target Acceleration Measurement
MMAE : Multiple Model Adaptive Estimation
MPSOG : Modified Particle Swarm Optimization Guidance
OGL : Optimal Guidance Law
OR : Optimal Rendezvous Guidance Law
PN : Proportional Navigation Guidance Law
PPN : Pure Proportional Navigation Guidance Law

PSOG : Particle Swarm Optimization Guidance
SAM : Surface to Air Missile
SRBM : Short Range Ballistic Missile
SSM : Surface to Surface Missile
STT : Skid to Turn
TACAN : Tactical Air Navigation
TF : Transfer Function
TSGL : Trajectroy Shaping Guidance Law
TPN : True Proportional Navigation Guidance Law
WG : Weave Guidance Law
WGC : Compansated Weave Guidance Law
ZEM : Zero Effort Miss

SYMBOLS

A, B, D	**:** State matrices
$\mathbf{a_p, a_y,}$	**:** Pitch and yaw accelerations
D	**:** Drag
E	**:** Expected value
g	**:** Gravitational acceleration
$\mathbf{G_{best}, P_{best}}$	**:** Global and Local best function value in PSOG
H	**:** Hamiltonian function
$\mathbf{j_T}$	**:** Target jerk
K	**:** Kalman gain matrix in KF
$\mathbf{\mathcal{L}}$	**:** Laplace transform
$\mathbf{n_c, n_L}$	**:** Commanded and lateral acceleration of missile
$\mathbf{n_T}$	**:** Target acceleration
P	**:** Error covariance matrix in KF
p, L, C	**:** Probability, likelihood and autocorrelation function in MMAE
Q, R	**:** Noise covariance matrices in KF
Q, R	**:** State penalty matricies in LQR
$\mathbf{Q_f}$	**:** Terminal penalty weighting matrix
R	**:** Relative distance
$\mathbf{R_s}$	**:** Radome slope
S	**:** Target span
T	**:** Missile Time Constant
$\mathbf{t_0, t_f,}$	**:** Initial and final time
$\mathbf{t_{go}}$	**:** Time to go
u, w	**:** Missile and target control commands
$\mathbf{V_c, V_m}$	**:** Closing and missile velocity
$\mathbf{w_{max}, w_{min}}$	**:** Inertial weights in PSOG
$\mathbf{x_m, y_m, z_m}$	**:** Cartesian coordinates of missile
$\mathbf{x_T, y_T, z_T}$	**:** Cartesian coordinates of target
$\mathbf{Y_m, Y_t,}$	**:** Relative seperation of missile and target from nominal LOS
$\mathbf{\alpha_m}$	**:** Missile heading angle

$\boldsymbol{\beta}$: The angle between target heading and initial reference frame

$\boldsymbol{\gamma_{m_0}, \gamma_{t_0}}$: Missile and target nominal heading angle

$\boldsymbol{\gamma_m}$: Missile flight path angle

$\boldsymbol{\varepsilon}$: Boresight error

$\boldsymbol{\zeta}$: Velocity ratio in EIG

$\boldsymbol{\tau_m}$: Missile time constant

$\boldsymbol{\theta_h}$: Gimbal angle

$\boldsymbol{\theta_m}$: Missile azimuth angle in LOS frame

$\boldsymbol{\theta_r}$: Reflection angle error

$\boldsymbol{\lambda}$: Line of sight angle

$\boldsymbol{\Phi}$: Power spectral density

$\boldsymbol{\Phi_k}$: State transition matrix in KF

$\boldsymbol{\phi_m}$: Missile azimuth angle

$\boldsymbol{\psi_m}$: Missile flight path angle in LOS frame

$\boldsymbol{\omega}$: Weaving frequency

$\boldsymbol{\omega, v}$: White noise process and measurement vectors in KF

LIST OF TABLES

Page

LIST OF FIGURES

Page

TACTICAL MISSILE GUIDANCE AND HOMING LOOP APPLICATIONS

SUMMARY

Modern missile guidance technology is based on the development of V1 and V2 missiles in Germany during World War II. Missiles are divided into guided missiles and strategic missiles. Guided missiles can be divided into missiles that may home to the target or follow a nonhoming preset course. Nowadays, most air defense systems use homing guidance methods. Homing missiles can be divided into active, semiactive or passive type. Active homing missiles may direct themselves to the target after launch. Following the use of the proportional navigation guidance law for the first time on the Lark missile, this guidance method has been used in almost all tactical radar and infrared missiles around the World. Proportional navigation guidance law has been the source of advanced guidance methods used today.

This study examined the classical and modern guidance law used in the terminal phase of today's tactical homing missiles. These guidance laws were obtained mathematically. The 2D non-linear missile target engagement geometry was linearized around collision course by assuming small angle approach for head-on collision and tail chase scenarios.

The homing loops have been modeled for the classical and modern guidance laws such as proportional navigation, optimal rendezvous, augmented proportional navigation and augmented optimal rendezvous which uses target acceleration, extended proportional navigation form using target jerk measurements, optimal guidance laws including control effort and impact angle constraint, weave guidance law used for spiral moving targets, biased proportional navigation guidance law that does not require time to go information, differential game guidance law and finally, particle swarm optimization guidance law as an heuristic method.

The disturbances are added into the models and measurements are filtered by using linear Kalman filters. The noise terms are in glint, range dependent and range independent noise form. Radome effect is also considered as a disturbance. Guidance delays are added into the simulation as a zero-order lag, first-order lag, and third order lag flight control system transfer functions. All guidance laws were simulated by taking account the different maneuvers of the target such as Barrel Roll, Vertical-S and constant maneuvers. Lastly, the approaches in the literature for multiple targets were examined. The centroid method and earliest intercept geometry method were performed.

TAKTİKSEL FÜZE GÜDÜMÜ VE HEDEF İZLEME DÖNGÜSÜ UYGULAMALARI

ÖZET

Modern füze güdüm teknolojisi V1 ve V2 füzelerinin ikinci dünya savaşı sırasında Almanya'da geliştirilmesine dayandırılabilir. Füzeler, güdüm füzeler ve stratejik füzeler olarak ikiye ayrılır. Güdümlü füzeler ise hedefi kendi kendine bulan veya önceden belirlenmiş bir rotayı takip eden füzeler olarak ikiye ayrılabilir. Günümüzde çoğu hava savunma sistemi kendi kendine bulan güdüm yöntemlerini kullanmaktadır. Kendi kendine bulan füzeler aktif, yarı aktif ve pasif füzeler olarak ayrılabilirler. Aktif tip füzeler fırlatıldıktan sonra kendilerini hedefe yönlendirebilirler. Oransal seyir güdüm kanunun ilk olarak Lark füzesinde kullanımının ardından, bu güdüm yöntemi dünya üzerinde neredeyse tüm takstiksel radar ve kızıl ötesi füzelerde kullanılmıştır. Bu güdüm kanunu günümüzde kullanılan ileri güdüm yöntemlerine kaynak olmuştur.

Bu çalışma günümüzün kendi kendine bulan taktiksel füzelerinin terminal safhasında kullanılan klasik ve modern güdüm kanunlarını incelemiştir. Bu kanunlar matematiksel olarak elde edilmiştir. Bazı güdüm kanunları doğrusal kuadratik kontrol kanunları uygulanarak elde edilmiştir. 2 boyutlu çarpışma geometrisi oluşturulmuş, doğrusal olmayan model, kafa kafaya veya kuyruktan yakalama durumları için küçük açı yaklaşımı kullanılarak doğrusallaştırılmıştır.

Oransal seyir güdümü, optimal birleşme, bunların hedef ivmesini kullanan arttırılmış oransal seyir ve optimal birleşme güdümleri, hedefin ivme değişimlerini kullanan genişletilmiş oransal seyir güdümü, vuruş açısı, kontrol eforu kısıtlarını içeren optimal güdüm kanunları, spiral hareket eden hedefler için kullanılan dönemeçli güdüm kanunu, kalan zaman bilgisine ihtiyaç duymayan sapmalı oransal seyir güdümü, diferansiyel güdüm ve son olarak sezgisel bir yöntem olan parçacık sürü optimizasyonu gibi klasik ve modern güdüm kanunları için güdüm model döngüleri modellenmiştir.

Oransal seyir güdümü literatürde en geniş kullanıma sahip güdüm kanunudur. Farklı tipte çeşitleri bulunmaktadır. Bu çalışmada yalın oransal seyir güdümü, gerçek oransal seyir güdümü, genelleştirilmiş gerçek oransal seyir güdümü hakkında bilgi verilmiştir. Benzetim çalışmalarında gerçek oransal seyir güdümü incelenmiştir. Yanal ivmenin görüş hattına dik uygulandığı gerçek oransal seyir güdümünde oransal seyir sabiti benzetimlere bağlı olarak 3 ve 4 şeklinde alınmıştır.

Optimal birleşme güdüm kanunu hareketsiz hedefler için vuruş açısı kısıtına dayanan bir yöntemdir. Aynı zamanda belirtilen güdüm kanunu Apollo uzay aracının Ay'a iniş maksadıyla kullanmış olduğu yöntemdir.

Arttırılmış oransal seyir güdümü hedefin ivmesini bir buçuk kat arttırarak hesaplamalara katmaktadır. Arttırılmış optimal seyir güdümü ise hareketli hedefler için vuruş açısı kısıtı içeren bir güdüm kanunudur.

Genişletilmiş oransal seyir güdümü hedefin ivme değişimlerini hesaba katmaktadır. Bu yüzden fazladan bir durum bilgisine daha ihtiyaç duymaktadır.

Füze güdüm döngüsü içerisinde bulunan gecikmeler, arayıcı başlık, güdüm ünitesi ve uçuş kontrol sisteminden kaynaklı olabilmektedir. Uçuş kontrol sistemindeki gecikmeler birinci ve üçüncü dereceden transfer fonksiyonları olarak modellenmiştir. Bu gecikmeler hedefin ivmesini kullanan güdüm kanunlarının performansını kötü yönde etkilemektedir. Bu maksatla optimal güdüm kanunları kullanılmaktadır. Minimum çaba güdüm kanunu veya diğer bir adıyla optimal güdüm kanunu füze güdüm gecikmelerinin etkisini yok edecek şekilde elde edilmektedir. Belirtilen güdüm yöntemi sistem gecikmelerini sıfıra indirgemeye çalışarak sıfır dereceli bir arttırılmış oransal seyir güdümü olarak görev almaktadır. Hedef ivme bilgisinin alınamadığı durumlarda ise bu güdüm yöntemi, füze güdüm gecikmelerini dengeleme üzerine çalışan oransal seyir güdüm kanunu formunda optimal bir güdüm kanununa dönüşür.

Hedefin spiral hareketi optimal bir kaçış manevrasıdır. Önceden belirtilmiş güdüm kanunları bu manevralara karşı etkisiz kalabilmektedir. Bu maksatla dönemeçli/zigzag güdüm kanunu elde edilebilmektedir. Bu çalışmada hedefin 1 ve 2 rad/s frekansa sahip 3g ve 6g yüksek fıçı tono, dikey-s manevraları ile, 2g sabit ivmeli artış yapan manevralar ve 3g, 6g sabit ivmeli manevralar incelenmiştir. Dönemeçli güdüm kanunu kullanan füzenin gecikmeleri dengelenebilmektedir ve böylece dengelenmiş dönemeçli güdüm kanunu elde edilir. Ancak hedefin spiral hareketinin frekansının hesaplanması gerektiği unutulmamaldır. Bu maksatla çalışmada filtre kümeleri kullanılarak önceden bilinmeyen hedefin spiral hareket frekansı hesaplanmıştır. Çoklu model uyarlanabilir kestirici yöntemi ile paralel çalışan kalman filtreleri hedefin hareket frekansını kestirebilmektedir.

Klasik ve modern güdüm kanunlarının yanında sezgisel yöntemler güdüm metodu olarak kullanılabilmektedir. Bu maksatla parçacık sürü optimizasyonu güdüm kanunu geliştirilmiştir. Burada füzeyi hedefe yaklaşırken bir sonraki adımda en az performans harcayacak konuma getirebilmek için anlık olarak en iyi oransal seyir sabiti bulunmaya çalışılmıştır. En iyileme problemi parçacık sürü yöntemi kullanılarak anlık olarak çözülmektedir.

Modellere bozuntular eklenmiş ve ölçümlerdeki hatalar doğrusal Kalman süzgeci kullanılarak minimize edilmiştir. 3 ve 4 durumlu doğrusal Kalman filtreleri benzetimlerde kullanılmıştır. Bozuntular yankının yer değişimi, mesafeye bağlı aktif ve mesafeden bağımsız formda olacak şekilde eklenmiştir.

Döngü modelleri Matlab Simulink programı kullanılarak oluşturulmuştur. Rastlantısal girdili modeller istatistiksel olarak incelenmiş ve sonuçlar Monte Carlo yöntemi ile elde edilmiştir. Sonuçlar ıskalama mesafesi, vuruş açısı, kontrol eforu cinsinden incelenmiştir. Benzetim sonundaki hedef ile mesafenin diğer bir adıyla ıskalama mesafesinin 10 metre altındaki sonuçları başarılı olarak yorumlanmıştır.

Bu çalışmada aynı zamanda çoklu hedef için literatürde bulunan yaklaşımlar incelenmiştir. Bu yöntemlerden merkezi yöntem ve erken yakalama geometri yöntemi uygulanmıştır.

Güdüm yöntemleri 16 farklı durum için ve bu durumlar 12 farklı güdüm yönteminin kullanılmasıyla incelenmiştir. Her bir güdüm yöntemi, uçuş süresinin 0 ile 10 saniye arasında ve 0.5 saniye arttırımla oluşabilecek çarpışma durumları için çalışılmıştır. Bu durumların incelemesi, Matlab/Simulink ortamında 100 saat üzerinde benzetim

süresinin ardından elde edilmiş. Modeller içerisindeki diferansiyel denklemler 4'üncü dereceden klasik Runge-Kutta yöntemiyle maksimum 0.01 zaman aralığı kullanılarak çözümlenmiştir.

İncelenen güdüm yöntemlerinin uygunluğu, hangi durumlarda kullanılabileceği sonuçlandırılmış ve gelecek çalışmalar için öneriler verilmiştir.

1. INTRODUCTION

Rockets have been used as a weapon in battles since the ancient times. The slow improvement of guidance and control system technology has led to the slow development of rockets. The missile can be defined as an object capable of being projected to hit a distant object. Unguided Missile is a missile, which cannot control its own trajectory. On the other hand, the guided missile can control its own flight path. Also the following definition of a guided missile, "a guided missile is a space traversing unmanned vehicle which carries within itself the means for controlling its flight path." was made by [1]. Another definition, "A guided missile is one which is usually fired in a direction approximately toward the target and subsequently receives steering commands from the guidance system to improve its accuracy." was made by [2].

The first thought of the use of guided missile in battles is based on the First World War. The first flight of a liquid propellant rocket happened in Germany on 1931 [3]. Then, the Peenemünde project was launched as guided missile development project. It can be said that modern missile guidance technology is based on the development of V-1 and V-2 surface to surface missiles during World War II. The new type of war weapon, V-1, was developed in 1942. V-1 was having 7.9m length, 5.3m wingspan, 2180kg weighted including 850kg warhead, powered by a pulsejet engine works with gasoline fuel, capable of propelling 724km/h and 370km range [4]. V-1's route was pursued with gyroscopes. When the preset range was reached, elevator deflects to dive ground. V-1 was not accurate enough and it could be destroyed by an anti aircraft guns.

The first liquid propellant long ranged missile and the most frightening weapon of World War II was V-2. It was developed by Dr.Werner-Von Braun and Dr.Walter Dornberger. V-2 had movable vanes on the outer tips of its fins. They were used for guidance and control purposes. Basically, hitting distribution of V-2 was within 16km from 322km firing distance. It was the first example of inertial guidance, making use of gyroscopes and accelerometers [5]. V-2 had two main parts, first one

was gyroscope which controls the altitude and pitch programmer. The second one was accelerometer senses the acceleration. It could cut off the engine and dive when preset velocity was reached. Germany continued to produce missiles during World War II.

Missiles can be divided into two categories according to operational area;

- Tactical Missiles or Guided Missiles
- Strategic Missiles or Unguided Missiles

Operational usage of Tactical Missiles is more likely for shorter range, maneuvering or non-maneuvering targets and endoatmospheric conditions. Its guidance and control technologies turn out to be more critical due to use for maneuvering targets [6]. Tactical Missiles can home to target or can follow preset path. Homing missiles can be divided into following forms, active, semi-active or passive. On the other hand, Strategic Missiles operate for long ranges, exo-atmospheric conditions and stationary targets.

Position of launch point and position of target point can be used for classification also. As a result, four main categories of missiles are;

- Surface to Surface Missile (SSM)
- Surface to Air Missile (SAM)
- Air to Surface Missile (ASM)
- Air to Air Missile (AAM)

Surface to Surface missiles are launched from surface of the earth or ship to hit the target on earth surface. Stationary targets fall into SSM category. The range of missiles can be up to thousands of kilometers. The accuracy required for large targets is not much as shorter range missiles. Strategic missiles are also known as long range target missiles. Short range, Intermediate range and Inter-Continental Ballistic Missiles (SRBM, IRBM and ICBM) are general names. Surface to surface missiles can be divided into categories as ballistic missiles and cruise missiles.

Surface to Air missiles are generally used for defensive purposes. Targets in this case have capable of evasive maneuvers. Thus guidance system of surface to air missiles has able to give proper commands in order to intercept air target.

Air to surface missiles are fired from an aircraft to hit targets on earth surface. Targets are usually stationary. Moving targets can be assumed stationary due to relatively very low speeds. Targets are not usually predetermined. Thus aircraft carries ASM seek the target in movement. This brings another problems to consider such as velocity and dynamic of aircraft.

Air to air missiles are possibly the most difficult to design. Target and launch point are in movement. Aircrafts have high maneuverability and capacity to achieve high speeds. Therefore advanced guidance methods are needed.

Essential parts of a guided missile can be divided into four groups, airframe and control surfaces, propulsion system, warhead system, guidance and control system. Movable control surfaces comply with the deflection commands from guidance and control system. Thus the guided missile tries to the hit target by following the proper path.

1.1 Missile Guidance

The guidance process is basically a feedback control system where the pursuer-evader engagement is considered part of the guidance navigation and control (GNC) loop [7]. The GNC loop has a couple of parts such as; information subsystem, control parts, an operator and pursuer dynamics. The guidance loop can be seen in Figure 1.1. Loop includes seeker to track target's dynamics. Then relative motion can be calculated with the information of missile's motion. The guidance processors use relative motion data to generate proper guidance command. Basically, lateral acceleration command is delivered to flight control system (FCS). Lateral acceleration is also known as latax. The guidance command generated by the guidance law is expressed as commanded lateral acceleration and is given as input the lateral autopilots. The FCS controls the deflection surfaces to change the missile's flight path due to time varying achieved lateral acceleration.

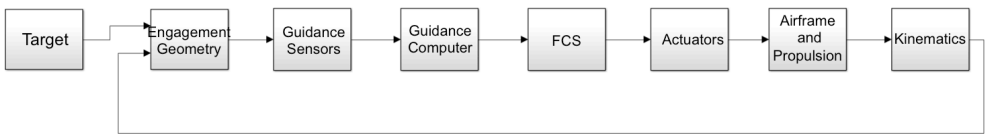

Figure 1.1 : Homing guidance loop.

The basic missile homing loop consists of a seeker to track target, a noise filter to estimate true value of the line of sight angle (LOS) rate, imaginary line joining the missile and the target at any given instant in time, an advanced guidance law to generate lateral acceleration command and lastly a flight control system to direct desired path to hit the target. Simplified homing loop can be seen in Figure 1.2. Miss distance is the distance of closest approach of the pursuer to the evader. Certainly, the guidance navigation and control system tries to bring zero miss distance. If the missile hits the target directly, miss distance will be zero. In some cases, missile can not hit the target perfectly and the fuze detonates the warhead to damage the target.

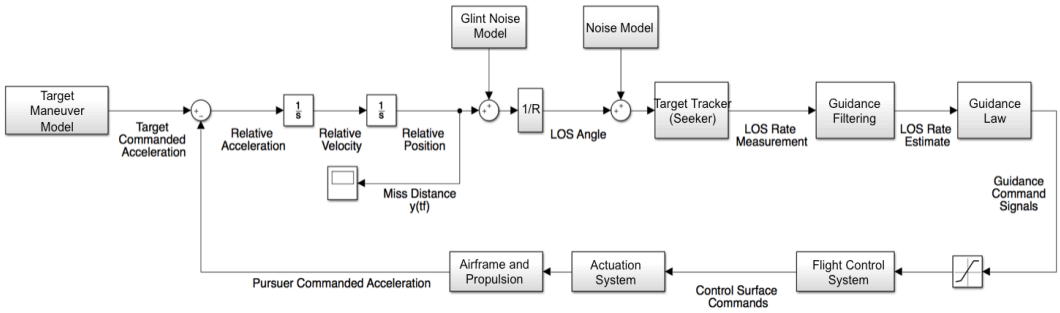

Figure 1.2 : Simplified homing guidance loop.

The sensor is needed to locate the target position and relative position. In order to do that, line of sight (LOS), range, altitude, LOS rate, range rate information may be needed. Some of the Line of sight (LOS) sensors are basically IR, EO Display Mapping Radar, Sonar, Optical. Range and its rate sensor examples are radar, laser, sonar, optical instruments and Doppler radar respectively. Altitude can be measured by baro-altimeter, radar-altimeter and LOS rate by EO Tracker. Lastly, GPS, TACAN or DME can be used as an external reference.

Guidance operator or computer's mission is to perform engagement perfectly. In order to do that, guidance steps are to be solved. These steps are basically; guidance performance, guidance phases and operation. There may be needed to use different guidance laws during engagement. Missile guidance is generally divided into three phases;

-Launch or Boost Phase

-Midcourse Phase

-Terminal Phase

The missile starts its flight after launching from the main platform. It starts with initial speed and altitude of the aircraft or launching platform. Boosted period lasts until the booster burns up its fuel. The missile should be has specific value of velocity. It is important to reach predetermined values in order to hit its target. The slant range is needed to shift boost phase to midcourse phase. If the interceptor cannot reach required slant range before terminal phase, the midcourse phase can be passed [8].

The midcourse phases starts when the missile reaches required slant range from the launching point. Phase lasts until the required slant range from the target is reached. Missile stays in phase until that point. During this midcourse phase major corrections to the missile's flight path are made. Subsequently, seeker scans a region looking for a target in both air to surface or air to air cases. Immediately after detecting target, seeker tracks target's position. After lock on period, midcourse phase can be said shifted to terminal phase. It is important to pass terminal phase with acceptable heading error. Heading error represents the difference in angle between actual velocity vector of the missile and the collision triangle.

The terminal phase occurs after lock on or required slant range is reached depend on the mission. The terminal phase is the most important among other phases. This requires high accuracy guidance commands from the guidance system in order to compensate target evasive maneuvers. The missile stays in terminal phase until hit the target. Depend on the mission classification the missile may have a single guidance system for all phases or more than one during engagement. Figure 1.3 represents the air to air operation.

Certain factors can be said to affect the mission success. In general, acquisition time of the seeker, the missile's kinematics capability, maneuverability. The radome that covers the seeker causes shifted position appearance of target instead of the actual position. In homing missiles, this affects guidance commands. It can be clearly said that non-maneuvering target is much easier to hit rather than maneuvering target. It is a challenging problem to hit maneuvering target [13][14]. Generation of guidance command can easily be affected by different type of noise. Also heading error has influence on terminal miss distance. Lastly, the missile's response to commanded acceleration has impact on terminal miss distance [6][12].

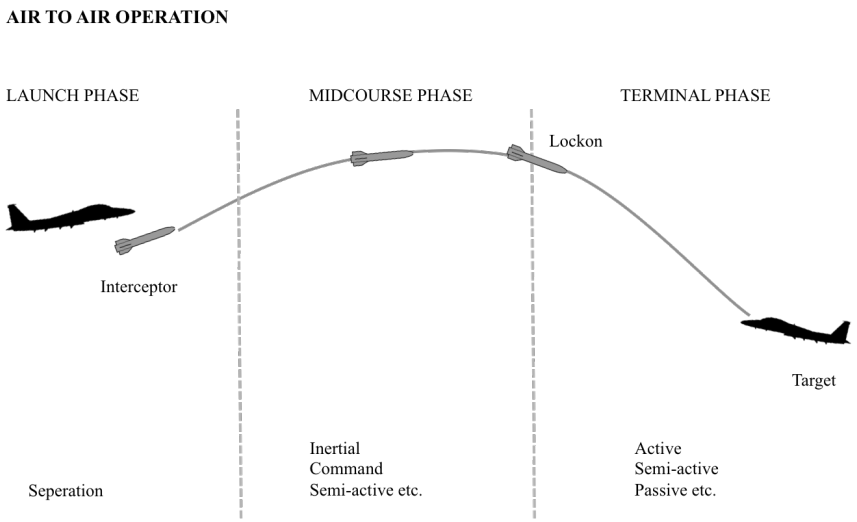

Figure 1.3 : Air to air operation.

During the engagement, different form of guidance laws may need to be complete mission perfectly. No one system is best for all phases. In midcourse phase, the missile usually uses a trajectory shaping guidance that a special form of proportional navigation guidance law in order to minimize energy loss [7]. In terminal phase, different from the midcourse guidance, dynamic requirements are significant. Trajectory errors should be overcome in a very short time. The strategy in this phase is called terminal guidance.

Another classification of guidance systems and algorithms could be as follows [4][13];

- Self-Contained Guidance (Preset, Terrestrial, Inertial and Celestial-Navigation)
- Command Guidance (CLOS)
- Beam Rider Guidance
- Homing Guidance (Active, Semi-Active, Passive)

The self-contained guidance group mostly applicable for surface to surface missiles. These systems do not transmit nor receive signals that can be interrupted. Thus countermeasures are ineffective [9]. Preset guidance is the guidance method used by the missile following predetermined path. Target position and trajectory information are implemented before launch. Thus, the trajectory cannot be changed after launch. Inertial guidance is similar to preset guidance. Main difference is that inertial guidance can make flight path corrections during engagement via accelerometers. On the other hand celestial-inertial system uses the stars to navigate the missile. The navigation system measures the angular elevation of known stars then tries to

determine its position. Terrestrial guidance simply compares the pre-loaded photos or maps with the earth surface. If the matching occurs, the missile moves towards the target.

Command guidance methods uses external source for guidance commands. There is such a tracking system that tracks both the target and the missile during engagement. Therefore, there is no seeker in the missile. Radar, optical or infrared system provides the necessary information such as range, range rate, elevations etc. Then, the computer on the earth surface calculates the lateral acceleration command then transmits the missile. The system is shown in Figure 1.4. These signals can be transmits with the missile tracking system or separately. A special type of command guidance is the command to line of sight (CLOS). In this type of system, the missile always to commanded lie on the line of sight (LOS). Command to line of sight is a line between the tracking system and the target. This guidance method is also known as three-point guidance that refers to the tracker, missile and target. Three-point guidance is also known in literature as constant bearing guidance [7].

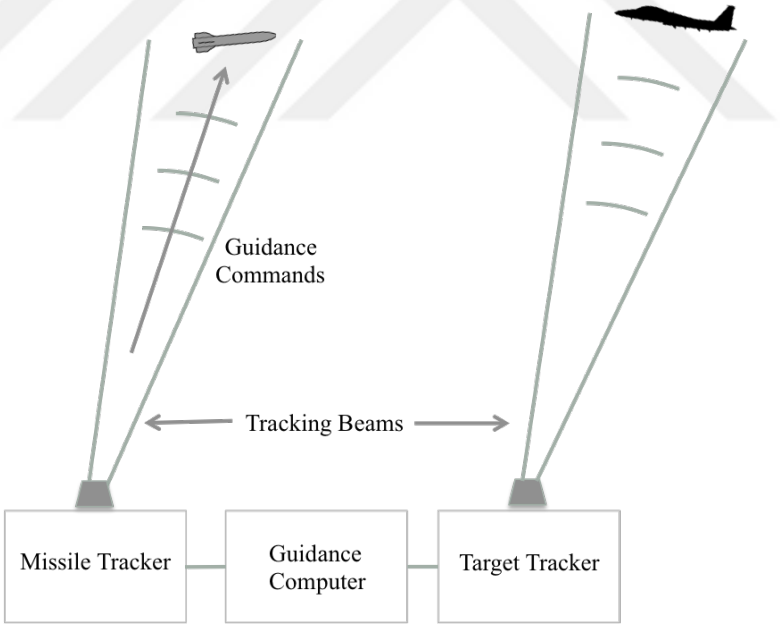

Figure 1.4 : Command guidance system.

Beam riding guidance is also a form of command guidance. A device in the missile tries it centered in the beam. Beam riding guidance can be seen in Figure 1.5. Thus, the missile is said to ride the beam. Advantage of this system is that a large number of launching missile may ride on the beam to hit the target. On the other hand, losing track of the target limits the usage of this system.

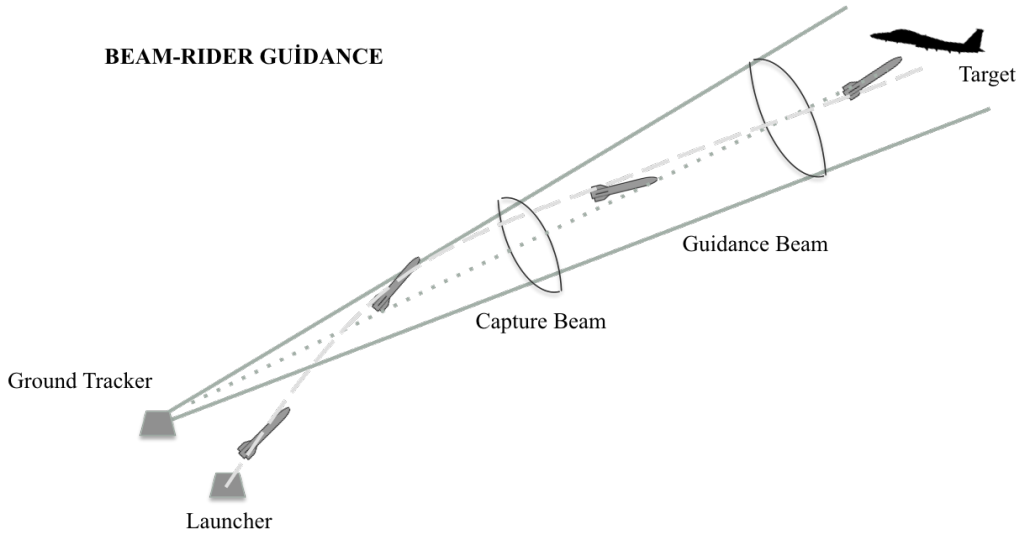

Figure 1.5 : Beam-rider guidance.

Homing guidance system can detect the target and direct itself to engagement. The missile detects the target passive or semi-active way. Then flight control system directs the missile to the target [10]. Accuracy in homing guidance cannot be obtained by any other type of missile guidance [11]. It explains the importance of homing guidance to us. Just because of the missile guides itself homing guidance systems are called fire and forget or leave and forget missiles. In homing guidance system, identifying and chasing a target should be done from target's distinctive features. The missile seeker can detect the radiated energy form; microwave, infrared, visible and ultraviolet. Active seeker illuminates the target in order to receive reflected signal. Passive seeker senses electromagnetic energy radiated by the target. Homing guidance systems have three general modes;

- Active Homing Guidance
- Semi-Active Homing Guidance
- Passive Guidance

In active homing guidance, the missile carries a transmitter and a receiver. Transmitted signals are reflected from the target. Simply, the missile illuminates the target. Reflected signals received from the receiver. Active guidance is generally used in the terminal phase. Figure 1.6 represents the active radar homing guidance. In this type of homing guidance, after the firing of missile, launch aircraft can maneuver immediately. In air to air combat case, active homing missiles have a superiority role. It can be said that disadvantage of active guidance is the unwanted

signals coming from surroundings. Also, susceptible to jamming is another important issue to turn over.

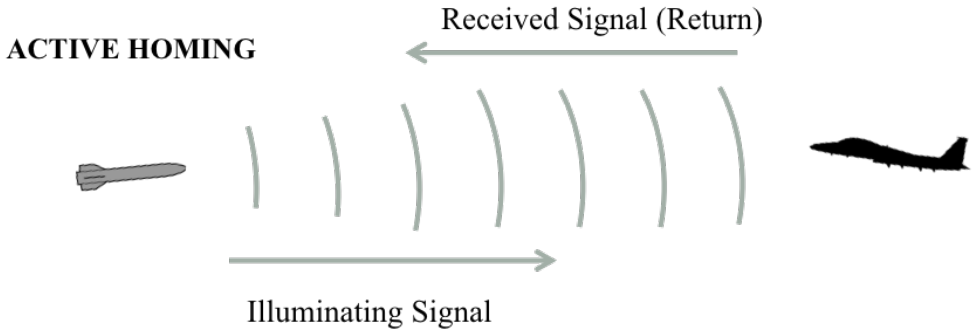

Figure 1.6 : Active homing guidance.

A semi-active homing guidance system chases the target with the help of an external source by illuminating the target. Tracking radar illuminates the target then the missile receives the reflected signals to hit the target. Tracking system can be placed on the earth surface or on an aircraft. During engagement, the missile receives signals and also tracking platform receives signals too in order to ensure that the target is illuminated. If the tracking platform is an aircraft there is a disadvantage of this system such that aircraft cannot maneuver immediately after firing the missile. In Figure 1.7 and 1.8 semi-active and passive homing guidance system can be seen respectively.

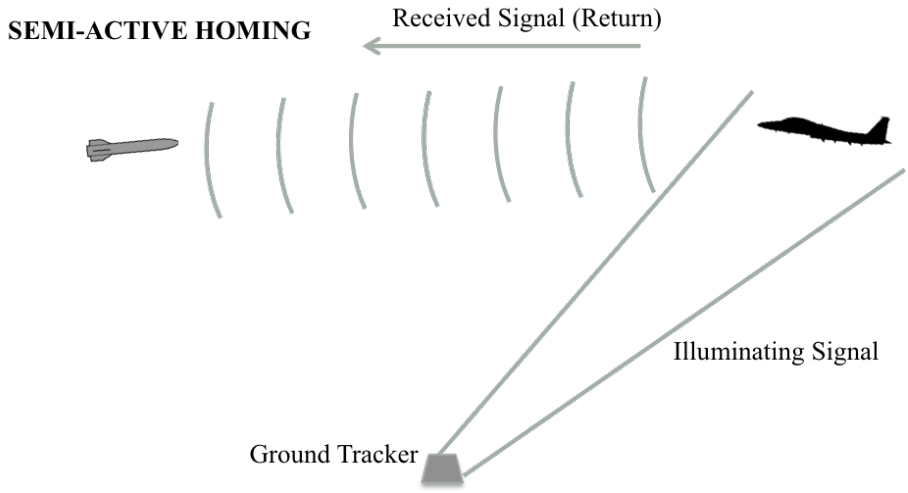

Figure 1.7 : Semi-active homing guidance.

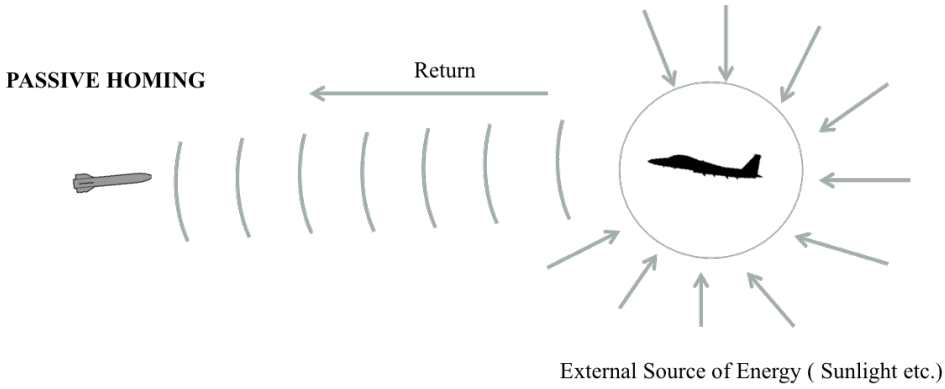

Figure 1.8 : Passive homing guidance.

Passive homing guidance system detects the presence of a target and tracks it by energy source that target propagates. The missile uses passive homing guidance cannot be detected or jammed by the target due to unsent signal. Energy characteristic of target should be different from the surroundings so that receiver detects the target. The missile may direct itself in this passive homing system such energy sources; electromagnetic energy, heat, light or natural energy sources as sun.

1.2 Literature Survey on Missile Guidance

In zero lag guidance system with non-maneuvering target case, the proportional navigation guidance law produces zero miss distance for the least integral square control effort. Subsequently modern control theory is used as a tool for development of modern guidance laws [4, 6, 20, 21].

Nesline et al compared the performance of modern guidance systems to a classical proportional navigation in homing missile guidance system [20].

Optimal control theory is used in Cottrell's study. The missile dynamics are represented as a single time lag. Certain miss distance reduction is obtained through the optimal guidance laws via high order missile dynamics are represented as a single time lag [22].

In missile guidance homing loop analysis, the closing velocity is mostly assumed constant. Primarily, the effect of aerodynamic drag on the missile is ignored. By doing so, the missile velocity is assumed constant after launching phase [15].

Adjoint analysis proposed by Zarchan can be used in miss distance analysis. Method based on linearized dynamics of missile, converting all step inputs to impulse and

inversing signal flows. Disadvantages of this method are firstly cannot be applied on nonlinear models, secondly, only give mean values of engagements not other statistical values such as variance and standard deviation like the monte carlo approach [6,16].

Hough proposed optimal guidance and nonlinear estimation algorithms for accelerated target using a nine state extended Kalman filter in a cartesian inertial frame [18].

Uhrmeister used a Kalman filter to estimate acceleration of maneuvering aircraft. LOS rate is estimated via radar measurement and target acceleration via imaging sensor [34].

Kim et al. studied on 3 dimensional augmented proportional guidance law. The Kalman filter and augmented proportional guidance law are generally represented in Cartesian coordinates in the literature. As a result, methods are not applicable to the real life guidance system applications. In this study, obtained guidance law and filter in Cartesian coordinates are transformed to the polar coordinates form. Then extended kalman filter is used to estimate relative position, velocity and target acceleration [35].

Vergez et al uses a passive seeker that only uses angle information in their study to estimate the relative position, velocity and acceleration. Four target acceleration models paired with an extended Kalman filter are presented in this study [36].

Uncertainty in the airframe time constant has an influence on the miss distance. Yaesh et al proposed a robust guidance law takes into account this issue and target evasive maneuver [19].

In order to hit target with time to go information required guidance laws, Ben-Asher et al proposed an optimal guidance method presents reduced sensitivity to the error in time to go estimations. Then proposed method is compared to the optimal guidance law and to proportional navigation guidance law [23].

Linear quadratic pursuit evasion games are considered in Ben-Asher et al study. In this study, the relative position, the relative velocity, pursuer's control effort and evader's control effort are weighted in cost function. Perfect interception (zero miss distance) and perfect rendezvous (zero terminal lateral velocity) cases are investigated [24].

Most classical and modern guidance laws solved for continuous time systems up to Gitizadeh et al proposed discrete-time optimal guidance method. In this study, discrete time versions of proportional navigation and augmented proportional navigation guidance laws are derived [25].

Sinusoidal or weave target maneuvers are difficult maneuvers for a missile to hit. Zarchan showed how to improve performance and reduce miss distance due to a weaving target by speeding up the guidance process and the missile acceleration capability [17]. Also proposed a guidance method against weaving or spiraling target is investigated [26].

Zarchan et al proposed a bank filter approach to hit spiraling or weaving target when the target weave frequency is unknown. In this study, linear Kalman filter bank approach is investigated. Each filter is adjusted to a different weave frequency. The superiority of bank filter approach against extended Kalman filter is shown [27].

Solving optimization problems using heuristic methods become popular lately. The missile guidance problem is investigated in Kung and Chen's study. In this study, proposed method is based on particle swarm optimization algorithm. The objective function is relative distance between the target and the missile. In that case, particle swarm optimization guidance method is similar to pure pursuit guidance law. Appropriate result from the point of terminal miss distance for head on or tail chase scenarios is obtained using proposed guidance method (PSOG) [30].

Particle swarm optimization guidance method guides the missile to the current position of the target. Thus, terminal miss distance becomes quite large if the target maneuvers. Chen, Lee, Liao and Kung are proposed improved particle swarm optimization guidance method (IPSOG). Objective function is selected as the line of sight rate. Hence, proposed method is similar to proportional navigation guidance law. The guidance performance is better than the particle swarm optimization guidance method [31]. Modified version of improved particle swarm optimization method is proposed in [32]. The Kalman filter algorithm is used to predict a target's dynamic. Proposed guidance method (MPSOG) has a better guidance performance than previous particle swarm optimization guidance methods.

Multiple target case has importance in missile guidance theory. Zarchan investigated the power centroid method. In this method, the missile is guided on the power

centroid of targets in close formation. When the one of the targets stays outside the seeker's view area, the missile guides itself to the other target [6].

Gutman et al. studied the effect of initial conditions on miss distance. The power centroid method is reviewed. Two types of proportional navigation guidance loop, numeric derivative and analytic derivative model, were modeled and compared [28].

Midcourse guidance strategy against multiple target was proposed by Shin et al. Method is based on the earliest intercept geometry guidance. Idea is that the missile can defend the area if the target stays in the area defined by the early intercept geometry [29, 33, 38].

1.3 Scope of the Thesis

In this study, the classical and modern guidance laws used in the terminal phase of the tactical missile are investigated. There are too many guidance laws to be examined in literature. The main ones are as follows; proportional navigation guidance, augmented proportional navigation guidance, optimal rendezvous, augmented optimal rendezvous, optimal guidance or minimum effort guidance, minimum effort guidance law without target acceleration information, extended proportional navigation, trajectory shaping guidance, weave guidance, compensated weave guidance, differential game guidance, biased proportional navigation and different version of particle swarm optimization guidance law. All these guidance laws are derived mathematically.

In order to investigate terminal phase guidance algorithms, two-dimensional planar engagement geometry is used. The engagement model is linearized around collision triangle using small angle approximations. This leads us to investigate head on collision or tail chase scenarios. The homing loops for all examined guidance laws have been modeled in Matlab Simulink platform. Because the flight control system design is beyond the scope of this thesis, autopilot, actuator and autopilot are represented in different cases as a single lag, fifth order binominal and a flight control transfer function for skid to turn missiles proposed in [35,37]. The response of the guidance system to disturbances such as target maneuver, heading angle error, radome error, missile time constant, glint noise, range depended and independent noise is studied. The relative distance, velocity and acceleration measurements are

corrupted by noise terms in reality. The Kalman filtering is the most excepted estimation theory used today. Therefore, states are estimated via linear Kalman filter. The guidance system performance based upon random noise input can vary. Hence, Monte Carlo approach is applied to obtain the terminal miss distance statistics. The guidance laws after designed are validated through simulation using nonlinear three-dimensional point-mass model.

Lastly, multiple target cases are investigated via two types of approach. The power centroid and early intercept geometry method are studied for a missile versus two targets cases. The simulation is made in order to validate proposed methods in two and three-dimensional nonlinear models.

1.4 Outline

The thesis contains eight chapters. In the first chapter, the general concepts in missile guidance, literature survey about homing missile guidance and scope of thesis are presented. In chapter 2, the mathematical modeling of homing missile, linearization of engagement geometry, missile homing loop and 3D point-mass equation of missile motion are described. Chapter 3 explains the missile and target characteristics. The noise input model, target maneuver model, flight control model and seeker model are discussed in detail. The classical and modern guidance laws are studied in chapter 4. Homing guidance system models are presented in this chapter. In chapter 5, three and four state Kalman filter models are presented as an optimal filtering method. Bank filter technique is applied to different target maneuver models in this chapter. Chapter 6 touches on multiple target cases by showing two main methods. Homing guidance algorithms are simulated through different scenarios in chapter 7. Simulink models are also showed in this chapter. Lastly, conclusion and future works are presented in chapter 8.

2. MATHEMATICAL MODELING FOR MISSILE GUIDANCE

2.1 Equations of Motion

2.1.1 Missile equations of motion

In this study, three-dimensional point-mass model is assumed for the missile and target dynamics. This type of approach is common in literature [4,6,31,39,40,41,42]. In order to minimize simulation time, three degrees of freedom (3DOF) model can be used without compromising the verity of six degrees of freedom (6DOF) model [39]. Gravitational, thrust and aerodynamic forces are included in missile dynamics. Inertial reference frame is fixed to earth surface for flat-earth and 3D earth models. Figure 2.1 shows the aerodynamic forces acting on the missile and pitch and yaw accelerations (latax) in body axis reference frame.

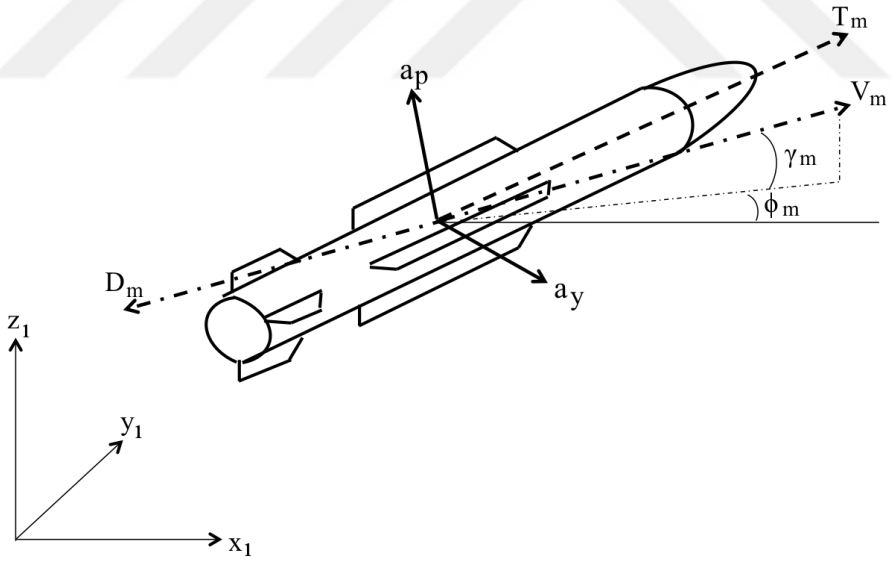

Figure 2.1 : Definition of a missile's aerodynamic vectors.

The missile equations of motion are in cartesian coordinate inertial reference frame as follows;

$$\dot{x}_m = V_m \, cos\gamma_m \, cos\phi_m \tag{2.1}$$

$$\dot{y}_m = V_m \, cos\gamma_m \, sin\phi_m \tag{2.2}$$

$$\dot{z}_m = V_m \, sin\gamma_m \tag{2.3}$$

x_m, y_m, y_m represent x, y and z coordinates of the missile respectively. $\dot{x}_m, \dot{y}_m, \dot{z}_m$ are the time derivative of the missile position.

$$\dot{\phi}_m = \frac{a_{ym}}{(V_m \, cos\gamma_m)} \tag{2.4}$$

$$\dot{\gamma}_m = \frac{a_{pm} - g \, cos\gamma_m}{V_m} \tag{2.5}$$

ϕ_m and γ_m are the azimuth angle and the flight path angle respectively. $\dot{\phi}_m$ and $\dot{\gamma}_m$ are the time derivative of the specified angles. In Light of Sight (LOS) reference frame, stated angles can be described as ψ_m and θ_m.

$$\dot{V}_m = \frac{T_m - D_m}{m} - g \, sin\gamma_m \tag{2.6}$$

$$D_m = k_1 \, V_m^2 + k_2 \, \frac{a_p^2 + a_y^2}{V_m^2} \tag{2.7}$$

$$\dot{a}_p = \frac{a_{pc} - a_p}{\tau_m} \tag{2.8}$$

$$\dot{a}_y = \frac{a_{yc} - a_y}{\tau_m} \tag{2.9}$$

V_m and $\dot{V}_m$ are the missile velocity and time derivative of velocity respectively. T is the time varying delivered thrust, D the drag, m the mass of missile and g the gravitational acceleration. k_1 and k_2 are the drag coefficients. a_p and a_y represents pitch and yaw accelerations. a_{pc} and a_{yc} are the commanded accelerations. τ_m is the time constant. 3D engagement geometry can be seen in Figure 2.2.

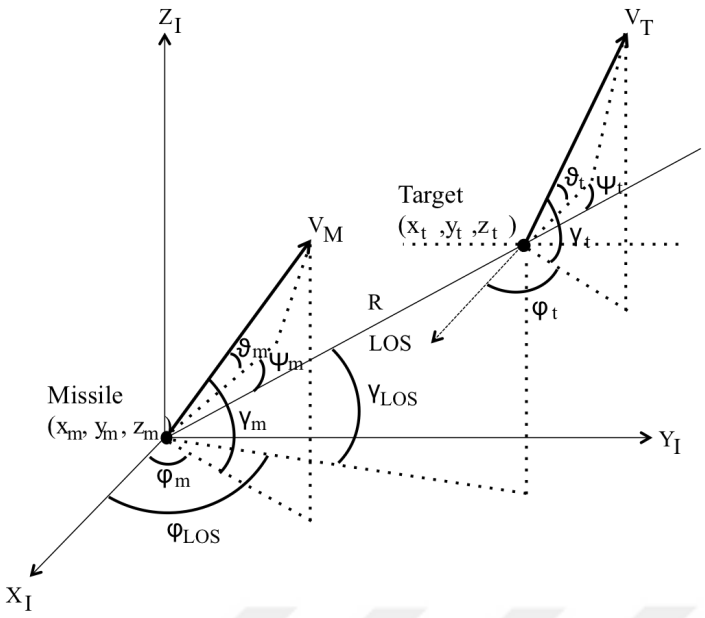

Figure 2.2 : Three dimensional engagement geometry.

2.1.2 Target equations of motion

Target is also considered as a point mass. Similar to the missile equation of motion, target's dynamic in cartesian coordinate reference frame can be shown as follow;

$$\dot{x}_t = V_t \, cos\gamma_t \, cos\phi_t \tag{2.10}$$

$$\dot{y}_t = V_t \, cos\gamma_t \, sin\phi_t \tag{2.11}$$

$$\dot{z}_t = V_t \, sin\gamma_t \tag{2.12}$$

$$\dot{\phi}_t = \frac{a_{yt}}{(V_t \, cos\gamma_t)} \tag{2.13}$$

$$\dot{\gamma}_t = \frac{a_{pt}}{V_t} \tag{2.14}$$

x_t, y_t, y_t represent x, y and z coordinates of the target respectively. $\dot{x}_t, \dot{y}_t, \dot{z}_t$ are the time derivative of the missile position. V_t is the target velocity, ϕ_m the azimuth angle, γ_m the flight path angle respectively. a_{pt} and a_{yt} represents the pitch and yaw accelerations of target. Important point is the evasive maneuver of target. Hence, the target maneuver modeling has a crucial importance.

$$\Delta x = x_t - x_m \tag{2.15}$$

$$\Delta y = y_t - y_m \tag{2.16}$$

$$\Delta z = z_t - z_m \tag{2.17}$$

$$R = \sqrt{(\Delta x^2 - \Delta y^2 + \Delta z^2)} \tag{2.18}$$

$$\gamma_{LOS} = tan^{-1}\left(\frac{\Delta z}{\sqrt{\Delta x^2 + \Delta y^2}}\right) \tag{2.19}$$

$$\phi_{LOS} = tan^{-1}\left(\frac{\Delta y}{\Delta x}\right) \tag{2.20}$$

Relative distance or length of the imaginary line between the missile and target in other words, line of sight is represented as R. ϕ_{LOS} and γ_{LOS} are the angles between line of sight and inertial reference frame.

2.2 Missile – Target Engagement Geometry

3D missile target engagement geometry can be seen in Figure 2.2. In this subsection, in order to design effective guidance algorithms, 3D engagement geometry is converted to 2D engagement geometry. Following assumptions will be made [21];

- The missile – target engagement is 2D in horizontal plane.
- Velocities of missile and target are constant.
- Flight paths can be linearized around collision course.

2D missile target engagement geometry can be seen in Figure 2.3.

The collision condition can be defined as;

$$V_t \sin(\gamma_{t_0}) - V_m \sin(\gamma_{t_0}) = 0 \tag{2.21}$$

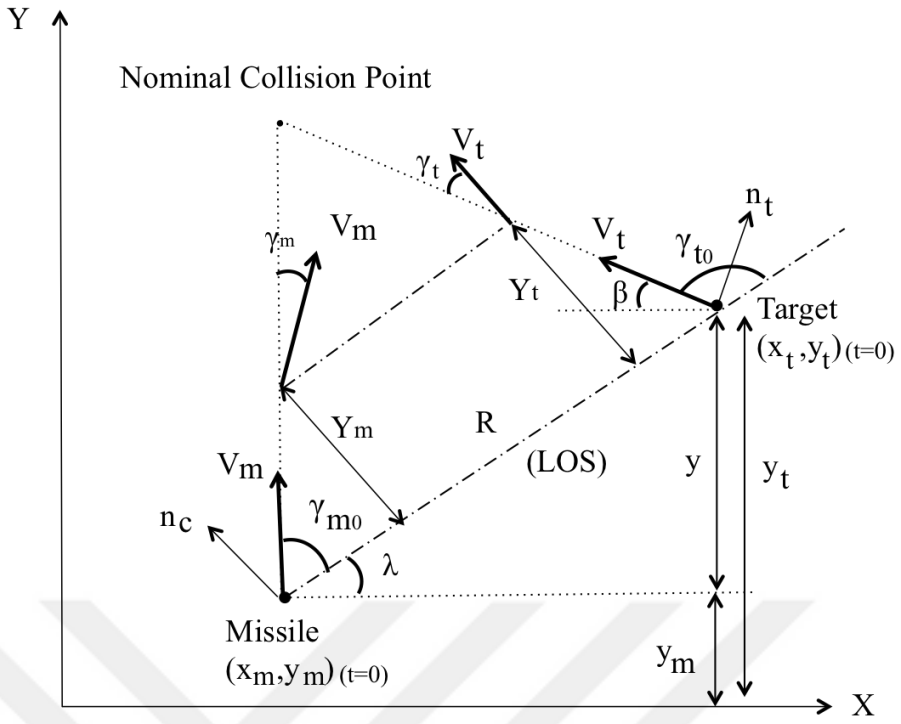

Figure 2.3 : Two dimensional engagement geometry.

$\gamma_{t_0}$are $\gamma_{m_0}$the missile and target nominal heading angles respectively. The closing velocity V_C is the negative rate of change of the relative distance between the missile and target as follow;

$$V_c = -\dot{R} = \mathrm{V_m}\cos(\gamma_{m_0}) - V_t\cos(\gamma_{t_0}) \tag{2.22}$$

At the end of engagement closing velocity will change its sign in other words when relative distance is minimum. $R(t)$ is the nominal lenght of the line of sight. Angular velocity of target and $R(t)$ can be specified as [6];

$$R = \sqrt{(R_{t_x} - R_{m_x})^2 + (R_{t_y} - R_{m_y})^2} \tag{2.23}$$

$$\dot{\beta} = \frac{\mathrm{n_t}}{V_t} \tag{2.24}$$

R_{t_x} , R_{t_y} , R_{m_x} and R_{m_y} are the target and missile position components repsectively. Hence, the target velocity components become;

$$\dot{R}_{t_y} = V_{t_y} = V_t sin\beta \tag{2.25}$$

$$\dot{R}_{t_x} = V_{t_x} = -V_t cos\beta \tag{2.26}$$

Target position vector can be found by integrating above equations. The closing velocity can also be express in other way by taking derivative of equation 2.23,

$$V_c = -\dot{R} = \frac{-[(R_{t_x} - R_{m_x})(V_{t_x} - V_{m_x}) + (R_{t_y} - R_{m_y})(V_{t_y} - V_{m_y})]}{\sqrt{(R_{t_x} - R_{m_x})^2 + (R_{t_y} - R_{m_y})^2}} \tag{2.27}$$

The line of sight angle can be seen from the figure as;

$$\lambda = tan^{-1}(\frac{R_{t_y} - R_{m_y}}{R_{t_x} - R_{m_x}}) \tag{2.28}$$

Taking derivative of above equation gives us the time derivative of line of sight angle as;

$$\dot{\lambda} = \frac{(R_{t_x} - R_{m_x})(V_{t_y} - V_{m_y}) - (R_{t_y} - R_{m_y})(V_{t_x} - V_{m_x})}{(R_{t_x} - R_{m_x})^2 + (R_{t_y} - R_{m_y})^2} \tag{2.29}$$

Relative seperation of the missile and target from the nominal line of sight are Y_m and Y_t. Relative seperation can be defiend as;

$$Y = Y_t - Y_m \tag{2.30}$$

$$\dot{Y} = \dot{Y}_t - \dot{Y}_m = V_t \sin(\gamma_{t_0} + \gamma_t) - V_m \sin(\gamma_{m_0} + \gamma_m) \tag{2.31}$$

γ_t and γ_m are the deviations of target and missile heading during engagement respectively. Lastly, nominal terminal time is expressed as;

$$t_f = t_0 + \frac{R(t_0)}{V_c} \tag{2.32}$$

2.3 Linearization of The Missile – Target Engagement Geometry

In this subsection, engagement model is linearized around collision triangle. It is better to develop simpler models for understanding and development of guidance algorithms. By doing so, we can apply linear control optimal theory to solve missile-

target guidance problem. Obviously, nonlinear engagement model will be used to verify generated guidance algorithms.

In fixed reference frame, y can be seen as relative separation between the missile and target in Figure 2.3. Also we defined previously Y as relative separation of the missile and target from the nominal line of sight angle. Either y or Y can be linearized as [6][21];

$$\ddot{y} = n_t cos\beta - n_c cos\lambda \tag{2.33}$$

Head-on or tail chase scenarios can be assumed and by using the small angle approach equation 2.28 and 2.33 becomes;

$$\ddot{y} = n_t - n_c \tag{2.34}$$

$$\lambda = \frac{y}{R} \; or \frac{Y}{R} \tag{2.35}$$

For head on or tail chase scenarios, small angle approach gives us;

$$\sin(\gamma_{m_0} + \gamma_m) \approx \sin(\gamma_{m_0}) + \cos(\gamma_{m_0})\,\gamma_m \tag{2.36}$$

$$\sin(\gamma_{t_0} + \gamma_t) \approx \sin(\gamma_{t_0}) + \cos(\gamma_{t_0})\,\gamma_t \tag{2.37}$$

Hence, equation 2.31 turns out a following form by substituting 2.36 and 2.37 as;

$$\dot{Y} = \dot{Y}_t - \dot{Y}_m = V_t cos(\gamma_{t_0})\gamma_t - V_m cos(\gamma_{t_0})\gamma_t \tag{2.38}$$

The cosine terms in closing velocity 2.22 becomes unity, therefore depend on the head on or tail chase case;

$$V_c = -\dot{R} = \mathrm{V_m} - V_t \tag{2.39}$$

$$V_c = -\dot{R} = \mathrm{V_m} + V_t \tag{2.40}$$

Defining the line of sight angle either in y or Y form, we can denote time derivative of line of sight angle $\dot{\lambda}$ as;

$$\dot{\lambda}(t) = \frac{d}{dt}\left(\frac{y}{R}\right) = \frac{y}{V_c(t_f - t)^2} + \frac{\dot{y}}{V_c(t_f - t)} = \frac{y + \dot{y}t_{go}}{V_c(t_{go})^2} \tag{2.41}$$

t_{go} is the time to go represents the $t_f - t$ in equation 2.41.

If we equate relative separation to x_1 and time derivative of the relative distance to x_2, normal accelerations become,

$$x_1 = y, \qquad x_2 = \dot{y}, \qquad w = V_m cos(\gamma_{t_0})\dot{\gamma}_t, \qquad u = -V_m \cos(\gamma_{m_0})\dot{\gamma}_m \tag{2.42}$$

After taking derivative of equation 2.38, state space representation can be obtained as,

$$\dot{x}_1 = x_2, \qquad \dot{x}_2 = u + w \tag{2.43}$$

In matrix form,

$$\dot{x} = Ax + Bu + Dw$$
$$A = \begin{bmatrix} 0 & 1 \\ 0 & 0 \end{bmatrix}, \qquad B = \begin{bmatrix} 0 \\ 1 \end{bmatrix}, \qquad D = \begin{bmatrix} 0 \\ 1 \end{bmatrix} \tag{2.44}$$

If the missile and target controls their acceleration without any time lag, this case referred as ideal form. If the missile's dynamics contains first order time lag with time constant T, this case has a following state space form;

$$A = \begin{bmatrix} 0 & 1 & 0 \\ 0 & 0 & 1 \\ 0 & 0 & -\frac{1}{T} \end{bmatrix}, \qquad B = \begin{bmatrix} 0 \\ 0 \\ \frac{1}{T} \end{bmatrix}, \qquad D = \begin{bmatrix} 0 \\ 1 \\ 0 \end{bmatrix} \tag{2.45}$$

If the missile and target dynamics have time lag, this case is referred as non-ideal,

$$A = \begin{bmatrix} 0 & 1 & 0 & 0 \\ 0 & 0 & 1 & 1 \\ 0 & 0 & -1/T & 0 \\ 0 & 0 & 0 & -1/\theta \end{bmatrix}, \qquad B = \begin{bmatrix} 0 \\ 0 \\ 1/T \\ 0 \end{bmatrix}, \qquad D = \begin{bmatrix} 0 \\ 0 \\ 0 \\ 1/\theta \end{bmatrix} \tag{2.46}$$

Here θ is the time constant of target's control system, u is the missile's control command and w is the target's acceleration command added system as a disturbance [21].

2.4 Linear Quadratic Differential Games in Missile Guidance Problem

The dynamic model of engagement geometry is as follow;

$$\dot{x} = Ax + Bu + Dw \tag{2.47}$$

Associated performance index;

$$J(u,w) = \int_0^{t_f} (x^T Q x + u^T R u - \gamma^2 w^T w) dt + x^T(t_f)\, Q_f\, x(t_f) \tag{2.48}$$

$u(t)$ is defined as missile's acceleration command with intent to minimize performance index equation 2.48. On the other hand, $w(t)$ is defined as target's accelerations so as to maximize same performance index. When γ goes to infinity, evader's action turns into stationary form as zero acceleration. In this case, problem becomes one sided linear quadratic optimal control problem. If the target and missile have a full control their acceleration, no lag in system, and target has stationary, solution of this problem will be in the form of proportional navigation guidance law with effective navigation ratio three as an example. Q, the state penalty matrix and R, the control matrix is assumed positive definite matrix. Q_f, the terminal penalty weighting matrix is positive definite. Linear Quadratic Optimal control problem is to find optimal acceleration command u. Stated problem will be solved using Lagrange multipliers λ. After adding multiplier to equation 2.47 then the resultant form will be added into equation 2.48. Hence, cost function will be in the form;

$$\begin{aligned} J(u,w) = \int_0^{t_f} [(x^T Q x + u^T R u - \gamma^2 w^T w) + \lambda^T ((Ax + Bu + Dw) \\ - \dot{x})] dt + x^T(t_f)\, Q_f\, x(t_f) \end{aligned} \tag{2.49}$$

Hamiltonian function H will be;

$$H(u,w) = (x^T Q x + u^T R u - \gamma^2 w^T w) + \lambda^T ((Ax + Bu + Dw) \tag{2.50}$$

Derivations, assumptions and conditions follow the lines of [21] and [43]. By application of the calculus of variations; state, costate, stationary and boundary conditions must be satisfied and following conditions are given below,

$$State\ Equation, \qquad \frac{\partial H}{\partial \lambda} = \dot{x}, \qquad for\ t \geq t_o \tag{2.51}$$

$$Costate\ Equation, \qquad \frac{\partial H}{\partial x} = -\dot{\lambda}, \qquad for\ t \le t_f \tag{2.52}$$

$$Stationarity, \qquad \frac{\partial H}{\partial u} = 0, \qquad \frac{\partial H}{\partial w} = 0, \qquad for\ t \ge t_o \tag{2.53}$$

$$Boundary, \qquad \frac{\partial \Phi}{\partial x} = \lambda(t_f), x(t_o) \quad given \tag{2.54}$$

Using stationary condition equation 2.53 missile and target acceleration commands can be found as;

$$u(t) = -R^{-1}B_2^T\lambda \tag{2.55}$$

$$w(t) = \gamma^2 B_1^T\lambda \tag{2.56}$$

Using equation 2.55 and 2.56 into state and costate equations, two-point boundary value problem is arised;

$$\begin{bmatrix}\dot{x}\\ \dot{\lambda}\end{bmatrix} = \begin{bmatrix} A & \gamma^2 B_1 B_1^T - B_2 R^{-1} B_2^T \\ -Q & -A^T \end{bmatrix}\begin{bmatrix} x \\ \lambda \end{bmatrix}$$
$$x(0) = x_0$$
$$\lambda(t_f) = Q_f x(t_f) \tag{2.57}$$

Sweep method is given to solve two-point boundary value problem in [21]. Based on the idea of the state $x(t)$ and costate $\lambda(t)$ satisfy the linear relation given below;

$$\lambda(t) = P_c\, x \tag{2.58}$$

P_c is the unknown matrix yet. Using equation 2.55, $u(t)$ and $w(t)$ can be written as;

$$u(t) = -R^{-1}B_2^T P_c\, x \tag{2.59}$$

$$w(t) = \gamma^2 B_1^T P_c\, x \tag{2.60}$$

Differentiate equation 2.58,

$$\dot{\lambda}(t) = \dot{P}_c\, x + P_c\dot{x} \tag{2.61}$$

Taking advantage of dynamic equations in 2.57,

$$\dot{x} = Ax + \gamma^2 B_1 B_1^T\lambda - B_2 R^{-1} B_2\lambda \tag{2.62}$$

$$\dot{\lambda} = -Qx - A^T\lambda \tag{2.63}$$

We can find a relation for P_c via substitute equation 2.61 into 2.63 and by the help of 2.58 after rearranging terms,

$$\dot{P}_c\, x + P_c\dot{x} = -Qx - A^T\lambda \tag{2.64}$$

$$\dot{P}_c\, x + P_c(Ax + \gamma^2 B_1 B_1^T\lambda - B_2R^{-1}B_2\lambda) = -Qx - A^T\lambda \tag{2.65}$$

$$\dot{P}_c\, x = -Qx - A^T P_c x - P_c Ax - P_c\gamma^2 B_1 B_1^T P_c x + P_c B_2 R^{-1} B_2 P_c x \tag{2.66}$$

$$-\dot{P}_c\ = Q + A^T P_c + P_c A + P_c\gamma^2 B_1 B_1^T P_c - P_c B_2 R^{-1} B_2 P_c \tag{2.67}$$

Optimal acceleration command depends on P_c. Above matrix riccatti differential equation 2.67 must be solved in order to find optimal acceleration command equation 2.59. There are ways to solve stated equation given in [21][43]. In chapter 4, a number of guidance laws will be solved via linear quadratic methods explained in this subsection.

3. GUIDANCE SYSTEM MODEL

3.1 System Design

Missile can be defined as an object capable of being projected to hit a distant object. Missiles are suitable for air-to-air, surface-to-air, surface-to-surface missions. They involve a propulsion system, guidance systems, control surfaces and warhead part. Following subsystems are part of a guided missile; Airframe, Guidance, Propulsion and Warhead. Airframe is extremely dependent on mission and guidance characteristic. Airframe types are basically, wing control, tail control and canard type. Each of these has advantages and disadvantages. Guidance selection is based on the propulsion, warhead and target characteristic. There are other factors to affect the system design. These are basically, the target, operational environment, cost and state of art [4]. Propulsion system can be clarified as; All-Boost, All-Sustain and Boos-Sustain. All-Boost type motor has rapid acceleration capability. As a result, short time of flight is inevitable. On the other hand, all-sustain type of motor has longer type of flight because of low missile acceleration capability. Boost-Sustain type of motor is combination of all-boost and all-sustain types. The missiles also can be classified as their airspeed. Modern air intercept missiles and surface to air missiles are in the supersonic section.

In simulation and analysis of air-to-air and surface-to-air missiles, skid-to-turn (STT) type of configuration is generally used in literature. The main reason is that cross coupling between roll, pitch and yaw is negligible in skid-to-turn type of missile. Table 2.1 shows the characteristics of the Sparrow, skid-to-turn type of missile [4]. In this thesis, skid-to-turn guidance mode is selected.

In order to evaluate the performance of guidance system, target and missile models must be in realistic form. Main subsections of guidance system can be seen in Figure 3.1.

Table 2.1 : Sparrow STT missile characteristics.

Missile System	Guidance Mode	Guidance System	Max. Acc.	Guidance Delay	Speed	Range
Sparrow III – AIM-7	Skid-to-Turn (STT)	Semi-active radar homing seeker	45g (32g per axis)	0.75s	Mach 4+	56km

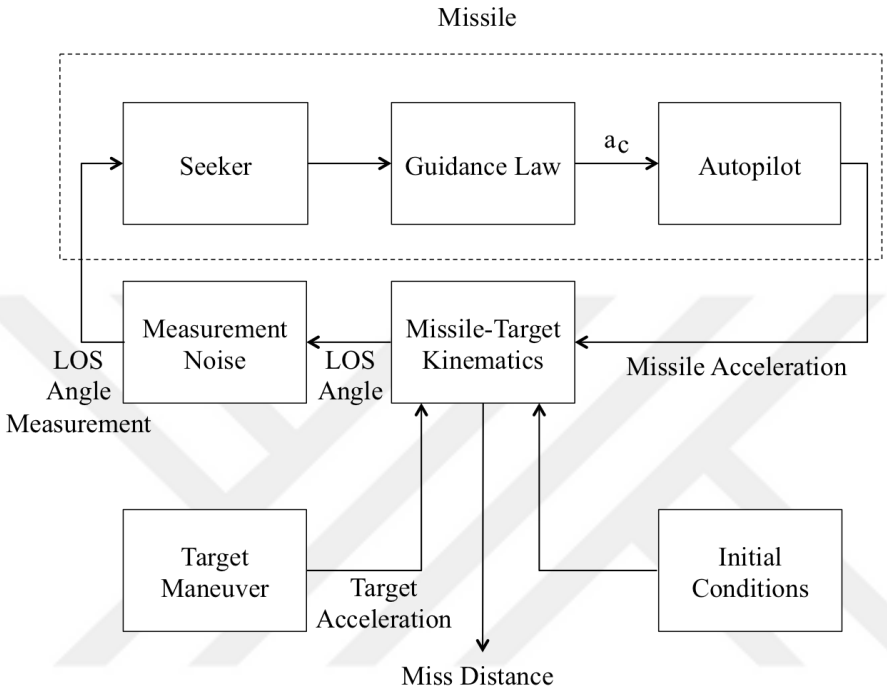

Figure 3.1: Guidance system.

As previously explained in introduction, sources of miss distance can be grouped as;

- Glint noise
- Range dependent noise
- Range independent noise
- Boresight-error
- Heading error
- Missile time constant
- Target maneuver

Problems listed above will be investigated in following sections.

3.2 Seeker Subsystem

In homing missiles, seeker has a function of tracking the target with the energy receiver such as in radar, infrared or optical form. Also it provides target's states,

time derivative of the line of sight angle and closing velocity information. There will be lag in the seeker tracking loop. Also, the missile radome causes unwanted effects. Refraction of the incoming radar wave will not give a true line of sight angle. As a result, the seeker will direct missile to apparent target as a false indication. Main causes of this error can be grouped as; radome shape, radome thickness, material selection and temperature. Boresight error in Figure 3.2 is expressed in following form;

$$\varepsilon = \lambda + \theta_r - \theta_m - \theta_h \tag{3.1}$$

Where the line of sight angle λ, refraction angle error θ_r, missile pitch angle θ_m and gimbal angle θ_h.

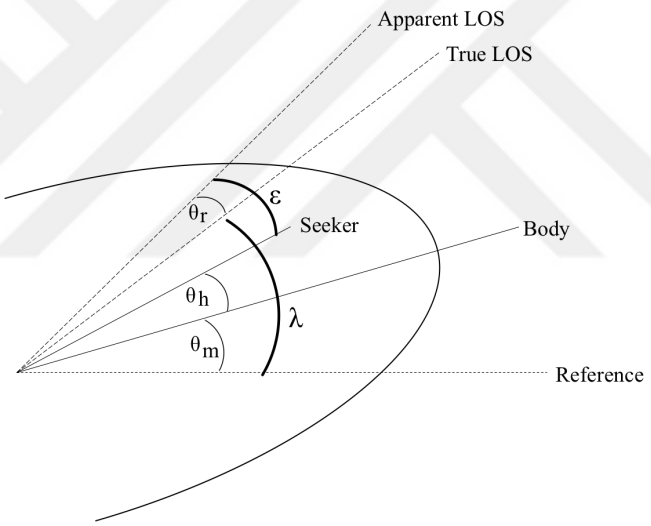

Figure 3.2 : Missile seeker, effect of radome error.

Zarchan, P. [6] stated that the radome refraction angle θ_r varies with the gimbal angle θ_h and θ_r is linearly proportional to the gimbal angle θ_h and radome slope R. According to Siouris [4], the radome effect becomes significant at high altitude and the boresight error can be neglect as compared to other errors. In analysis, the radome slope will be in the range from -0.1 to 0.1 as proposed in [4]. The Block diagram of the seeker model can be seen in Figure 3.3.

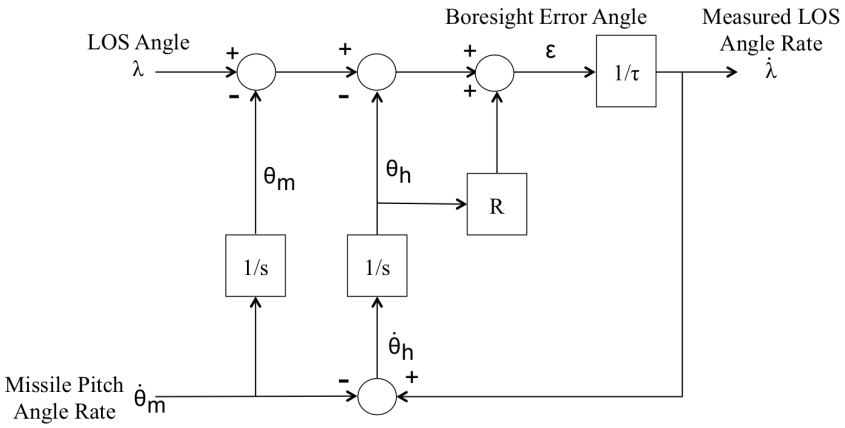

Figure 3.3 : Block diagram of the seeker subsystem.

3.3 The Missile Noise Input

Another important issue in missile guidance problem is that noise in measurements. The line of sight measurements is corrupted by noise during engagement. No matter how a measurement method is used, infrared or radar, noise affects the miss distance. The effect of noise is revealed by the hiding true value of the line of sight rate. There are different types of noise related with the guidance system as follows;

3.3.1 Glint noise

Glint Noise is caused by two or more sources arrised from random flactuations of propogated waves [4][6]. Because glint depends on the relative distance between target and missile, it can be said as a distance error. It varies as $1/R$. Glint will be modeled in this study as white gaussian noise random. Since standard deviation σ depends on target span, perpendicular to the LOS, glint will be modeled as [4];

$$\sigma = 0.25\, S/R \tag{3.2}$$

where S is target span and R is the relative distance between target and missile.

3.3.2 Thermal noise

Noise is present in all receivers. Even if semi-active or active type seeker is used, thermal noise has an impact on the terminal miss distance. Thermal noise produced in receiver, is dependent on the radar range equation. According to Zarchan, P. [6] range dependent noise or thermal noise can be grouped as active range dependent and semiactive range dependent noise and stated that semiactive range dependent

noise is directly proportional to the distance between missile and target. On the other hand, active range dependent noise is square of the relative distance. Important point is that noise goes down during approach. It will be modeled white Gaussian noise in simulation proportional to;

$$\sigma^2 \, V_c \, t_{go} \, / \, R \tag{3.3}$$

3.3.3 Range independent noise

Other noise sources can be said as range independent noise. Range independent noise is subsistent in the missile receiver [7]. The noise can be modeled zero mean white Gaussian noise and power spectral density.

$$\phi = 2\tau_f r_f \tag{3.4}$$

where r_f is the variance and τ_f is the range independent noise correlation time constant.

3.4 Target Maneuver Model

An evasive manuver is determined by target lateral acceleration. The second derivative of the target position models are referred to as acceleration model. The target motion models of the highest order available in literature include terms up to the target acceleration. In tracking a highly manuvering target, the target can be modeled as a jerk model [4,44]. Jerk model refers to the inclusion of the acceleration rate of the target motion. The third derivative of the target position.

Deterministic and stochastic maneuvers are widely used in missile guidance analysis. Constant acceleration step maneuver is an example of deterministic maneuver model. On the other hand, target can perform maximum positive or negative acceleration then switches its direction anytime during engagement. This type of maneuver is an example of the stochastic maneuver. Moving target may be in the form of an aircraft or a missile. Hence, we can assume that if target is an aircraft, target maneuver level is limited as +/- 9g. If target is a missile, maneuver level is around +/- 45g this time.

Optimal evasive maneuver is a manuver that produces the most miss at the terminal. According to the previous studies on evasive operations [6,45,46,47,48], Vertical-S,

Horizontal-S and Barrel Roll maneuvers are the best practical maneuvers that target can perform.

3.4.1 Vertical-S and horizontal-s maneuvers

Vertical-S and Horizontal-S maneuvers are in the form of S maneuver. According to the studies [49,50], there is not main difference between these maneuvers. Same maneuver model can be used for the two dimensional analysis. Target stays at maximum acceleration and periodically reverse its sign by 180 degrees rolling. It can be implemented into the model as [45];

$$\ddot{y}(t) = \frac{4n_{T\,max}}{\pi} \sum_{n=1,3,5\ldots}^{inf} \frac{1}{n} \sin \frac{n_{T\,max}\pi t}{L} \tag{3.5}$$

where $n_{t\,max}$ represents the target's maximum acceleration limit. $n_{t\,max}$ is limited by the pilot's physical attributes. L is the half period of maneuver.

3.4.2 Barrel roll maneuver

The Barrel Roll maneuver can be modeled in two dimensional space as sinusoidal wave;

$$\ddot{y}(t) = n_T \sin \frac{\pi t}{L} \tag{3.6}$$

where n_T represents the target's acceleration. L is the half period of maneuver.It can be clearly seen that maximum acceleration occurs some of the time. Imado, F. et al [47] studied high-barrel roll maneuver against a proportional navigation guided missile and according to the results, the high g-barrel roll maneuver produces a large miss distance more then a vertical-s maneuver. However, the miss distance caused by barrel roll maneuvers does not depend on maneuver initiation time. On the other hand, initiation time of the vertical-s maneuver effects the miss distance results. Typical 3g barrel roll maneuver and 3g vertical-s maneuver can be seen in Figure 3.4.

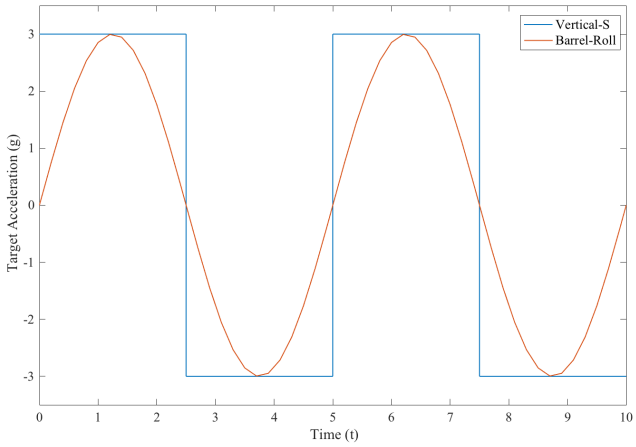

Figure 3.4 : Bank roll and vertical-s maneuver model.

3.4.3 Other basic maneuvers

Barrel Roll, Vertical-S, Horizontal-S and other relative maneuvers are complex maneuvers. Such repositioning and energy saving maneuvers require pilot skill. There are also other types of maneuvers; High and Low Yo-Yos, Scissors, Immelmann etc. [48]. In this thesis, objective is to study the effect of target evasive maneuvers on the miss distance. For this reason, Barrel Roll and S-maneuvers are selected as target evasive maneuvers. On the other hand, primary basic fighter maneuvers are usually the simple maneuvers such as climbs, dives and turns. These basic maneuvers are also implemented in simulations as constant target maneuvers.

3.5 Flight Control System Model

Flight Control System consists of three main parts; Autopilot, Actuator and Airframe. Autopilot takes acceleration commands from guidance computer and converts to a fin deflection command. Then angular deflection is achieved through actuators using fin deflection commands and control surfaces such as wings, tails. Lastly, airframe provides the lateral acceleration using angular deflections.

Flight Control System design is beyond scope of this thesis. But in order to how overall system is influenced by the flight control system, various type of transfer functions are implemented into simulations. The objective of the flight control system is that converting acceleration command n_c to lateral acceleration command n_L. In zero lag homing loops, the miss distance will always be zero. The missile system lags or in other words, time constants cause misses as previously mentioned.

The flight control system can be modeled as a single lag transfer function to investigate how flight control system time constant T influence guidance performance.

$$\frac{n_L}{n_c} = \frac{1}{1 + sT} \tag{3.7}$$

Another form of representation can be in fifth order binomial transfer function. Two time constants stand for the seeker and the noise filter. The other three represent the flight control system.

$$\frac{n_L}{n_c} = \frac{1}{(1 + sT)^3} \tag{3.8}$$

Zarchan,P. [6] stated that; if the total guidance system time constant is same, all fifth order guidance system configurations give almost same miss distance at the end. Hence, we can deduce that important point is the total time constant. As previously stated; in simulation and analysis of air-to-air and surface-to-air missiles, skid-to-turn (STT) type of configuration is generally used in literature. In this study, flight control system is also modeled in case of skid-to-turn missile. The pitch and the yaw dynamics are independent. Thus, we took in consideration only the pitch dynamics in homing loop analysis. Following transfer function which represents the aerodynamics including accelerometer is used in Kim et al [35] and Blakelock [37] studies and It will be implemented in homing loop without changing the parameters.

$$\frac{n_L}{n_c} = \frac{-108.3\ (s + 2)(s + 34.41)\ (s - 34.41)}{(s + 1.96)(s + 13.58)(s^2 + 37.48s + 4830.81)} \tag{3.9}$$

All three types of transfer function will be used alternately in all simulations.

4. GUIDANCE LAWS

In this chapter, a brief description of the guidance laws that has appeared in the literature will be given. Guidance laws may be in the form of proportional navigation guidance law which is the most important classical guidance law. Two dimensional engagement geometry given in Figure 2.3 is used to derive guidance laws. In order to derive guidance laws using linear quadratic optimization theory, linear engagement kinematics in Figure 4.1 will be used.

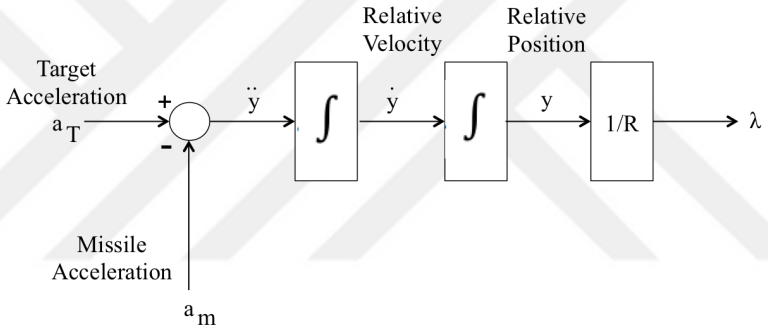

Figure 4.1: Linear engagement kinematics.

Integral of relative acceleration yields relative velocity, double integration yields relative position. After dividing relative position to range gives line of sight angle for near collision course. In the following subsections guidance laws will be obtained in different ways.

4.1 Proportional Navigation Guidance Law

Proportional Navigation Guidance Law is the most widely known guidance method and used for homing missiles. Since the implementation to homing missile can be dealed with easily. If the missile and target closes on each other and the line of sight angle between them does not change relative to the inertial space, they will intercept at the end. We can clearly say from that PN guidance law is directly proportional to

the rate of change of the missile heading and the rate of change of the line of sight angle.

From the above natural definiton of proportional guidance law;

$$\frac{d\alpha_m}{dt} = N\frac{d\lambda}{dt} \tag{4.1}$$

where N is navigation constant, α_m is the missile heading and λ is the line of sight angle in Figure 4.2. On-going derivations will follow the lines of [4]. The time rate of change or R;

$$\frac{dR}{dt} = V_T\cos(\alpha_t - \lambda) - V_m\cos(\alpha_m - \lambda) \tag{4.2}$$

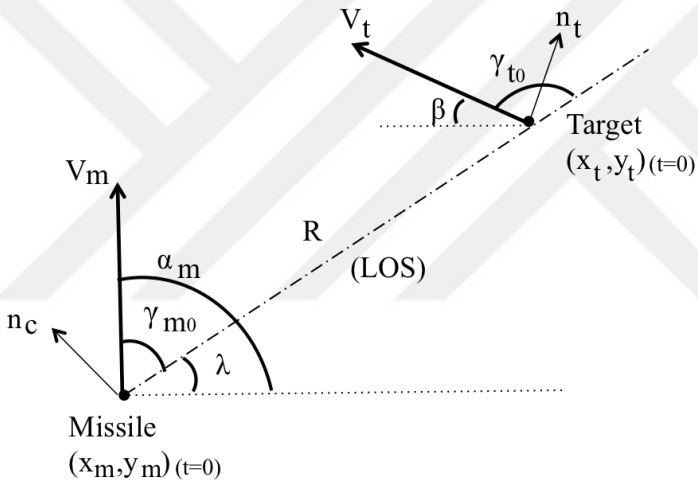

Figure 4.2 : Engagement geometry.

The rate of rotation of the line of sight angle, using small angle approximations;

$$R\frac{d\lambda}{dt} = V_T\sin(\alpha_t - \lambda) - V_m\sin(\alpha_m - \lambda) \tag{4.3}$$

Taking derivative of above equations yields;

$$\frac{dR}{dt}\frac{d\lambda}{dt} + R\frac{d^2\lambda}{dt^2} = (\dot{\alpha_T} - \dot{\lambda})V_T\cos(\alpha_t - \lambda) - (\dot{\alpha_m} - \dot{\lambda})V_m\cos(\alpha_m - \lambda) \tag{4.4}$$

Substituting equation (4.1) and (4.2) into (4.4),

$$\frac{d^2\lambda}{dt^2} + \left(\frac{d\lambda}{dt}\frac{1}{R}\right)\left[2\frac{d^2R}{dt^2} + NV_m\cos(\alpha_m - \lambda)\right] = \left(\frac{1}{R}\right)\dot{\alpha_T}V_T\cos(\alpha_T - \lambda) \tag{4.5}$$

For a straight-line course, time derivative of target's flight path becomes zero as $\dot{\alpha_T} = 0$.

$$\frac{d^2\lambda}{dt^2} + \left(\frac{d\lambda}{dt}\frac{1}{R}\right)\left[2\frac{d^2R}{dt^2} + NV_m\cos(\alpha_m - \lambda)\right] = 0 \tag{4.6}$$

Hence, a homogenous differential equation for $\dot{\lambda}$ is in the form of equation (4.6) In order for $\dot{\lambda}$ to approximate the zero line;

$$2\left(\frac{dR}{dt}\right) + [NV_m\cos(\alpha_m - \lambda)] > 0 \tag{4.7}$$

From that Navigation ratio N will be;

$$N > -2\left(\frac{dR}{dt}\right)/V_m\cos(\alpha_m - \lambda) \tag{4.8}$$

Substituting equation (4.2) into (4.8) will give us;

$$N > 2[1 - [\frac{\cos(\alpha_t - \lambda)}{\frac{V_m}{V_T}\cos(\alpha_m - \lambda)}] \tag{4.9}$$

Equation 4.9 can be written in the form as; [4]

$$N' = -N[\frac{(V_m\cos(\alpha_m - \lambda)}{\dot{R}}] \tag{4.10}$$

where N' is called the effective navigation ratio. The missile normal acceleration can be defined as;

$$a_m = V_m(\frac{d\alpha_m}{dt}) \tag{4.11}$$

Substituting (4.1) into (4.11);

$$a_m = N\,V_m\frac{d\lambda}{dt} \tag{4.12}$$

This is the Pure Proportional Navigation guidance law (PPN). Here, lateral acceleration guidance command is perpendicular to the missile velocity. If we ignore the angle of attack of the missile, direction of the lift force of the missile becomes the

direction of the lateral acceleration. Problem here is that angle of attack is different from zero. Pure Proportional Navigation guidance law becomes unapplicable totally. Another important issue arrises when missile velocity is not directly available. But closing velocity can easily obtained by using doppler radar. We can write equation (4.12) into such form that including closing velocity. True Proportional Navigation guidance law (TPN) is the following form after substituting (4.10) into (4.12) and by the definition of $\dot{R} = -V_c$;

$$a_m = [\frac{N\,V_c}{\cos(\alpha_m - \lambda)}]\frac{d\lambda}{dt} \tag{4.13}$$

Problem in True Proportional Navigation guidance law is that, lateral acceleration command is perpendicular to the line of sight and implementation of lateral acceleration is an issue. $\cos(\alpha_m - \lambda)$ in (86) is the missile gimbal angle, can be assumed unity for head-on or tail chase scenarios. Then it can be written in a more convenient form ;

$$a_m = N'\,V_c\,\dot{\lambda} \tag{4.14}$$

Another form of True Proportional Navigation (TPN) is the Generalized True Proportional Navigation guidance law (GTPN). GTPN stated that direction of the lateral acceleration can be deviated by some angle to be fully applicable in real applications. The various types of the Proportional Navigation guidance law can be seen in Figure 4.3, 4.4 and 4.5.

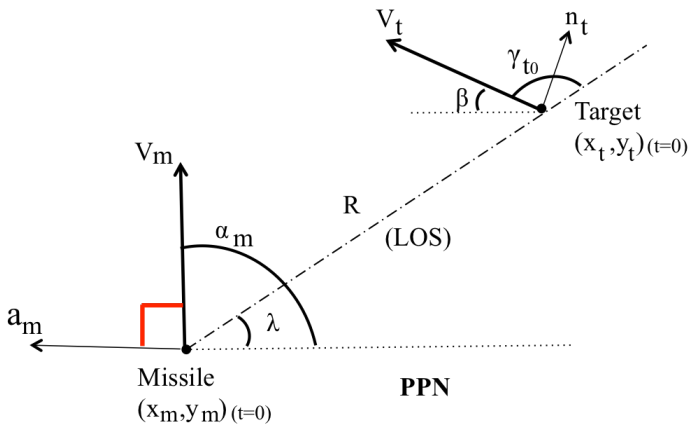

Figure 4.3 : Pure proportional navigation.

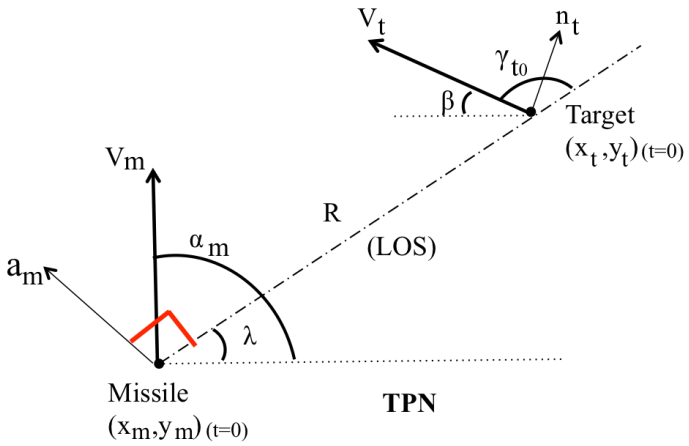

Figure 4.4 : True proportional navigation.

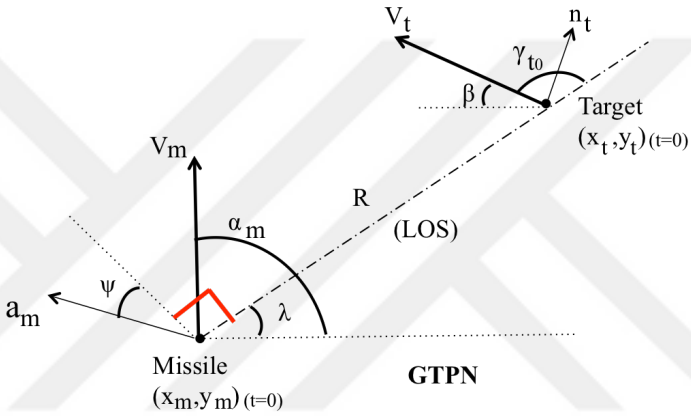

Figure 4.5 : Generalized proportional navigation.

Proportional Navigation guidance law can also be obtained by using linear quadratic optimization techniques. General solution of the nonmaneuvering target case will be discussed later on. Linear quadratic optimization problem for ideal missile and target is stated as [21,24,43];

$$\min_{u(t)} J = \frac{b}{2}x_1^2(t_f) + \frac{c}{2}x_2^2(t_f) + \frac{1}{2}\int_0^{t_f} u^2(t_f)dt \tag{4.15}$$

By using (2.55) and (2.61) optimality conditions for this case becomes;

$$\dot{\lambda}_1 = 0, \qquad \dot{\lambda}_2 = -\lambda_1, \qquad u = -\lambda_2 \tag{4.16}$$

Boundry conditions are;

$$\lambda_1(t_f) = bx_1(t_f), \qquad \lambda_2(t_f) = cx_2(t_f) \tag{4.17}$$

After rearranging (4.17);

$$\lambda_1 = bx_1(t_f), \qquad \lambda_2 = bx_1(t_f)(t_f - t) + cx_2(t_f) \tag{4.18}$$

Substituting λ_2 into u and ideal state space form $\dot{x} = Ax + Bu$;

$$\dot{x}_1 = x_2, \qquad \dot{x}_2 = -bx_1(t_f)(t_f - t) + cx_2(t_f) \tag{4.19}$$

Integrating (4.19) from t_0 to t;

$$\begin{aligned} x_1(t) = {} & \left[\frac{1}{2}b\left(\frac{t^3}{3} - \frac{t_o^3}{3}\right) - \frac{1}{2}bt_0^2(t - t_0)\right]x_1(t_f) - \frac{1}{2}b(t - t_0)^2 t_f x_1(t_f) \\ & - \frac{1}{2}c(t - t_0)^2 x_2(t_f) + x_1(t_0) + x_2(t_0)(t - t_0) \end{aligned} \tag{4.20}$$

$$\begin{aligned} x_2(t) = {} & \frac{1}{2}b(t^2 - t_0^2)x_1(t_f) - b\, t_f(t - t_0)x_1(t_f) - c(t - t_o)x_2(t_f) \\ & + x_2(t_0) \end{aligned}$$

At $t = t_f$ (4.20) we can find an expression for $u(t)$,

$$\begin{aligned} u(t) = -(& \frac{b(t_f - t_0)\left(\frac{1}{2}(t_f - t_0)c + 1\right)}{\frac{(t_f - t_0)^4 cb}{12} + (t_f - t_0)c + \frac{(t_f - t_0)^3 b}{3} + 1} x_1(t) \\ & + \frac{\frac{1}{3}(t_f - t_0)^3 cb + (t_f - t_0)^2 b + c}{\frac{(t_f - t_0)^4 cb}{12} + (t_f - t_0)c + \frac{(t_f - t_0)^3 b}{3} + 1} x_2(t)) \end{aligned} \tag{4.21}$$

$(t_f - t_0)$ is the time to go and equation (4.21) is the general solution for non-manuvering target. This problem can also be solved by using matrix ricatti equation in (2.67). The optimal solution will be in the form of (2.55). Symbolic solver may be needed to solve riccati equations.

Special case comprises in equation (94) when $c = 0$ and taking limit $b \to \infty$;

$$u_{PN}(t) = -(\frac{3}{(t_f - t_0)^2}x_1(t) + \frac{3}{(t_f - t_0)}x_2(t)) = -\frac{3}{t_{go}^2}[x_1(t) + x_2(t)t_{go}] \tag{4.22}$$

Using the $x_1 = y$ and $x_2 = \dot{y}$ we can write equation (4.22) as;

$$u_{PN} = \frac{3}{t_{go}^2}[y + \dot{y}\, t_{go}] \tag{4.23}$$

Line of sight rate $\dot{\lambda} = \frac{y+\dot{y}t_{go}}{V_c(t_{go})^2}$ is previously given in (2.41) and using this, equation (4.23) will be in the form of proportional navigation,

$$u_{PN} = -N'V_C\dot{\lambda}, \qquad N' = 3 \tag{4.24}$$

Equation (4.24) is the well known proportional navigation guidance law with effective navigation ratio = 3. Hence, we can clearly say that optimal proportional navigation gain for non-maneuvering target is $N' = 3$. $(y + \dot{y}\, t_{go})$ is known as Zero Effort Miss (ZEM) of PN guidance law. Zero effort miss is the distance at the end that if the target continues on its path and the missile did not manuver during engagement. Guidance performance is directly related to the ZEM. Equation derived in (4.24) is in the form of True Proportional Navigation. In this study, PN guidance law is used in the form of TPN.

4.2 Optimal Rendezvous Guidance Law

Another special form of non-manuvering target general solution is the optimal rendezvous guidance law (OR) and it can be obtained from equation (4.21) by letting $b \to \infty$ and $c \to \infty$;

$$u_{OR}(t) = -\frac{6}{\left(t_f - t_0\right)^2}x_1(t) - \frac{4}{(t_f - t_0)}x_2(t) \tag{4.25}$$

Using $x_1 = y$, $x_2 = \dot{y}$, $\dot{\lambda} = \frac{y+\dot{y}t_{go}}{V_c(t_{go})^2}$, and $\lambda = \frac{y}{V_c(t_{go})}$ it can also be written as;

$$u_{OR} = -V_c(4\dot{\lambda} + \frac{2\lambda}{t_{go}}) \tag{4.26}$$

Equation (4.26) is the Optimal Rendezvous guidance law (OR) and it uses the same structure of the proportional navigation with effective navigation ratio 4. It requires an extra information as line of sight angle. Also this guidance law is known as Apollo guidance law [6]. The Apollo spacecraft used the former guidance law in

1969. Basically, the relative velocity and the relative position are desired to be zero at intercept.

4.3 Augmented Proportional Navigation Guidance Law

Proportional Navigation guidance law with effective navigation ratio 3 is the optimal solution for non-maneuvering target as stated before. From here, the issue of guidance law for maneuvering targets arises. It does not mean that proportional navigation guidance law can not hit target, but target's constant maneuver can be implemented into the guidance law to achieve better results. Augmented Proportional Navigation guidance law (APN) deals with the constant maneuvering target. We enhance the model to include target acceleration w. As previously shown in equation (2.44), we can model the target and the missile as an ideal case and zero lag system;

$$\dot{x} = Ax + Bu + Dw$$
$$A = \begin{bmatrix} 0 & 1 \\ 0 & 0 \end{bmatrix}, \qquad B = \begin{bmatrix} 0 \\ 1 \end{bmatrix}, \qquad D = \begin{bmatrix} 0 \\ 1 \end{bmatrix} \tag{4.27}$$

The cost function is;

$$\min_{u(t)} J = \frac{b}{2} x_1^2(t_f) + \frac{1}{2}\int_0^{t_f} u^2(t_f)dt \tag{4.28}$$

The cost function here (4.28) is different from the cost function in proportional navigation by equating $c = 0$ (88). It means that there is no velocity constraints at the end. By using (2.55) and (2.63), optimality conditions are same as in proportional navigation;

$$\dot{\lambda}_1 = 0, \qquad \dot{\lambda}_2 = -\lambda_1, \qquad u = -\lambda_2 \tag{4.29}$$

Boundry conditions are;

$$\lambda_1(t_f) = bx_1(t_f), \qquad \lambda_2(t_f) = 0 \tag{4.30}$$

After rearranging (4.30);

$$\lambda_1 = bx_1(t_f), \qquad \lambda_2 = bx_1(t_f)(t_f - t) \tag{4.31}$$

Substituting λ_2 into u and state space form (4.27);

$$\dot{x}_1 = x_2, \qquad \dot{x}_2 = -bx_1(t_f)(t_f - t) + w_0 \tag{4.32}$$

It can be clearly seen in equation (4.29) that optimal missile control command u is only related with the x_1. Therefore we only need to get x_1. Integrating (4.32) from t_0 to t and with inital conditions;

$$\begin{aligned} x_1(t) = &-\frac{b}{6}x_1(t_f)(t_f - t)^3 + \frac{w_0}{2}(t_f - t)^2 + x_2(t_0)(t - t_0) \\ &- \left[\frac{b}{2}x_1(t_f)(t_f - t_0)^2 - w_0(t_f - t_0)\right](t_f - t_0) + x_1(t_0) \\ &+ \frac{b}{6}x_1(t_f)(t_f - t_0)^3 - \frac{w_0}{2}(t_f - t_0)^2 \end{aligned} \tag{4.33}$$

$$x_2(t) = \frac{b}{2}x_1(t_f)(t^2 - t_0^2) - b\, t_f x_1(t_f)(t - t_0) + w_0(t - t_0) + x_2(t_0)$$

At $t = t_f,\ x_1(t)$ in equation (4.33) becomes;

$$x_1(t_f) = x_2(t_0)(t_f - t_0) - \frac{b}{3}x_1(t_f)(t_f - t_0)^3 + \frac{w_0}{2}(t_f - t_0)^2 + x_1(t_0) \tag{4.34}$$

Substitute equation (4.34) into λ_2 (4.31) then through $u = -\lambda_2$ in (4.29), we can find an expression for $u(t)$;

$$u(t) = -\frac{1}{\frac{1}{b} + \frac{1}{3}(t_f - t)^3}\left[x_1(t)(t_f - t) + x_2(t)(t_f - t)^2 + \frac{w_0}{2}(t_f - t)^3\right] \tag{4.35}$$

Zero miss can be obtained by letting $b \to \infty$,

$$u(t) = -\frac{3}{(t_{go})^2}\left(x_1(t) + x_2(t)t_{go} + \frac{w_0}{2}t_{go}^2\right) \tag{4.36}$$

Equation (4.36) is the well known Augmented Proportional Navigation guidance law (APN). Also it can be expressed in more convenient form as;

$$u_{APN} = -N'V_c\dot{\lambda} - \frac{3}{2}w_0, \qquad N' = 3 \tag{4.37}$$

Zero effort miss of APN guidance law is now represented as $(y + \dot{y}\, t_{go} + \frac{1}{2}a_T t_{go}^2)$.

4.4 Extended Proportional Navigation Guidance Law

Target acceleration can be increased linearly during engagement. It means that target accelerates in a particular direction with constant jerk. Here, the states are augmented by adding x_3 and x_4 which represent the target acceleration and the target jerk respectively.

$$\dot{x} = Ax + Bu$$

$$A = \begin{bmatrix} 0 & 1 & 0 & 0 \\ 0 & 0 & 1 & 0 \\ 0 & 0 & 0 & 1 \\ 0 & 0 & 0 & 0 \end{bmatrix}, \qquad B = \begin{bmatrix} 0 \\ -1 \\ 0 \\ 0 \end{bmatrix} \tag{4.38}$$

The cost function is;

$$\min_{u(t)} J = \frac{b}{2} x_1^2(t_f) + \frac{1}{2} \int_0^{t_f} u^2(t_f) dt \tag{4.39}$$

By using (2.55) and (2.63), optimality conditions;

$$\dot{\lambda}_1 = 0, \qquad \dot{\lambda}_2 = -\lambda_1, \qquad \dot{\lambda}_3 = -\lambda_2, \qquad \dot{\lambda}_4 = -\lambda_3, \quad u = -\lambda_2 \tag{4.40}$$

Boundry conditions are;

$$\lambda_1(t_f) = b x_1(t_f), \qquad \lambda_2(t_f) = 0, \qquad \lambda_3(t_f) = 0, \qquad \lambda_4(t_f) = 0 \tag{4.41}$$

After rearranging (4.41);

$$\lambda_1 = b x_1(t_f), \qquad \lambda_2 = b x_1(t_f)(t_f - t) \tag{4.42}$$

Substituting λ_2 into u and state space form (4.38);

$$\dot{x}_1 = x_2, \qquad \dot{x}_2 = x_3 - b x_1(t_f)(t_f - t), \qquad \dot{x}_3 = x_4, \qquad \dot{x}_4 = 0 \tag{4.43}$$

It can also be clearly seen in equations (4.42) and (4.40) that optimal missile control command u is only related with the x_1. Therefore we only need to get x_1. Again, integrating (4.43) from t_0 to t and with inital conditions and evaluating x_1 at $t = t_f$ as in previous guidance laws;

$$x_1(t_f) = x_2(t_0)(t_f - t_0) - \frac{b}{3}x_1(t_f)(t_f - t_0)^3 + \frac{1}{2}x_3(t_0)(t_f - t_0)^2 + \frac{1}{6}x_4(t_0)(t_f - t_0)^3 + x_1(t_0) \tag{4.44}$$

Substitute equation (4.44) into λ_2 (4.42) then through $u = -\lambda_2$ in (4.40), we can find an expression for $u(t)$ and by letting $b \to \infty$,

$$u_{EPN}(t) = -\frac{3}{(t_{go})^2}\left(x_1(t) + x_2(t)t_{go} + \frac{1}{2}x_3(t)t_{go}^2 + \frac{1}{6}x_4(t)t_{go}^3\right) \tag{4.45}$$

Equation (4.45) is the Extended Proportional Navigation guidance law (EPN). Also it can be expressed in more convenient form as;

$$u_{EPN} = -N'V_c\dot{\lambda} + \frac{3}{2}w_0 + \frac{1}{2}\,j_T\,t_{go}, \qquad N' = 3 \tag{4.46}$$

Where w_0 is the constant target acceleration and j_T is the constant target jerk. Zero effort miss of EPN guidance law is now represented as $(y + \dot{y}\,t_{go} + \frac{1}{2}a_T t_{go}^2 + \frac{1}{6}j_T t_{go}^3)$. EPN guidance law requires more information than APN such as target jerk measurement. It can be used against constant jerk maneuvering target.

4.5 Augmented Optimal Rendezvous Guidance Law

As stated previously optimal rendezvous guidance law is a special form of non-maneuvering target's general solution when $b \to \infty$ and $c \to \infty$. Also we can derive to find optimal rendezvous solution of maneuvering target. This brings us to investigate Augmented Optimal Rendezvous guidtırıcance law (AOR). In Augmented Proportional Navigation guidance law (APN), it was assumed that $b \to \infty$ and $c = 0$. Here, we will study on the same model used in APN but by letting $b \to \infty$ and $c \to \infty$;

$$\dot{x} = Ax + Bu + Dw$$
$$A = \begin{bmatrix} 0 & 1 \\ 0 & 0 \end{bmatrix}, \qquad B = \begin{bmatrix} 0 \\ 1 \end{bmatrix}, \qquad D = \begin{bmatrix} 0 \\ 1 \end{bmatrix} \tag{4.47}$$

The cost function is;

$$\min_{u(t)} J = \frac{b}{2}x_1^2(t_f) + \frac{c}{2}x_2^2(t_f) + \frac{1}{2}\int_0^{t_f} u^2(t_f)dt \tag{4.48}$$

The cost function (4.48), following adjoint equations are identical to the nonmaneuvering target case (4.15). By using (2.55) and (2.67),

$$\dot{\lambda}_1 = 0, \qquad \dot{\lambda}_2 = -\lambda_1, \qquad u = -\lambda_2 \tag{4.49}$$

Boundry conditions are;

$$\lambda_1(t_f) = bx_1(t_f), \qquad \lambda_2(t_f) = cx_2(t_f) \tag{4.50}$$

After rearranging (4.50);

$$\lambda_1 = bx_1(t_f), \qquad \lambda_2 = bx_1(t_f)(t_f - t) + cx_2(t_f) \tag{4.51}$$

Substituting λ_2 into u and state space form (4.47);

$$\dot{x}_1 = x_2, \qquad \dot{x}_2 = -bx_1(t_f)(t_f - t) + cx_2(t_f) + w_0 \tag{4.52}$$

Integrating (4.52) from t_0 to t and with inital conditions;

$$\begin{aligned} x_1(t) = bx_1(t_f)\Bigg[-t_f\frac{(t^2 - t_0^2)}{2} + t_f t_o(t - t_0) + \frac{(t^3 - t_0^3)}{6} \\ - \frac{t_0^2}{2}(t - t_0)\Bigg] + cx_2(t_f)\left[\frac{(t^2 - t_0^2)}{2} - t_0(t - t_0)\right] \\ + w_0\left[\frac{(t^2 - t_0^2)}{2} - t_0(t - t_0)\right] + x_2(t_0)(t - t_0) + x_1(t_0) \end{aligned} \tag{4.53}$$

$$\begin{aligned} x_2(t) = \frac{b}{2}x_1(t_f)(t^2 - t_0^2) - bx_1(t_f)(t - t_0) + cx_2(t_f)(t - t_0) \\ + w_0(t - t_0) + x_2(t_0) \end{aligned}$$

If we repeat the method as before. Substituting equation (4.53) into λ_2 (4.52) after evaluating x_1 and x_2 at $t = t_f$, then through $u = -\lambda_2$ in (4.50), we can find an expression for $u(t)$ and by letting $b \to \infty$ and $c \to \infty$ [21],

$$u_{AOR}(t) = -\frac{6}{\left(t_f - t_0\right)^2} x_1(t) - \frac{4}{\left(t_f - t_0\right)} x_2(t) - w_0 \tag{4.54}$$

It can be written in more convenient form as;

$$u_{OAR} = -V_c \left(4\dot{\lambda} + \frac{2\lambda}{t_{go}}\right) - w_0 \tag{4.55}$$

In some applications we may want not only to hit a target but also at certain angle to improve effectiveness. Relative velocity can be expressed in terms of hitting angle by using definition of line of sight angle;

$$\dot{y} = \frac{\dot{\lambda} V_c t_{go}^2 - y}{t_{go}} = \frac{\dot{\lambda} V_c t_{go}^2 - \lambda V_c t_{go}}{t_{go}} = \dot{\lambda} V_c t_{go} - \lambda V_c \tag{4.56}$$

At intercept $\dot{y}(t_f)$, t_{go} goes to zero and preceding equation becomes;

$$\dot{y}(t_f) = \lambda(t_f) V_c \tag{4.57}$$

We can shape the λ in the equation (128) at intercept with desired hitting angle as;

$$u_{TSG} = -V_c \left(4\dot{\lambda} + \frac{2(\lambda - \lambda_f)}{t_{go}}\right) - w_0 \tag{4.58}$$

Equation (4.58) is also known as Trajectory Shaping guidance law (TSG) [6]. AOR and OR guidance laws hit the target at zero angle relative to reference frame. TSGL is not only hit the target but also control the hitting angle.

4.6 Optimal Guidance Law

Augmented Proportional Navigation guidance law (APN) reduces the missile acceleration requirements by taking advantage of target acceleration measurements. As previously stated that one of the sources of miss distance is missile guidance system lags. Up to now, all system models have been represented by a zero lag system. The missile response to a commanded acceleration can be modeled as a first order lag transfer function;

$$\frac{a_c}{a_L} = \frac{1}{Ts+1} \tag{4.59}$$

Where the a_c is the commanded acceleration, a_L the missile lateral acceleration and T, missile time constant. In state space form;

$$\dot{x} = Ax + Bu + Dw$$

$$A = \begin{bmatrix} 0 & 1 & 0 \\ 0 & 0 & 1 \\ 0 & 0 & -\frac{1}{T} \end{bmatrix}, \qquad B = \begin{bmatrix} 0 \\ 0 \\ \frac{1}{T} \end{bmatrix}, \qquad D = \begin{bmatrix} 0 \\ 1 \\ 0 \end{bmatrix} \tag{4.60}$$

Here x_3 represents the commanded acceleration a_c. The cost function is;

$$\min_{u(t)} J = \frac{b}{2} x_1^2(t_f) + \frac{1}{2}\int_0^{t_f} u^2(t_f)dt \tag{4.61}$$

Necessary conditions are identical to the ideal maneuvering target case (101). By using (2.55) and (2.67),

$$\dot{\lambda}_1 = 0, \qquad \dot{\lambda}_2 = -\lambda_1, \qquad \dot{\lambda}_3 = -\lambda_2 + \frac{\lambda_3}{T}, \qquad u = -\frac{1}{T}\lambda_3 \tag{4.62}$$

Boundry conditions are;

$$\lambda_1(t_f) = bx_1(t_f), \qquad \lambda_2(t_f) = 0, \qquad \lambda_3(t_f) = 0 \tag{4.63}$$

Integrating (4.62);

$$\lambda_1 = bx_1(t_f) \quad \lambda_2 = bx_1(t_f)(t_f - t) \quad \lambda_3 = bx_1(t_f)[(t_f - t)T - T^2 + T^2 e^{\frac{t-t_f}{T}}] \tag{4.64}$$

Substituting λ_2 into u and state space form (4.60);

$$\dot{x}_1 = x_2, \qquad \dot{x}_2 = x_3 + w_0,$$
$$\dot{x}_3 = -\frac{1}{T}x_3 - \frac{1}{T}bx_1(t_f)[(t_f - t) - T + Te^{\frac{t-t_f}{T}}] \tag{4.65}$$

The calculations for the gains are too complicated to be derived here. Ben-Asher et al. (1998) is derived all necessary equations. [21] Procedure is same here and If we repeat the methods as before in PN, OR, APN, EPN, AOR, integrating (4.65) from t_0 to t and with inital conditions. Then evaluating x_1 at $t = t_f$ and substituting results into λ_3 (137). Hence making use of $u = -\frac{1}{T}\lambda_3$ in (135), we can find an expression for $u(t)$ and by letting $b \to \infty$, $h = \frac{t_{go}}{T}$,

$$u_{OG/MEL} = N'V_c\dot{\lambda} + \frac{N'}{2}w_0 - n_L\frac{N'}{t_{go}^2}T^2(e^{-h} + h - 1),$$
$$N' = \frac{6h^2(e^{-h} - 1 + h)}{2h^3 + 3 + 6h - 6h^2 - 12he^{-h} - 3e^{-2h}} \tag{4.66}$$

Equation (4.66) is the well-known Optimal Guidance Law (OGL). In literature, former equation is also known as Minimum Effort Law (MEL) [19,21,23,24]. OGL attempts to make first order system lag to be appear zero lag system. [6] If the guidance system lag disappears, our guidance system turns into APN model. It should be hit the target perfectly. Problem here is that; time constant, T, is a function of flight conditions and depends on missile aerodynamic characteristic [43]. It is hard to get the true value of T. Another issue, OGL/MEL is required the target acceleration information. If target acceleration measurements are not available, optimal guidance law can be modified as zero target acceleration. Latter guidance law is referred as MELN, minimum effort law without target acceleration measurements [21].

$$u_{MELN} = N'V_c\dot{\lambda} - n_L\frac{N'}{t_{go}^2}T^2(e^{-h} + h - 1),$$
$$N' = \frac{6h^2(e^{-h} - 1 + h)}{2h^3 + 3 + 6h - 6h^2 - 12he^{-h} - 3e^{-2h}} \tag{4.67}$$

MELN works in the same way as optimal guidance law. Guidance system now turns into PN guidance model when system lags disappear.

4.7 Biased Proportional Navigation Guidance Law

In all guidance law so far, time to go information was needed. Time to go may be available in radar homing missiles but not in IR homing missiles. It can be usefull to derive a guidance law that does not require time to go information for non-maneuvering target. We can equate the PPN (4.12) to TPN (4.14);

$$u_c = NV_m\dot{\lambda} = N'V_c\dot{\lambda} \Longrightarrow N = N'\frac{V_c}{V_M} \tag{4.68}$$

We can clearly see that navigation ratio (N) is equal to effective navigation ratio (N') for stationary target case. In equation (4.1), we defined the definition of proportional navigation guidance law. Here, we can add an additional bias term to flight path angle rate $(\dot{\alpha}_m)$ in equation (4.1) as;

$$\dot{\alpha}_m = N\dot{\lambda} + bias \tag{4.69}$$

If we integrate former equation from t_0 to t_f and at the intercept $\alpha_m(t_f) = \lambda(t_f)$;

$$\alpha_m(t_f) - \alpha_m(t_0) = N[\lambda(t_f) - \lambda(t_0)] + bias\ \Delta t \tag{4.70}$$

$$bias = \frac{-\alpha_m(t_f)(N-1) + N\lambda(t_0) - \alpha_m(t_0)}{\Delta t} \tag{4.71}$$

Thus, Biased Proportional Navigation guidance law (BPN) can be expressed by the help of perpendicularity between acceleration command and velocity vector;

$$u_{BPN} = V_m\dot{\alpha}_m = V_m[N\dot{\lambda} + bias] \tag{4.72}$$

$$u_{BPN} = NV_m\dot{\lambda} + V_m\frac{-\alpha_m(t_f)(N-1) + N\lambda(t_0) - \alpha_m(t_0)}{\Delta t} \tag{4.73}$$

Where $\alpha_m(t_f)$ represents the final flight path angle (hitting angle), $\lambda(t_0)$ initial line of sight angle, Δt bias duration. Here we can adjust the bias duration. Equation (4.73) is in the trajectory shaping and pure proportional navigation guidance forms. Simply, desired hitting angle can be controlled. Here, the missile does not require any time to go or closing velocity informations.

4.8 Weave Guidance Law

If the target is weaving, a special guidance law can be derived according to sinusoidal maneuver. Zarchan, P. [6] stated the engagement model and found an optimal guidance law against weaving target maneuver. State space form is represented as;

$$\dot{x} = Ax + Bu$$

$$A = \begin{bmatrix} 0 & 1 & 0 & 0 \\ 0 & 0 & 1 & 0 \\ 0 & 0 & 0 & 1 \\ 0 & 0 & -w^2 & 0 \end{bmatrix}, \qquad B = \begin{bmatrix} 0 \\ -1 \\ 0 \\ 0 \end{bmatrix} \tag{4.74}$$

The cost function is;

$$\min_{u(t)} J = \frac{b}{2} x_1^2(t_f) + \frac{1}{2} \int_0^{t_f} u^2(t_f) dt \tag{4.75}$$

Solution technique is similar to previous ones. Here, x_3 and x_4 represents the target acceleration and target jerk respectively. w is the target weaving frequency. Weave maneuver is the planar version of bank roll maneuver. As previously stated that maneuver can be expressed as $n_T \sin wt$. Optimal Weave guidance law can be stated as;

$$u_{WG}(t) = \frac{3}{(t_{go})^2} \left(x_1(t) + x_2(t) t_{go} + \left(\frac{1 - coswt_{go}}{w^2} \right) x_3(t) + \left(\frac{wt_{go} - sinwt_{go}}{w^3} \right) x_4(t) \right) \tag{4.76}$$

$$u_{WG}(t) = 3V_c \dot{\lambda} + \frac{3}{t_{go}^2} \left[\left(\frac{1 - coswt_{go}}{w^2} \right) n_t + \left(\frac{wt_{go} - sinwt_{go}}{w^3} \right) j_T \right] \tag{4.77}$$

Weave Guidance law (WG) can be seen in equation (4.77). When target weaving frequency goes to zero, former guidance law turns into extended proportional navigation guidance law (EPN) form in equation (4.46). Also the missile time lag can be compansated via time varying effective navigation ratio as used before in optimal guidance law (OGL). This type of approach brings us the Compansated Weave guidance law (WGC) and can be expresed as;

$$u_{WGC}(t) = N'V_c\dot{\lambda} + \frac{N'}{t_{go}^2}\left[\left(\frac{1-coswt_{go}}{w^2}\right)n_t + \left(\frac{wt_{go}-sinwt_{go}}{w^3}\right)j_T\right],$$
$$N' = \frac{6h^2(e^{-h}-1+h)}{2h^3+3+6h-6h^2-12he^{-h}-3e^{-2h}} \tag{4.78}$$

4.9 Differential Game Guidance Law

This guidance law uses the structure of proportional navigation. More precisely Differential Game guidance (DG) uses the proportional navigation form of zero effort miss concept. Missile performs its own acceleration limits either positive of negative. Thus, there is no optimal control on acceleration and it is bang bang in nature [6]. Following guidance law can be expressed as;

$$u_{DG} = n_{max}sign(ZEM_{DG}),$$
$$ZEM_{DG} = y + \dot{y}t_{go} - n_L T^2(e^{-h}+h-1) \tag{4.79}$$

Where $h = t_{go}\,/\,T$ and n_{max} represents the missile acceleration limit. Here, zero effort miss does not depend on the target maneuver level or type. Only compansation term is added to eliminate the effect of missile time lag.

4.10 Particle Swarm Optimization Guidance Law

Classical and modern guidance laws have been investigated up to now. In this subsection, guidance problem is investigated in optimization point of view. Solving optimization problem with heuristic methods is quite popular in recent years. Particle Swarm Optimization (PSO) is a heuristic method based on the idea of social behaviour in biological populations. In literature, PSO guidance algorithm is applied on relative distance, R, as a cost function [30]. In such a case, miss distance can diverge if the missile does not approach from front or rear.

In proportional navigation guidance, we were tried to minimize line of sight rate $\dot{\lambda}$. Now, we can define cost function of the optimization problem as in ZEM_{PN} form. Algorithm tries to find optimal control solution of guidance problem in each iteration. During engagement, ZEM_{PN} is minimized by PSO algorithm to be more

precise. If target acceleration or target jerk information is available, ZEM_{APN} or ZEM_{EPN} can be used to find optimal control solution. Here, ZEM_{PN} is used to clarify proposed guidance law. Algorithm starts with the distribution of particles in solution space randomly. Each particle is a possible solution of guidance problem. Here, particles refer to effective navigation ratio and solution space is bounded between 3 and 5. In each iteration, particles are manipulated according to following equations,

$$V_{i,j} = wV_{i,j} + c_1 rand_1 \left(P_{best_{i,j}} - X_{i,j}\right) + c_2 rand_2 (G_{best_i} - X_{i,j})$$
$$X_{i,j} = X_{i,j} + V_{i,j} \tag{4.80}$$

P_{best} is the first fitness function and represents the local best fitness values each particle has achieved. On the other hand, G_{Best} is the global best fitness value that any particle has achieved so far [30]. $X_{i,j}$ is the position of particle, $V_{i,j}$ is the velocity of particle. c_1 and c_2 are two positive constant. w is the inertial weight. Lastly, $rand_1$ and $rand_2$ are two random values between [0,1]. The subscript j is a number of generation and i is number of particles. Block diagram of the algorithm can be seen in Figure 4.6.

In this study, parameters are $w_{max} = 0.9, w_{min} = 0.4, c_1 = 2, c_2 = 2$. Population size is choosen as $n = 100$. Maximum and minimum effective navigation ratio, N', are selected as 3 and 5 respectively. Maximum iteration was set to 10. Previously ZEM_{APN} is defined as $y + \dot{y}\,t_{go} + \frac{1}{2}a_T t_{go}^2$. If we use APN guidance law form and after rearrange, we can define cost function as;

$$\min_{ZEM_{PN}} J = \left(y + \dot{y}t_{go}\right)^2 = \left(\frac{n_c t_{go}^2}{N'} - \frac{1}{2}t_{go}^2 n_t\right)^2 \tag{4.81}$$

Algorithm tries to find minimum function value, equation (4.81), in each iteration by testing different values of effective navigation ratio N′ defined between 3 and 5. In each iteration, 100 particles are firstly distributed in solution space. At the end of 10 iterations, optimal effective navigation ratio N' will be found. N' must be stay in predetermined limits. Then we can substitute optimal N' into proportional navigation or augmented proportional navigation guidance law form.

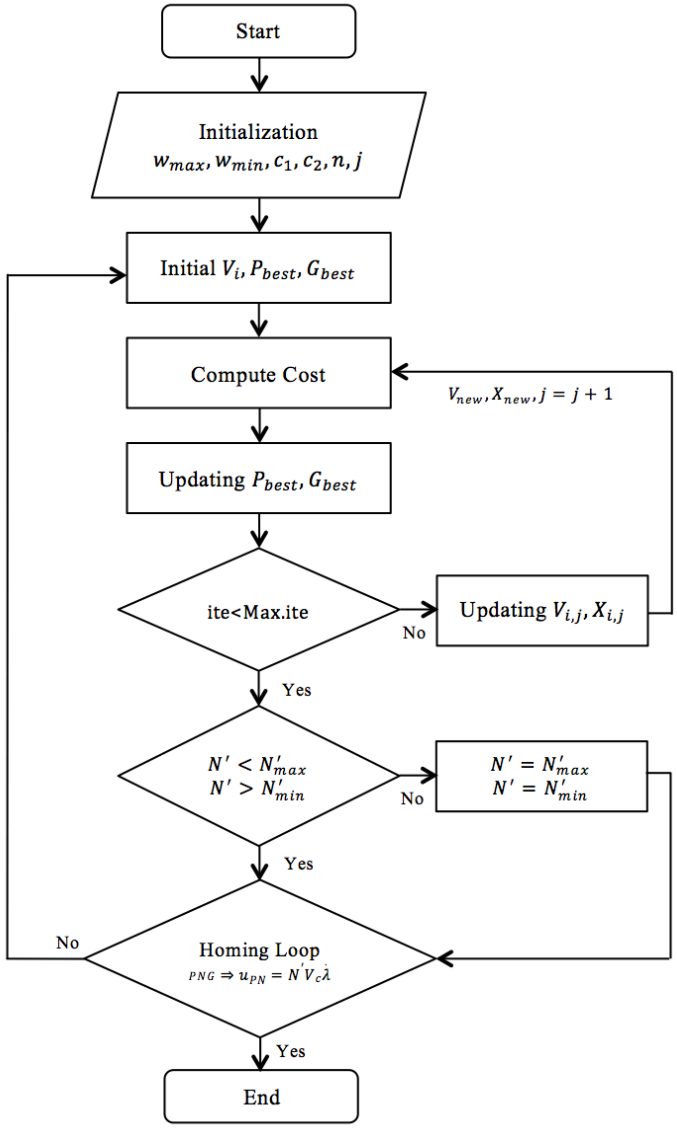

Figure 4.6 : Block diagram of the particle swarm optimization guidance.

$$u_{PSOG} = N'_{PSO} V_c \dot{\lambda} \tag{4.82}$$

Here, Particle Swarm Optimization guidance law (PSOG) uses previous acceleration command n_c and target acceleration n_T during engagement to find optimal effective navigatino ratio N'_{PSO} in each time step. Basically, PSOG tries to arrange the missile on a flight path that does not require any maneuver in the next step to hit the target.

5. KALMAN FILTERING

In chapter 4, essential guidance laws are derived. Therein, states are basically expressed as relative position, relative velocity, target acceleration and target jerk. In reality, those states are not measured perfectly and corrupted by noise. Therefore, the filtering is necessary to extract signal from the noisy measurements. The purpose of the filtering is to estimate the certain states of the system from the given noisy measurements. Kalman filtering is generally used in missile guidance theory to produce an optimal digital noise filter. The Kalman filter requires models of the states, and the relationship between states and measurements. Also, filter predicts the states forward in time then updates the estimate with measurements [51]. The mean value obtained from the kalman filter provides the optimal estimate of the states that have minimum mean square error. [6,51,52,53]. In Kalman filter applications discrete time models are generally preferred. The derivation of the Kalman filter is beyond the scope of this thesis. Theoretical equations are given below. Firstly, we can start with a continous time linear model representation of dynamic system;

$$\begin{aligned} \dot{x} &= Ax + Bu + w \\ y &= Cx + v \end{aligned} \tag{5.1}$$

In here, x is the state vector, u is the guidance control command vector, y is the measurement vector, w and v are white noise process and measurement vector. The process and measurement noise covariance matrices Q and R;

$$\begin{aligned} Q &= E[ww^T] \\ R &= E[vv^T] \end{aligned} \tag{5.2}$$

State transition matrix can be obtained by $\Phi(t) = \mathcal{L}^{-1}([sI - A]^{-1}),\ \Phi_k = \Phi(T_s)$ if the dynamic system is linear and time invariant. Γ_k defined below is obtained from $\Gamma_k = \int_0^{T_s} \Phi_{\mathrm{k}}(\tau)B(\tau)d\tau$. Discrete time representation of (5.1) as given;

$$x_{k+1} = \Phi_k x_k + \Gamma_k u_k + w_k$$
$$y_k = H_k x_k + v_k \tag{5.3}$$

Equation (5.3) is the sampled version of the contionus time model in (5.1). Process and measurement noise covariance matrices can be expressed as;

$$Q_k = E[w_k w_k^T] = \int_0^{T_s} \Phi(\tau)\, Q(\tau) \Phi^T(\tau) d\tau$$
$$R_k = E[v_k v_k^T] = \sigma_n^2 \tag{5.4}$$
$$0 = E[w_k v_k^T]$$

The Kalman filter as stated before, has two steps; firstly, prediction then measurement update. x_k^- represents the a priori estimate constructed before a measurement at time k and x_k^+ represents the posteriori estimate constructed after a measurement at time k. Estimation error covariance matrix P_k where,

$$P_k^- = E[x_k - \hat{x}_k^-][x_k - \hat{x}_k^-]^T$$
$$P_k^+ = E[x_k - \hat{x}_k^+][x_k - \hat{x}_k^+]^T \tag{5.5}$$

The discrete time Kalman filter algorithm can be expressed as in order of formation and firstly initialization [6,51,52,53];

Initial conditions,

$$\hat{x}_0^+ = E[x(0)]$$
$$P_0^+ = E[x_0 - \hat{x}_0^+][x_0 - \hat{x}_0^+]^T \tag{5.6}$$

Prediction;
State prediction,

$$\hat{x}_k^- = \Phi_{k-1} x_{k-1}^+ + \Gamma_{k-1} u_{k-1} \tag{5.7}$$

Error covariance prediction,

$$P_k^- = \Phi_{k-1} P_{k-1}^+ \Phi_{k-1}^T + Q_{k-1} \tag{5.8}$$

Correction;

Kalman gain update,

$$K_k = P_k^- H_k^T [H_k P_k^- H_k^T]^{-1} \tag{5.9}$$

Measurement update,

$$\hat{x}_k^+ = x_k^- + K_k(y_k - H_k x_k^-) \tag{5.10}$$

Error covariance update,

$$P_k^+ = [I - K_k H_k] P_k^- \tag{5.11}$$

5.1 Kalman Filter Application to Homing Loop

In this subsection, utility of Kalman filtering concept will be investigated. Linear Three-State Discrete Time and Linear Four-State Weave Discrete Time Kalman filter design will be demonstrated in the following sections.

5.1.1 Linear three-state discrete time Kalman filter

Previously stated that, APN guidance law and related model can be expressed as;

$$u_{APN} = \frac{N'}{t_{go}^2}\left[x_1(t) + x_2(t)t_{go} + \frac{1}{2}x_3(t)t_{go}^2\right], \qquad N' = 3$$

$$\dot{x} = Ax + Bu + Dw \tag{5.12}$$

$$A = \begin{bmatrix} 0 & 1 & 0 \\ 0 & 0 & 1 \\ 0 & 0 & 0 \end{bmatrix}, \qquad B = \begin{bmatrix} 0 \\ -1 \\ 0 \end{bmatrix}, \qquad D = \begin{bmatrix} 0 \\ 0 \\ 1 \end{bmatrix}$$

APN guidance command u_{APN} requires to estimate relative position $y = x_1(t)$, relative velocity $\dot{y} = x_2(t)$, and target acceleration $a_T = x_3(t)$ states. Measurement and process statistics are given;

$$Q = E[ww^T], \qquad E[w] = 0$$

$$R = E[vv^T], \qquad E[v] = 0 \tag{5.13}$$

$$E[wv^T] = 0$$

Discrete time dynamics and covariance matrices are shown below;

$$x_{k+1} = \Phi_k x_k + \Gamma_k u_k + w_k$$
$$y_k = H_k x_k + v_k \tag{5.14}$$

$$\Phi_k = \begin{bmatrix} 1 & T_s & 0.5T_s^2 \\ 0 & 1 & T_s \\ 0 & 0 & 1 \end{bmatrix}, \qquad \Gamma_k = \begin{bmatrix} -0.5T^2 \\ -T \\ 0 \end{bmatrix},$$

$$Q_k = \begin{bmatrix} \frac{1}{20}T_s^5 & \frac{1}{8}T_S^4 & \frac{1}{6}T_s^3 \\ \frac{1}{8}T^4 & \frac{1}{3}T^3 & \frac{1}{2}T^2 \\ \frac{1}{6}T^3 & \frac{1}{2}T^2 & T \end{bmatrix} Q, \qquad H_k = [1 \quad 0 \quad 0], \tag{5.15}$$

$$R = \sigma_n^2$$

By using (5.6)-(5.11), estimation equation can also be expressed as;

$$\hat{x}_k^+ = [I - KH_k][\Phi_{k-1} x_{k-1}^+ + \Gamma_{k-1} u_{k-1}] + K y_k \tag{5.16}$$

Kalman Gain matrix, K, is given below;

$$K = \begin{bmatrix} K_1 \\ K_2 \\ K_3 \end{bmatrix} = \begin{bmatrix} \frac{p_{11}}{p_{11} + \sigma_n^2} \\ \frac{p_{22}}{p_{22} + \sigma_n^2} \\ \frac{p_{33}}{p_{33} + \sigma_n^2} \end{bmatrix} \tag{5.17}$$

A priori covariance and posteriori covariance matrix can be expressed by using (5.8) and (5.11) as;

$$P_k^- = \begin{bmatrix} p_{11} & p_{12} & p_{13} \\ p_{12} & p_{22} & p_{23} \\ p_{13} & p_{23} & p_{33} \end{bmatrix}$$

$$P_k^+ = \begin{bmatrix} p_{11} - p_{11}K_1 & p_{12} - p_{12}K_1 & p_{13} - p_{13}K_1 \\ p_{12} - p_{11}K_2 & p_{22} - p_{12}K_2 & p_{23} - p_{13}K_2 \\ p_{13} - p_{11}K_3 & p_{23} - p_{12}K_3 & p_{33} - p_{13}K_3 \end{bmatrix} \tag{5.18}$$

This Kalman filter scheme will be used in this study for zero lag guidance systems required three states information such as PN, APN, OR, AOR, OGL, MELN, BPN, DG, PSOG. In order to apply filter, measurement noise variance σ_n^2 is required.

5.1.2 Linear four-state weave discrete time Kalman filter

Here, four state linear kalman filter will be investigated against a sinusoidal target maneuver. As previously investigated in weave guidance law (WG) section, stated optimal control command and related dynamic models can be seen below;

$$u_{WG}(t) = N'V_c\dot{\lambda} + \frac{N'}{t_{go}^2}\left[\left(\frac{1-coswt_{go}}{w^2}\right)n_t + \left(\frac{wt_{go}-sinwt_{go}}{w^3}\right)j_T\right],$$

$$N' = \frac{6h^2(e^{-h}-1+h)}{2h^3+3+6h-6h^2-12he^{-h}-3e^{-2h}} \tag{5.19}$$

$$\dot{x} = Ax + Bu + Dw$$

$$A = \begin{bmatrix} 0 & 1 & 0 & 0 \\ 0 & 0 & 1 & 0 \\ 0 & 0 & 0 & 1 \\ 0 & 0 & -w^2 & 0 \end{bmatrix}, \quad B = \begin{bmatrix} 0 \\ -1 \\ 0 \\ 0 \end{bmatrix}, \quad D = \begin{bmatrix} 0 \\ 0 \\ 0 \\ 1 \end{bmatrix} \tag{5.20}$$

In this filter design, relative position $y = x_1(t)$, relative velocity $\dot{y} = x_2(t)$, target acceleration $a_T = x_3(t)$ and target jerk $\dot{a}_T = x_4(t)$ measurements are required. Discrete time dynamics and covariance matrices are shown below;

$$x_{k+1} = \Phi_k x_k + \Gamma_k u_k + w_k$$
$$y_k = H_k x_k + v_k \tag{5.21}$$

$$\Phi_{\mathrm{k}} = \begin{bmatrix} 1 & T_s & \frac{1-\cos x}{w^2} & \frac{x-\sin x}{w^3} \\ 0 & 1 & \frac{\sin x}{w} & \frac{1-\cos x}{w^2} \\ 0 & 0 & \cos x & \frac{\sin x}{w} \\ 0 & 0 & -w\sin x & \cos x \end{bmatrix},$$

$$\Gamma_k = \begin{bmatrix} -0.5T_s^2 \\ -T_s \\ 0 \\ 0 \end{bmatrix}, \tag{5.22}$$

$$Q_k = \begin{bmatrix} Q_{11} & Q_{12} & Q_{13} & Q_{13} \\ Q_{12} & Q_{22} & Q_{23} & Q_{24} \\ Q_{13} & Q_{23} & Q_{33} & Q_{34} \\ Q_{14} & Q_{24} & Q_{34} & Q_{44} \end{bmatrix},$$

$$\mathrm{H_k} = [1 \quad 0 \quad 0 \quad 0],$$

where

$$\mathrm{Q_{11}} = \frac{\Phi_s}{w^5}[0.333x^3 - 2\sin x + 2x\cos x + 0.5x - 0.25\sin 2x],$$

$$\mathrm{Q_{12}} = \frac{\Phi_s}{w^4}[0.5x^2 - x\sin x + 0.5\sin^2 x],$$

$$\mathrm{Q_{13}} = \frac{\Phi_s}{w^3}[\sin x - x\cos x - 0.5\,x + 0.25\sin 2x],$$

$$\mathrm{Q_{14}} = \frac{\Phi_s}{w^2}[\cos x + x\sin x - 0.5\sin^2 x - 1],$$

$$\mathrm{Q_{22}} = \frac{\Phi_s}{w^3}[1.5x - 2\sin x + 0.25\sin 2x], \tag{5.23}$$

$$\mathrm{Q_{23}} = \frac{\Phi_s}{w^2}[1 - \cos x - 0.5\sin^2 x],$$

$$\mathrm{Q_{24}} = \frac{\Phi_s}{w}[\sin x - 0.5\,x - 0.25\sin 2x],$$

$$\mathrm{Q_{33}} = \frac{\Phi_s}{w}[0.5x - 0.25\sin 2x],$$

$$\mathrm{Q_{34}} = 0.5\Phi_s\, sin^2 x,$$

$$\mathrm{Q_{44}} = w\Phi_s\,[0.5x + 0.25\sin 2x],$$

$$\Phi_s = \frac{w^2 n_{T_{max}}^2}{t_F}, \qquad x = wT_S$$

Process noise covariance matrix calculations (5.23) can be obtained by any symbolic solver. Estimation equations are as described in the previous three-state linear Kalman filter section.

$$\hat{x}_k^+ = [I - KH_k][\Phi_{k-1} x_{k-1}^+ + \Gamma_{k-1} u_{k-1}] + Ky_k \tag{5.24}$$

Kalman gain matrix, a priori covariance and posteriori covariance matrix equations can be obtained from (5.8),(5.9) and (5.11). If we have any knowledge of the target weave frequency, linear four states Kalman filter can be used to estimate target acceleration and its rate, target jerk. As already mentioned that when target weaving frequency approaches to zero, WG turns into EPN guidance law form. Therefore, proposed Kalman filter can also be used in such guidance systems.

5.2 The Multiple Model Adaptive Estimator Approach

In order to apply linear four state Kalman filter against weaving target, weave frequency must be known. Lack of knowledge of the weave frequency will effect the miss performance of the guidance system. Previous Kalman filter will not give a good result when target frequecny is unknown. It can be used when this type of problem arises. Multiple model adaptive estimation (MMAE) is a recursive estimator uses a bank of M filters and It can be used against unknown target weaving frequency cases [6,27,54]. Multiple Kalman filters operate at the same time and each one is configurated to a different weave frequency. Each filter is independent from others. At every time step, bank filter approach can determine the probability that a given filter is the correct one [6]. The states estimates of each kalman filter is multiplied by the related probability then all the multiplications are added to be used in the guidance system. MMAE process can be seen in Figure 5.1

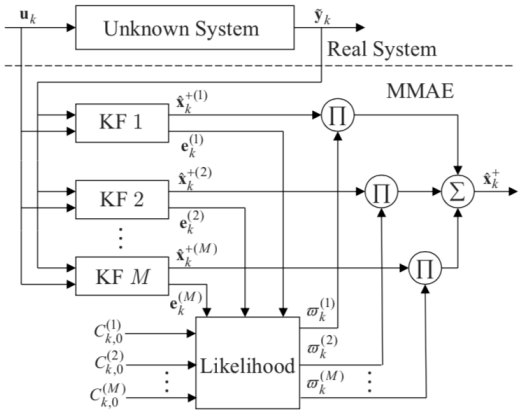

Figure 5.1 : Multiple model adaptive estimator process [54].

Application of Bayes' rule yields;

$$p_k(i) = \frac{p_{k-1}(\mathrm{i})\ \mathrm{p}(\mathrm{y}|\hat{\mathrm{x}}_\mathrm{k}^-(\mathrm{i}))}{\sum_{j=1}^{M} p_{k-1}(\mathrm{j})\ \mathrm{p}(\mathrm{y}|\hat{\mathrm{x}}_\mathrm{k}^-(\mathrm{j}))} \tag{5.25}$$

$p_k(i)$ represents the probability of ith filter. Since $\mathrm{p}\left(\mathrm{y}|\hat{\mathrm{x}}_\mathrm{k}^-(\mathrm{i})\right) = L_k(i)$ Likelihood function which is defined by,

$$L_k(i) = \frac{1}{\{\det[2\pi(H_k P_k^-(i) H_k^T + R_k)]\}^{1/2}} \exp[-\frac{1}{2} e_k^T(i)(H_k P_k^-(i) H_k^T + R_k)^{-1} e_k(i)] \tag{5.26}$$

Here in (178) Likelihood function for the measurement residual is shown. $H_k P_k^-(i) H_k^T + R_k$ represents the autocorrelation matrix $C_k = E[e_k e_k^T]$. Discrete time residual equation e_k is given by using (5.22);

$$e_k = y_k - H_k \hat{x}_k^- = H_k x_k + v_k - H_k \hat{x}_k^- = -H_k \tilde{x}_k^- + v_k \tag{5.27}$$

Where $\tilde{x}_k^- \equiv \hat{x}_k^- - x_k$. The residual and residual covariance are scalars here. Thus, we can also express Likelihood function of M filters in the filter bank as by equating $Res = e_k$ and rearrange equation (5.25);

$$p_k(i) = \frac{p_{k-1}(i)\ L_k(i)}{\sum_{j=1}^{M} p_{k-1}(j)\ L_k(j))}, \qquad p_0(i) = \frac{1}{M} \tag{5.28}$$

$$L_k(i) = \frac{1}{\{\det[2\pi(C_k(i))]\}^{1/2}} \exp[-\frac{1}{2} Res_k^2(i) C_k(i)^{-1}]$$

The spesific estimate of weaving frequency, ω, at time t_k is given by;

$$\widehat{\omega}_k = \sum_{i=1}^{M} p_k(i)\, \omega(i) \tag{5.29}$$

The resultant state estimates , $\hat{x}$, can also be expressed in the same way;

$$\hat{x}_k = \sum_{i=1}^{M} p_k(i)\, \hat{x}_k(i) \tag{5.30}$$

$\hat{x}_k(i)$ represents the state estimates of each filter. Here, in equations (5.29) and (5.30) each of state estimates and weaving frequencies are weighted by the probability that the filter is correct.

6. MULTIPLE TARGETS

In this section case of multiple targets is investigated. Here, multiple targets are limited to two targets. Power centroid method proposed by Zarchan, P.[6,28] and Earliest Intercept Geometry (EIG) method proposed by Shin, H.S. et al [29,33] were selected as subjects to be examined in the following subsections.

6.1 Power Centroid Method

Basic idea behind this method is that the missile is guided on the power centroid of multiple targets in close formation [6, 28]. When one of the two targets goes out the viewpoint of missile seeker, then interceptor decides to direct itself to other target. Problem is that whether there is enough time left to hit the target or not. Multiple target application to homing loop can be implemented into blocks as initial conditions. One way to model this case is an initial displacement error, other one initial heading error [28]. In Figure 6.1 first way is to assume X, Y reference frame for initial dispacelement, other way is to assume X', Y' reference frame for initial heading error.

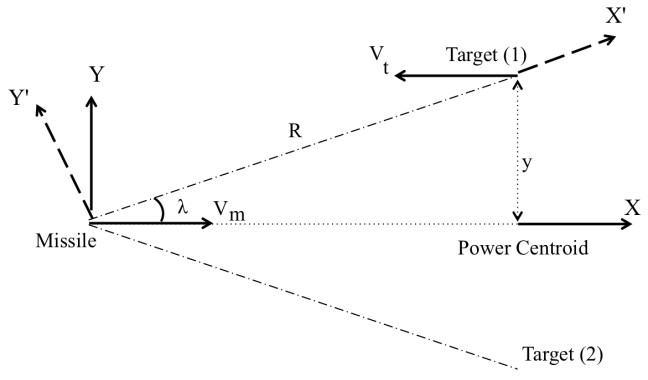

Figure 6.1 : Multiple target engagement geometry [28].

Implementation into homing loop can be seen in Figure 6.2.

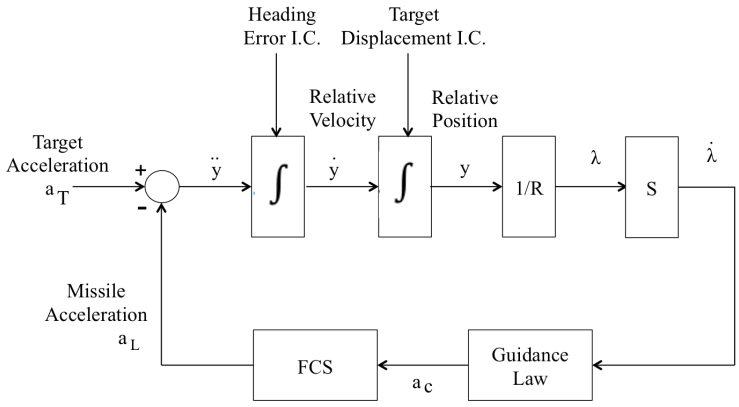

Figure 6.2 : Homing loop with initial conditions.

It does not important how to implement initial conditions into homing loop or how to choose reference line. Since we know that miss distance is independent of referance frame. Therefore, they must result in the same miss distance at the end.

6.2 Earliest Intercept Geometry Method

Shin, H.S. et al [29,33,38] proposed a method based on a geometric approach. Idea is that the missile can defend the area if the target stays in the area defined by the early intercept geometry (EIG). The boundries of possible interception regions are obtained by earliest intercept geometry method wtihout considering any target maneuvers. Minimum safetly distance between any defended asset and boundry of interception region is calculated simultaneously by EIG. According to minimum safety distance values, the interceptor can decide which target should be directed.

In Figure 6.3 two cases are shown. In the first case, the distance, d_1, between Target-1 and defended asset is shorter than the distance, d_2, between Target-2 and defended asset. Thus, missile directs itself to Target-1. On the other hand, in the second case, the missile steers itself to Target-2 since $d_2 < d_1$. Algorithm starts with the finding the set of all possible allocations. Then, computes the earliest intercept geometries and calculates the minimum safety distances $\min d_i$. Lastly, the missile is guided to the target. Interception geometry can be seen in Figure 6.4.

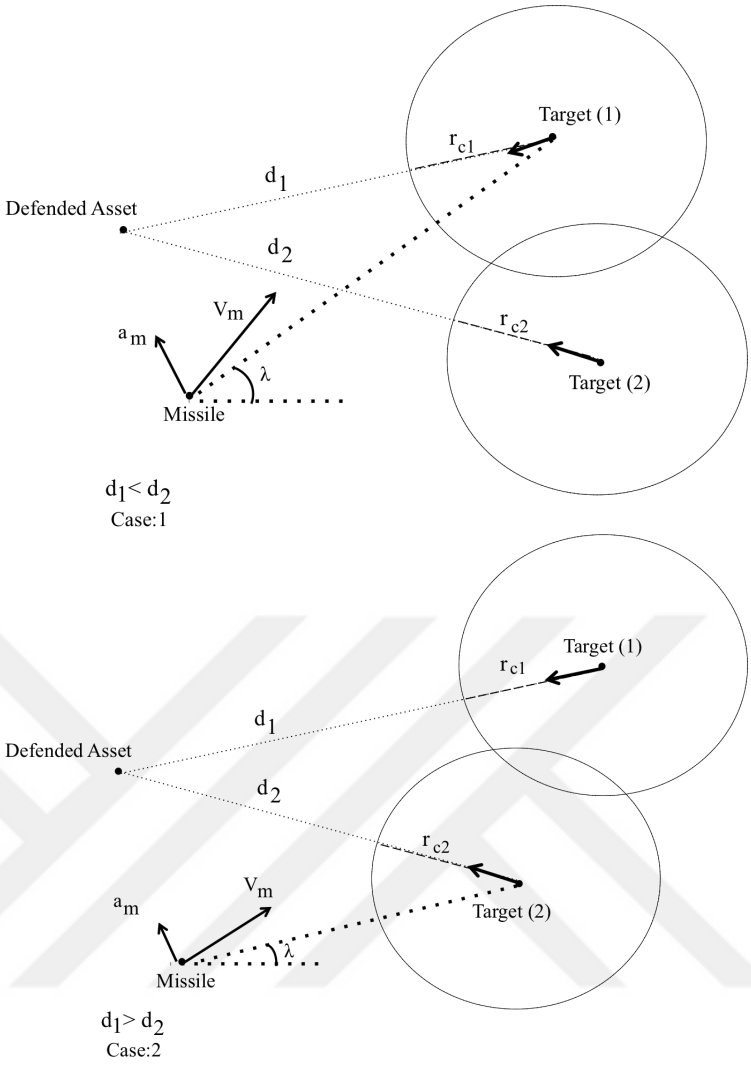

Figure 6.3 : Earliest intercept geometry concept [33].

Theoritical equations are given below; [29,33,38]

$$D_M^2 = x^2 + y^2, \qquad D_T^2 = (R - x)^2 + y^2 \tag{6.1}$$

$$D_M^2 = \zeta^2 D_T^2 \tag{6.2}$$

ζ represents the velocity ratio and R represents the sightline range. After substituting (6.1) into (6.2) yields;

$$(x - r_c)^2 + y^2 = c_l^2, \qquad r_c = \frac{\zeta^2 R}{|\zeta^2 - 1|}, \qquad c_l = \frac{\zeta R}{|\zeta^2 - 1|} \tag{6.3}$$

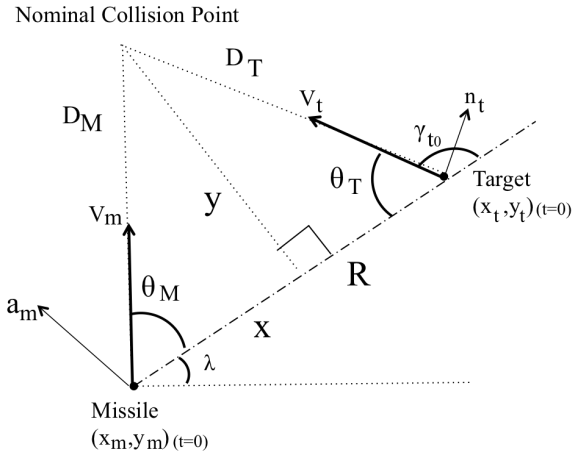

Figure 6.4 : Missile-target intercept geometry [33].

Here, equation (6.3) represents a circle with radius r_c and centre c_l. In order to apply this method velocity ratio ζ is required. In this study, $\zeta > 1$ case, missile velocity greater than the target velocity, is assumed. During the engagement the missile can evaluate earliest intercept geometry to decide which target should be directed by using minimum safety distance.

7. SIMULATION SCENARIOS, COMPARISON AND ANALYSIS

Following cases will be investigated through this section. In homing loop, various type of disturbances are added. Mainly, target maneuvers, radome slope, guidance delay, noise terms such as range dependent, independent and glint are investigated.

Target maneuvers are in 3g constant acceleration, 3g Barrel roll, 3g Vertical-S, 2g constant jerk, white gaussian random and 6g high Barrel roll form. Effect of guidance delay is investigated through flight control system time lag. Three different form of flight control system model is studied such as zero lag, first order lag and skid to turn type missile flight control system transfer function in equation (3.9). First order lags are assumed as 0.5 and 0.75 seconds alternately. Noise terms are added into three different form. Glint noise, range independent noise and active range dependent noise are studied as 3 to 10m, 1 MR and 2 to 4 MR respectively. Radome slope is added into simulation as -0.01. In order to see effect of initial conditions, relative distance and relative velocity/heading error are examined. Relative seperation is assumed 1000m in some cases. On the other hand, initial heading error is assumed 20deg. Scenarios in Table 7.1 are set up taking into consideration those mentioned disturbances.

Flight time for each case is set from 0 to 10 seconds with 0.5 second increment. In each time step 50 run monte carlo simulations were performed. Standard deviation results are obtained with the help of monte carlo simulation. Statistical results are shown only in noise term added cases.

In order to show flight path, relative velocity and commanded acceleration results, flight times of 10 seconds were selected for each case. Relative velocity results are shown in heading angle form. Also, control effort results are in integral squared of commanded acceleration form.

Table 7.1 : Simulation scenarios.

Scenarios	Disturbances (Target Maneuver in g, Radome Slope, Noise in MR Standard Deviation,	Initial Conditions (Relative Seperation, Heading Error)	Guidance Delay (FCS Time Lag)
Case 1	$3g$ constant target maneuver	$y = 0, \dot{y} = 0$	Zero Order
Case 2	$3g$ constant target maneuver	$y = 0, \dot{y} = 0$	First Order (T=0.5s)
Case 3	$3g$ constant target maneuver	$y = 500m,$ $\dot{y} = 0$	First Order (T=0.5s)
Case 4	$3g$ constant target maneuver	$y = 0,$ $\dot{y} = 20 \deg HE$	First Order (T=0.5s)
Case 5	$3g$ constant target maneuver, Radome slope $R_s = -0.01$	$y = 0,$ $\dot{y} = 0$	First Order (T=0.5s)
Case 6	$3g$ Barrel-Roll maneuver, $w = 2\ rad/s,$ Radome slope $R_s = -0.01$	$y = 1000m,$ $\dot{y} = 0$	First Order (T=0.5s)
Case 7	$3g$ Vertical-S maneuver, $w = 2\ rad/s$ Radome slope $R_s = -0.01$	$y = 1000m,$ $\dot{y} = 0$	First Order (T=0.5s)
Case 8	2g constant jerk maneuver Radome slope $R_s = -0.01$	$y = 0,$ $\dot{y} = 0$	First Order (T=0.5s)
Case 9	$3g$ constant target maneuver Range independent noise = 2MR	$y = 0,$ $\dot{y} = 0$	First Order (T=0.5s)
Case 10	$3g$ constant target maneuver Range independent noise = 2MR	$y = 1000m,$ $\dot{y} = 20 \deg HE$	First Order (T=0.5s)
Case 11	WG random maneuver $\sim N(0, \sigma^2 = 9g^2)$ Range independent noise = 2MR	$y = 0,$ $\dot{y} = 0$	First Order (T=0.5s)
Case 12	$3g$ constant target maneuver Glint noise = 3m, Range independent noise = 1MR, Active range dependent Noise = 4MR	$y = 0,$ $\dot{y} = 0$	First Order (T=0.5s)

Table 7.1 : Simulation scenarios (continued).

Scenarios	Disturbances (Target Maneuver in g, Radome Slope, Noise in MR Standard Deviation,	Initial Conditions (Relative Seperation, Heading Error)	Guidance Delay (FCS Time Lag)
Case 13	$3g$ constant target maneuver Glint noise = 3m, Range independent noise = 1MR, Active range dependent noise = 4MR	$y = 1000m,$ $\dot{y} = 20 \deg HE$	Third Order STT type FCS TF in eqn (3.9)
Case 14	$3g$ Barrel Roll target maneuver Glint noise = 3m, Range independent noise = 1MR, Active range dependent noise = 4MR	$y = 0,$ $\dot{y} = 20 \deg HE$	Third Order STT type FCS TF in eqn (3.9)
Case 15	$6g$ high Barrel Roll target maneuver Glint noise = 3m, Range independent noise = 1MR, Active range dependent noise = 4MR	$y = 0,$ $\dot{y} = 0,$	Third Order STT type FCS TF in eqn (3.9)
Case 16	$6g$ Barrel roll maneuver, $w = 2\ rad/s,$ + WG Random maneuver $\sim N(0, \sigma^2 = 1)$ Glint noise = 10m, Range Independent Noise = 1MR, Active range dependent Noise = 4MR	$y = 0,$ $\dot{y} = 0,$	First Order (T=0.75s)

Noise term added cases are filtered via three state linear and four state linear Kalman filter depend on the guidance law used. The bandwidth of kalman filter is adjusted equal to actual noise level in some cases. In cases where range dependent noise and glint noises were added, kalman filter measurement noise statistics were kept higher than actual noise level. Kalman filter bandwidth is decreased on purpose to do more filter. Simply, it was assumed by filter that there is more measurement noise in system.

12 types of guidance laws were studied in this thesis. All this guidance laws are described in chapter 4. Proportional navigation guidance law (PN) is in the True Proportional navigation guidance form. Effective navigation ratio, N, is assumed 3 in

noise free cases. In other cases, it is assumed 4. The effect of navigation ratio is not investigated in this study. Augmented Proportional Navigation (APN), Optimal Rendezvous (OR), Augmented Optimal Rendezvous (AOR) are other variety of former guidance law. Extended Proportional Navigation (EPN) uses target jerk information in addition to them. Bias duration in Biased Proportional Navigation guidance (BPN) is assumed 3 seconds in all cases. Final flight path angle/hitting angle is adjusted zero. Particle Swarm Optimization guidance law (PSOG) tries to find optimal effective navigation ratio that minimizes zero effort miss. Therefore it uses different effective navigation ratio during engagement. Differential Guidance law (DG) uses $\pm 45g$ maximum/minimum acceleration as a command. Compansation terms are also added in DG. Optimal guidance law or Minimum Effort Law (MEL) tries to eliminate missile time lag. In first order time lag cases, guidance law compansation term is equalized to the actual time lag value. In third order cases, it was adjusted as 0.1 second. Minimum effort law without target acceleration measurement (MELN) is another form of MEL. The actual value of target weaving frequeny is implemented into Weave guidance law (WG). When target maneuver is constant, weaving frequency is assumed nearly zero. Also, missile time lag is eliminated in Compansated Weave Guidance (WGC) via true value of time lag as in MEL/MELN. Acceleration commands generated from all these guidance laws are limited to $\pm 45g$.

In order to investigate multiple target case, centroid method is used firstly. As previously mentioned, if initial condition as relative seperation or heading angle is given sufficiently, multiple target case can be examined. Initial condition approach is considered for multiple target case in this thesis. As an example, it can be clearly seen in initial condition column that, in some cases, relative seperation is given as 1000m.

Results are examined according to following parameteres: miss distance, control effort and hitting angle. The most important parameter among them is miss distance. Kill-zone is generally defined as below 10 meters. Therefore, miss distance results below 10 meters are considered acceptable in this study. Estimated and actual values of target states in noise added cases are given in following sections. In order to avoid confusion, all results will not be given in case studies. Only important points and results will be shown. In this study cases are divided into two main groups as basic

homing loops and noise filter added homing loops. Also for further subgrouping, constant acceleration target maneuvers and optimal evasive target maneuvers are used.

7.1 Basic Homing Loops

Scenarios from Case 1 to Case 8 belong to this section. Here, noise terms are not added into homing loops. Only target maneuvers, radome effects and guidance delays are considered. Firstly constant acceleration target maneuver cases will be shown then barrel roll and vertical-s evasive maneuvers will be investigated.

7.1.1 Constant acceleration target maneuvers

Case 1 represents the basic homing loop such that there is no time lag in guidance loop. Therefore all guidance laws are expected to hit the target perfectly. Only disturbance in the loop is the 3g constant acceleration target maneuver. It can be seen from Figure 7.1 that miss distance results are all zero which means all guidance laws hit the target perfectly at all flight times.

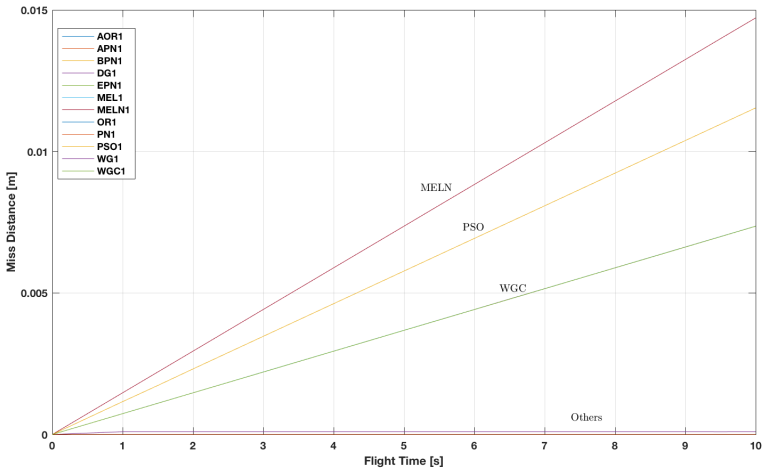

Figure 7.1 : Case 1 - miss distance results.

As an initial condition relative seperations and initial headings are adjusted as zero. 10 seconds flight's trajectory can be seen in Figure 7.2.

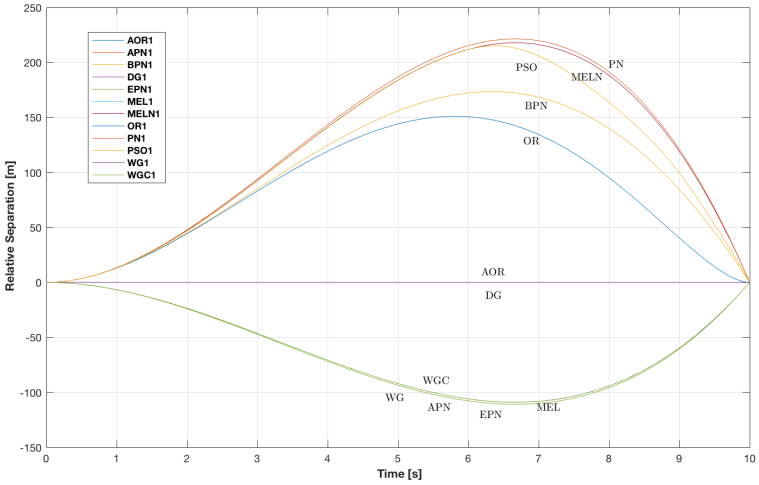

Figure 7.2 : Case 1 - flight paths.

Control effort results can be seen in Figure 7.3. It can be clearly seen that the best/minimum results are achieved by EPN, MEL, WG, WGC and APN. Hitting angles can be seen in Figure 7.4. As previously mentioned OR and AOR are the trajectory shaped guidance laws. Therefore these guidance laws hit the target with the desired angles such that zero angle in this case.

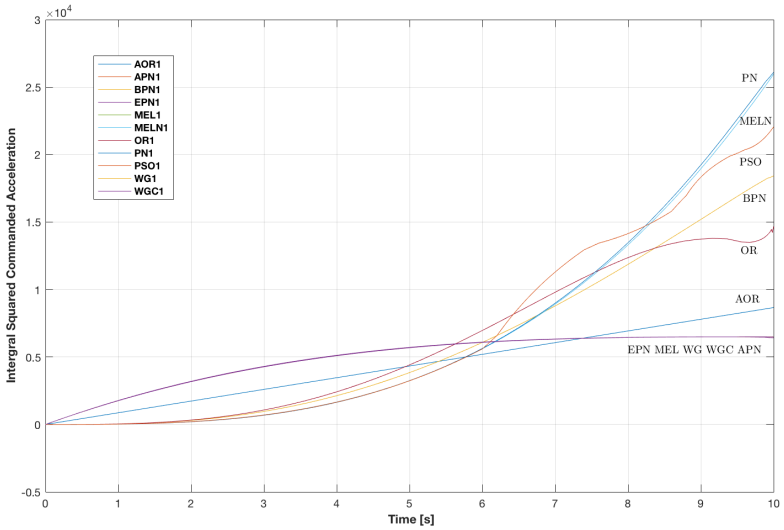

Figure 7.3 : Case 1 - control effort results.

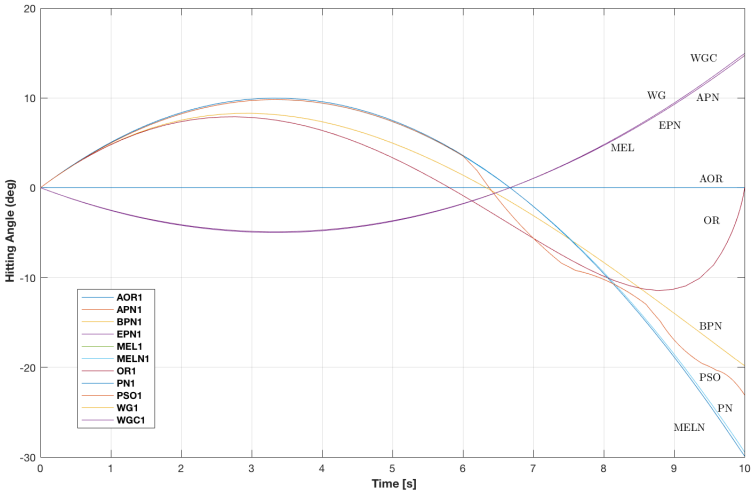

Figure 7.4 : Case 1 - hitting angle results

Case 2 represents the first order lag homing loop. As a flight control system, first order transfer function with time constant 0.5 second is used. Guidance delay and target maneuver are the two disturbances here. Miss distance results at all flight times can be seen in Figure 7.5. Minimum miss distance results are achieved by MEL, WG and WGC when flight lasts 10 seconds. All guidance laws hit the target in desired range at all flight times. Flight paths and hitting angles results are the almost same as in case 1. Therefore results are not given here. In control effort point of view, results can be seen in Figure 7.6. Minimum integral squared commanded acceleration results are achieved by MEL and WGC.

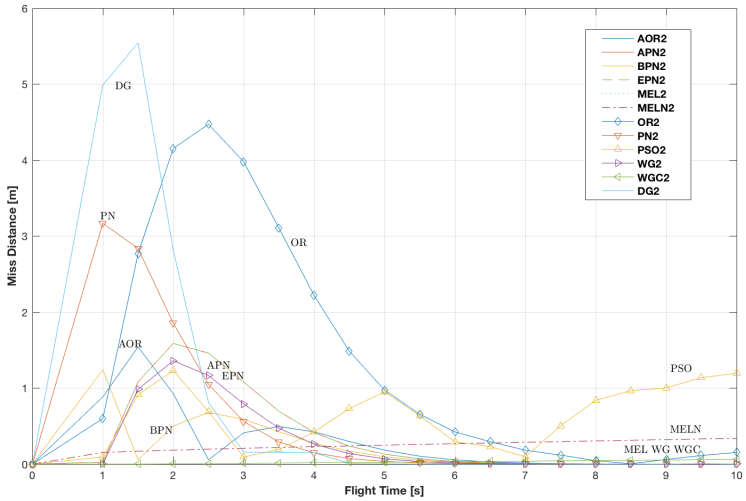

Figure 7.5 : Case 2 - miss distance results.

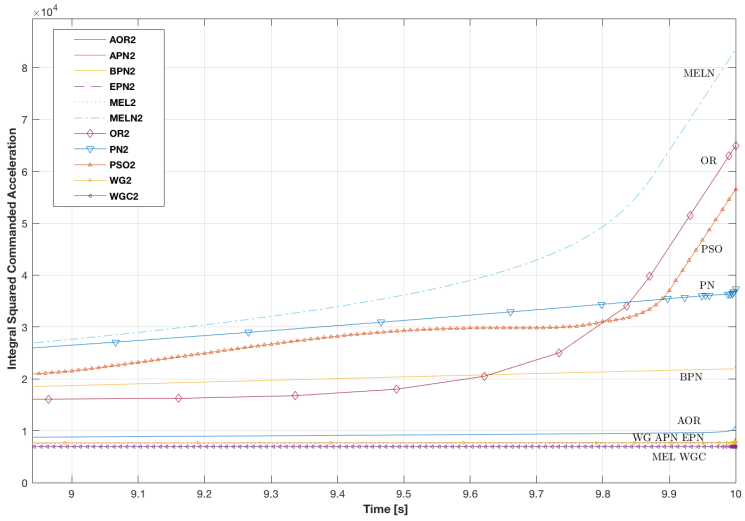

Figure 7.6 : Case-2 integral squared commanded acceleration results.

Case 3 represents the first order lag homing loop with given initial relative distance. It means that the missile did not fired head on or tail side of the target. As previously mentioned it can be considered as a multiple target case. In relation to that missile is engaged one of the targets. Alternatively it can be considered as a not perfectly fired missile and in that case this is reflected as an initial condition in homing loop. Miss distance results can be seen in Figure 7.7. In order to understand better, flight time between 3 and 10 seconds are displayed. It is reasonable to show like that because it takes couple of seconds to hit target from 500m. It can be concluded that the missile can hit the target less than a meter with any of the guidance law if flight time greater than 7 seconds.

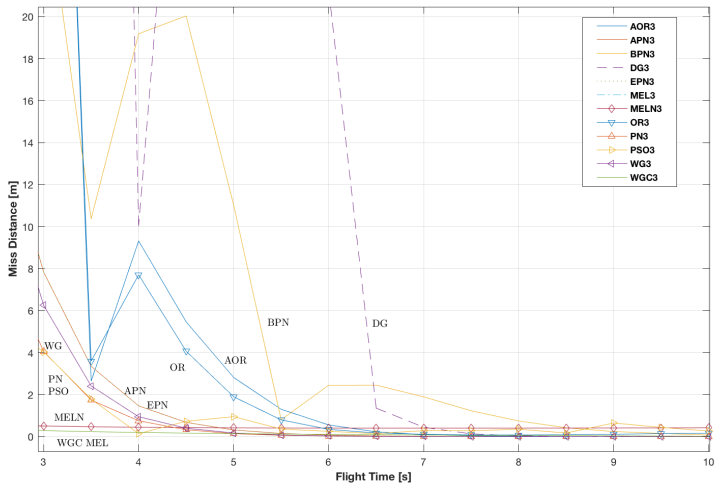

Figure 7.7 : Case 3 - miss distance results.

It can be seen in Figure 7.8 that missile starts to approach target from 500m as an initial condition. During 10 seconds of engagement all guidance laws follow different trajectory.

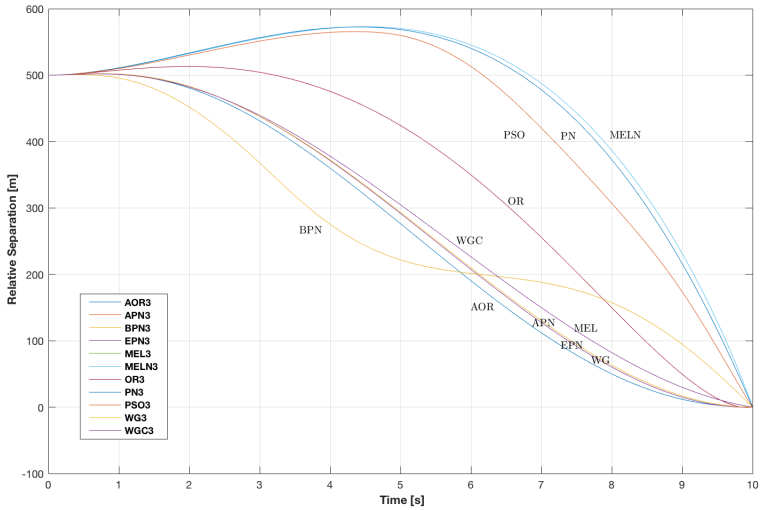

Figure 7.8 : Case 3 - flight paths.

Hitting angles can be seen in Figure 7.9. As previously mentioned AOR is the optimal trajectory guidance law against moving targets. AOR hits the target with zero angle. Also, WG, APN and WG hit the target with almost zero angle. In order to increase impact of the hit, trajectory shaping is one of the methods that can be used.

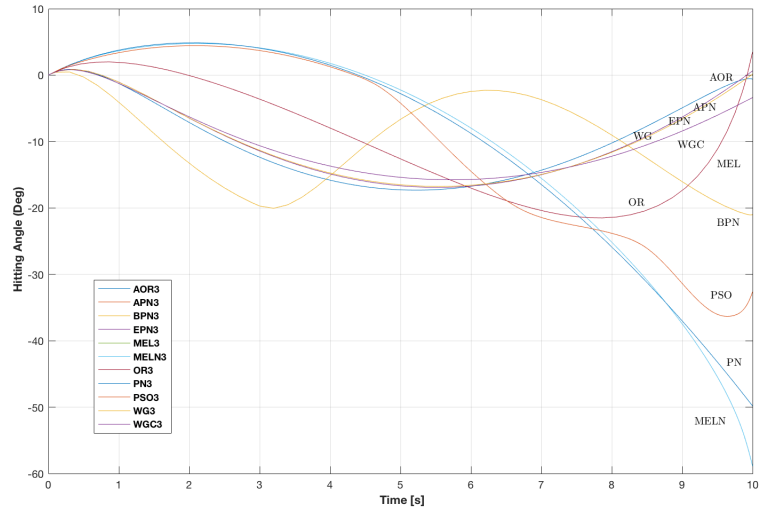

Figure 7.9 : Case -3 hitting angles.

Case 4 represents the first order lag homing loop with given initial heading error of 20 deg. It means that the missile heading is not pointed to that target. In real life application, missiles can not fired directly to the target. Initial heading error of 20 deg is an applicable value. From miss distance results seen in Figure 7.10, compansated guidance laws, MEL, MELN and WGC, are found to be the best choice with less than 0.15m miss distance results at 3 to 10 seconds of flight time. DG is found to be inapplicable if the missile does not directly fired to the target. Also OR and AOR are highly sensitive to initial heading errors.

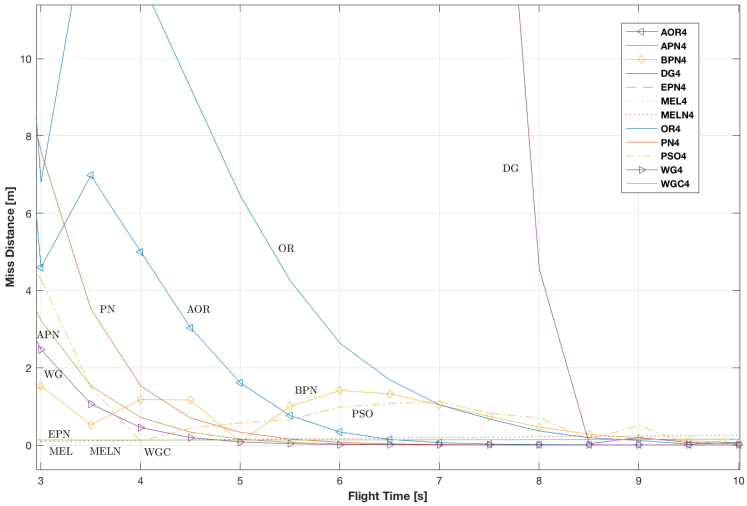

Figure 7.10 : Case 4 - miss distance results.

This sensitivity is reflected on hitting angle results too in Figure 7.11. OR in Case 1 and 2 hits the target with zero hitting angle, but in here 5 degrees is achieved even if there was 10 seconds of flight time. Also, OR requires the most control effort among guidance laws together with MELN in Figure 7.12. In Figure 7.13, commanded acceleration results can be seen. Commanded acceleration is generated from guidance module and transmitted to flight control system as previously explained. It can be clearly seen that OR and MELN acceleration commands are reached the previously defined physical limit of the missile $\pm 45g$. Also even if it is not perfectly seen in figures, AOR is also reached the minimum acceleration limit $-45g$ before hit the target.

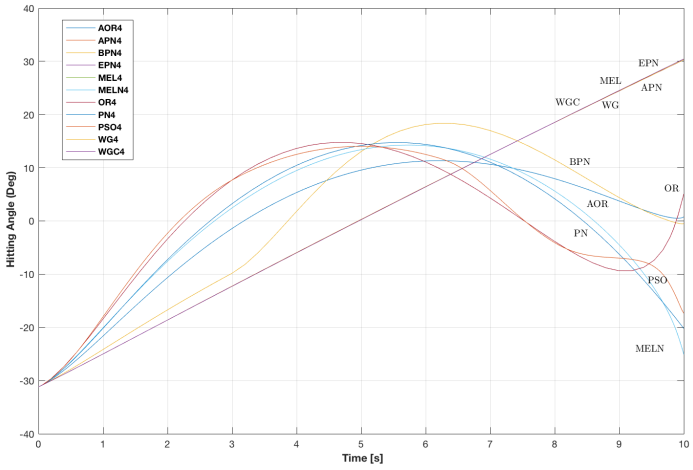

Figure 7.11 : Case 4 - hitting angle results.

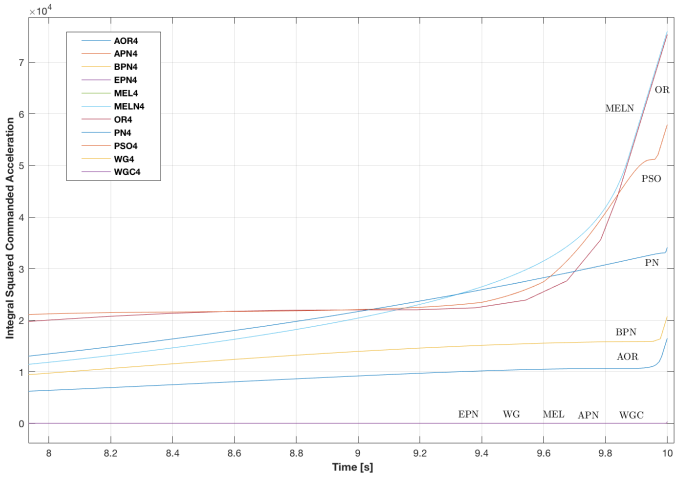

Figure 7.12 : Case 4 - control effort results.

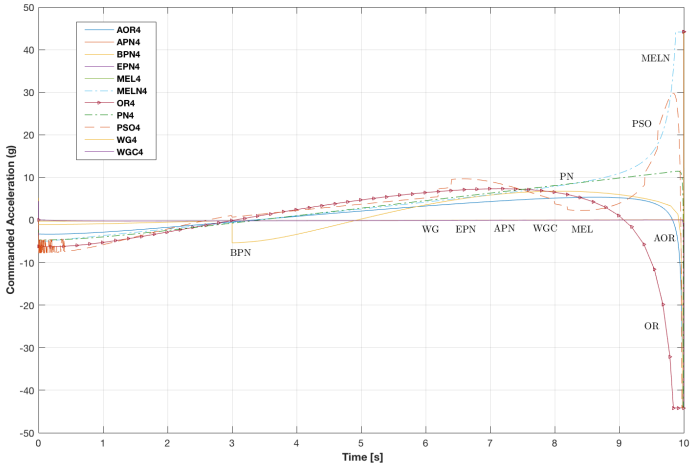

Figure 7.13 : Case 4 - commanded acceleration results.

Case 5 represents the first order lag homing loop with the radome effect. In this case disturbances are 3g constant target acceleration and -0.01 radome slope. Miss distance results can be seen in Figure 7.14 and Figure 7.15. In order to be more descriptive, results are divided into two figures. Compansated guidance laws, MEL, MELN and WGC miss distances are all stable at all the flight time and less than a 3 meter. PSO tries to find optimal effective navigation ratio between 3 and 5. Fluctuations in results can be seen in PSO. On the other hand PN uses effective navigation ratio 3. It can be concluded that PN gives better results than PSO in this case. It means that radome slope affects on the PSO miss distance results. All the guidance laws hit the target in desired range if flight time is greater than 5 seconds. Hitting angles and flight path results are similar to former cases.

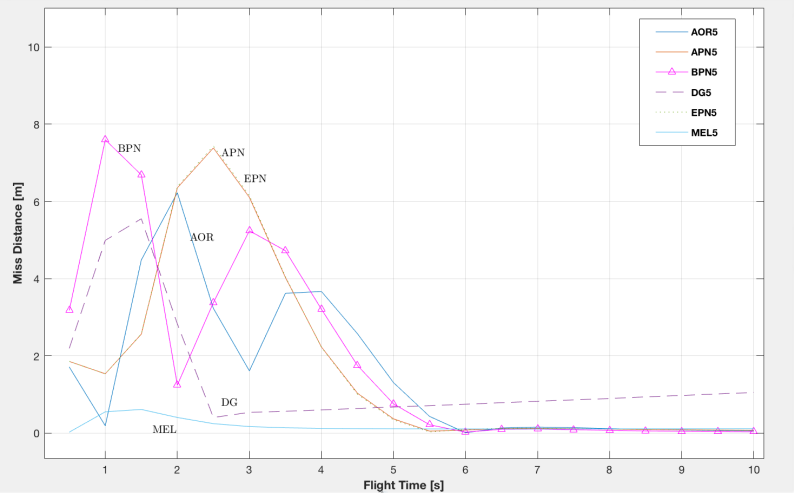

Figure 7.14 : Case 5 - miss distance results.

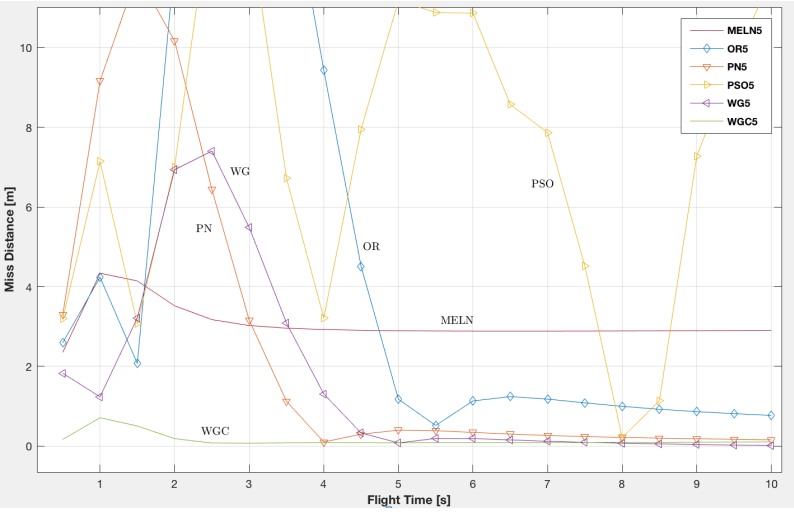

Figure 7.15 : Case 5 - miss distance results.

7.1.2 Optimal evasive target maneuvers

Case 6 represents the first order lag homing loop with optimal target evasive maneuver Barrel-Roll and given initial 1000m relative distance. Disturbances are 3g Barrel Roll maneuver and radome slope. In order to make case difficult, relative seperation as an initial condition was added. Miss distance results can be seen in Figure 7.16 and 7.17. Terminal velocity contrained guidance laws OR and AOR gave poor results by higher than 10m at all the flight time. PN and EPN have similar characteristics after 5 seconds. In BPN and DG, It took time to get into stable phase after 7 seconds. Best results are achived by compansated guidance laws such that MEL, MELN and WGC at all the flight time. Also APN and WG are found to be useful against weaving target.

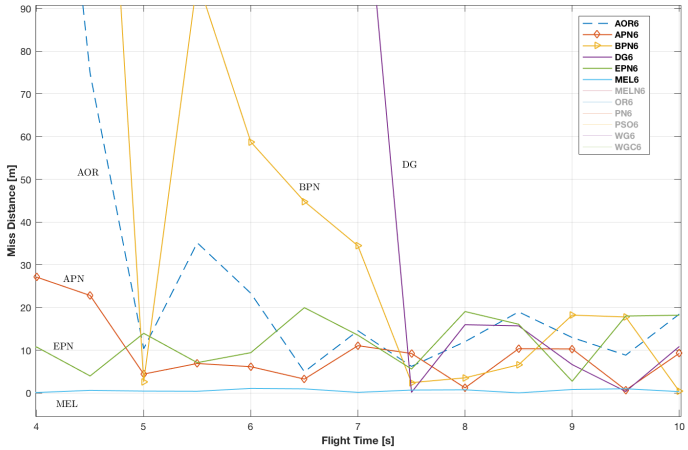

Figure 7.16 : Case 6 - miss distance results.

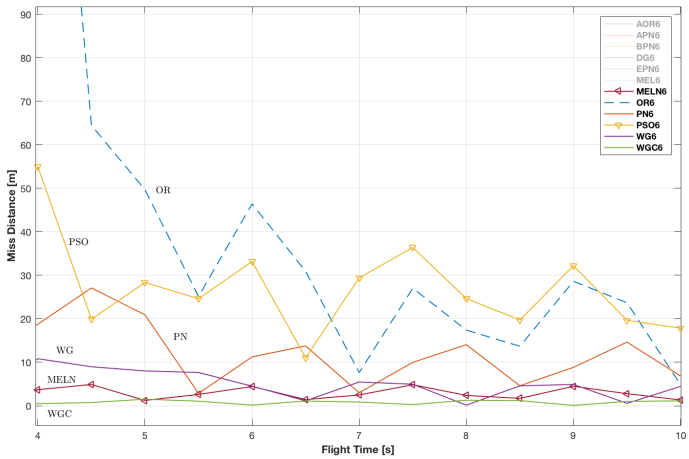

Figure 7.17 : Case 6 - miss distance results.

It can be seen in Figure 7.18 and 7.19 that WGC requires less control effort than any other guidance law against weaving target. Classical PN requires two times higher control effort than WGC. Also WG can be useful against weaving target even if compansation term is not included in guidance law. It can deduced with the help of miss distance and control effort results that, target's weaving maneuver has much more effect on missile performance than guidance delay in this case.

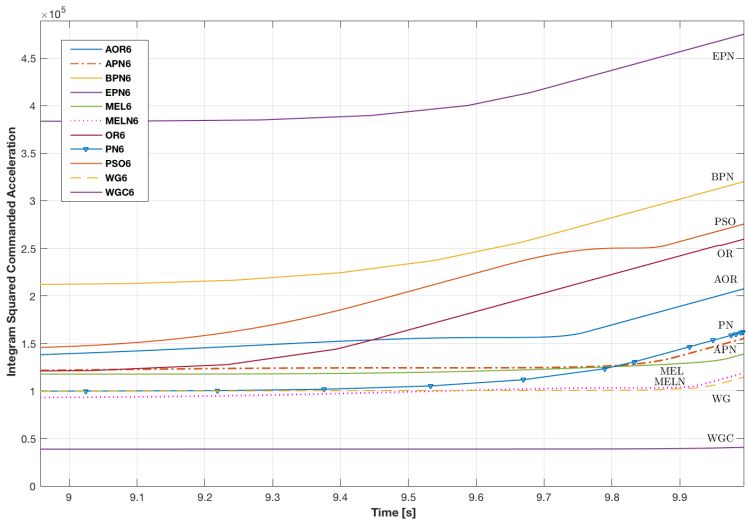

Figure 7.18 : Case 6 - control effort results.

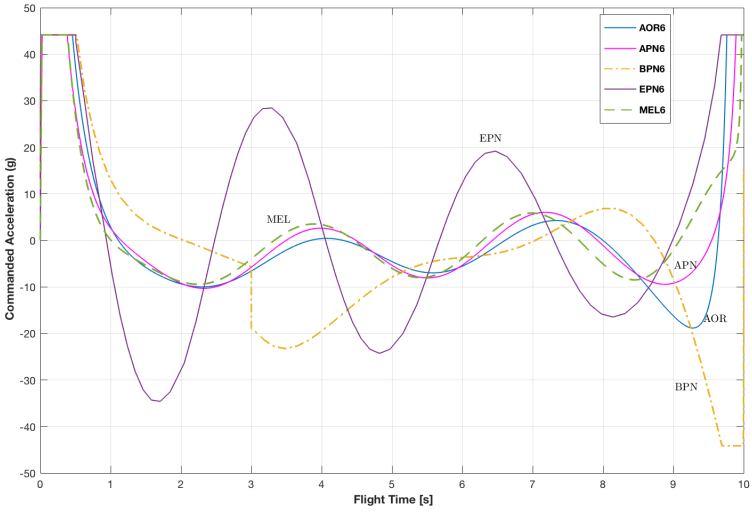

Figure 7.19 : Case 6 - commanded acceleration results.

It can be seen in Figure 7.20 that, only WGC does not use physical limits of the missile. Maximum achieved acceleration in WGC law is +25g in this case. On the

other hand other guidance laws are reached the $\pm 45g$ acceleration limit at the beginning and the end of the simulation in 10 seconds run. Hitting angle results can be seen in Figure 7.21 and 7.22. Trajectory shaped guidance law AOR hits the target with 10 deg. It can be said that trajectory shaping with AOR is ineffective against weaving target.

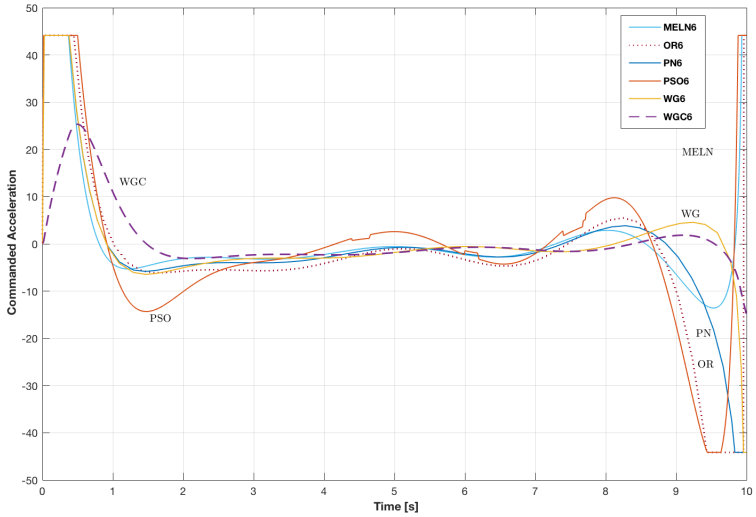

Figure 7.20 : Case 6 - commanded acceleration results.

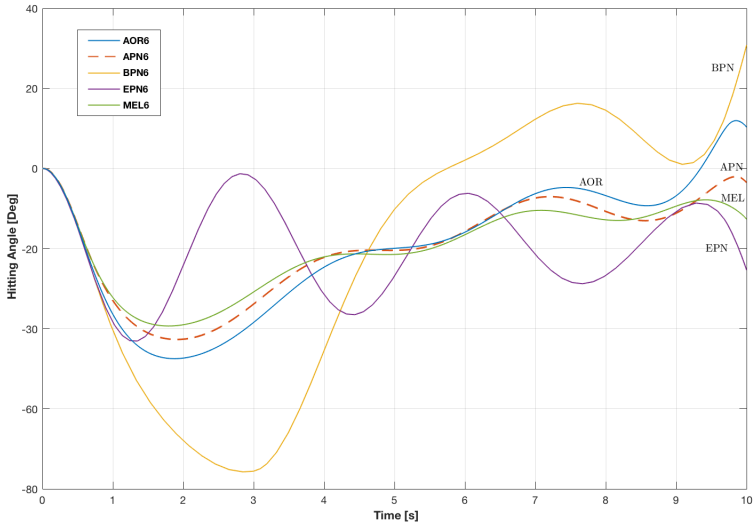

Figure 7.21 : Case 6 - hitting angle results.

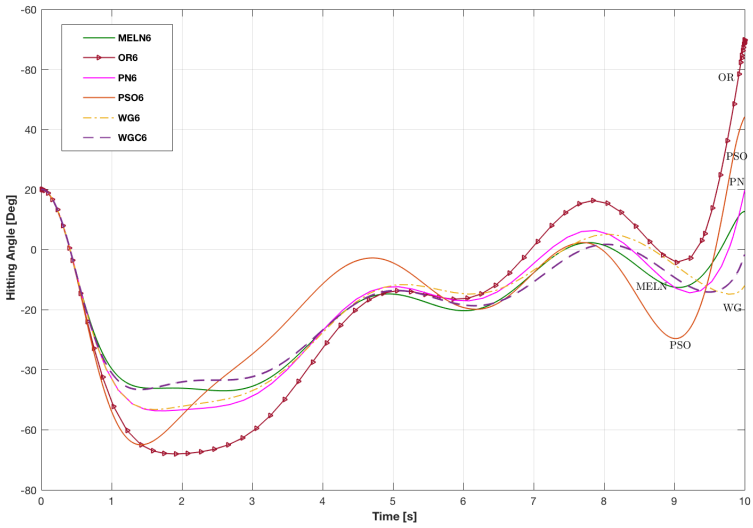

Figure 7.22 : Case 6 - hitting angle results.

Case 7 represents the first order lag homing loop with optimal target evasive maneuver Vertical-S and given initial 1000m relative distance. In this case only difference from former one is the target maneuver type. In literature Barrel-Roll maneuver is more optimal than Vertical-S type evasive maneuver. It is reasonable to compare these evasive weaving maneuvers and results. Miss distance results can be seen in Figure 7.23 and 7.24. It can be seen that miss distance results of Vertical-S maneuver are similar to Barrel-Roll maneuver expept PN and PSO results. PN and PSO gave a little bit poor results against Vertical-S maneuver. Even if target is not moving sinusoidal in Vertical-S maneuver, WGC and WG are found to be applicable against such target. Also, MEL and MELN gave superior results in this case.

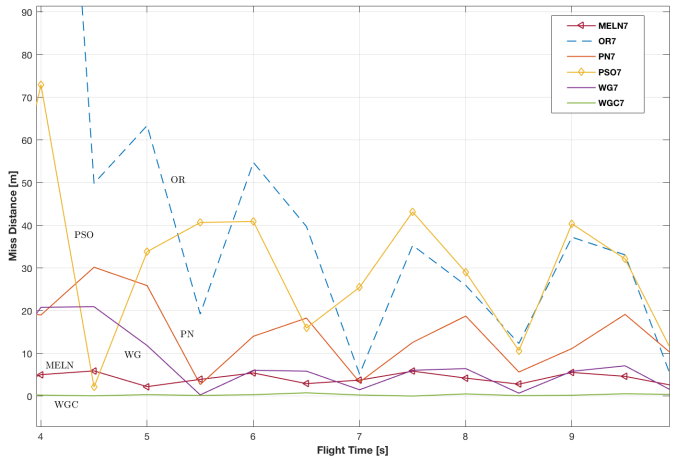

Figure 7.23 : Case 7 - miss distance results.

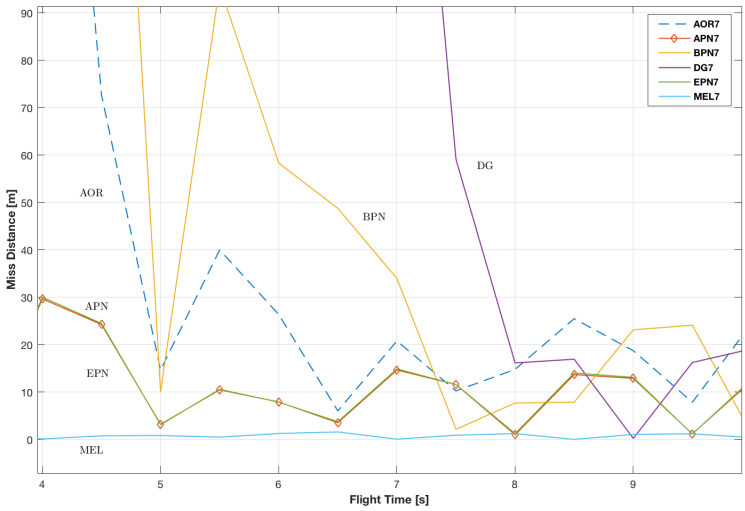

Figure 7.24 : Case 7 - miss distance results.

Control effort results for 10 seconds of flight time can be seen in Figure 7.25. Main difference from former case is WG and WGC which gave same optimal results in here. Also EPN reduces its control effort here from 4.7e5 to 1.7e5.

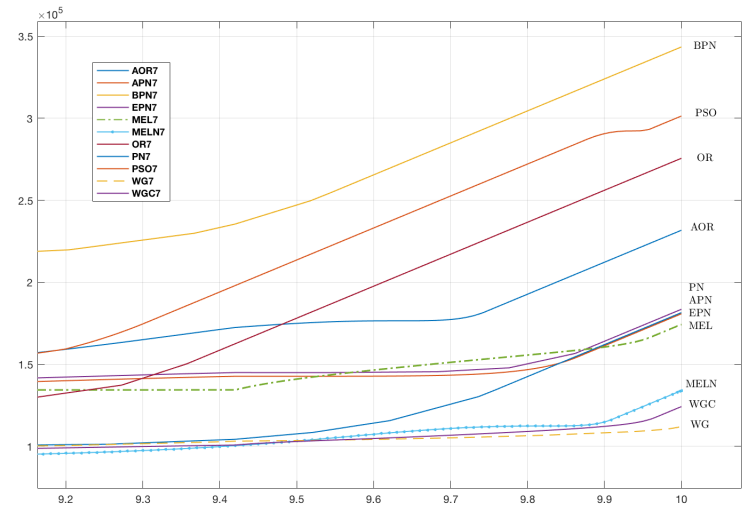

Figure 7.25 : Case 7 - control effort results.

Case 8 represents the first order lag homing loop with 2g constant jerk target maneuver. It means that target constantly increases its acceleration in one direction. Also, radome slope distrubance is added into guidance loop. Maneuver starts with the 2g acceleration at the beginning and reaches up to 20g acceleration at t=10s. Miss distance results can be seen in Figure 7.26. It may be concluded that PN, MELN and OR guided missiles can not accomplish the mission in desired range if flight time is

more than 3s. On the other hand target acceleration limit does not effect the EPN, AOR, APN, MEL, WG, WGC in this case.

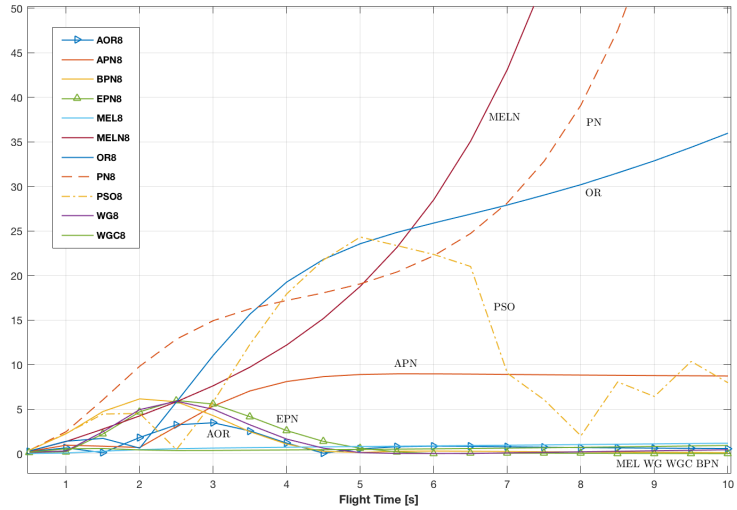

Figure 7.26 : Case 8 - miss distance results.

Control effort results of 10 seconds flight time can be seen in Figure 7.27. It may be reviwed that minimum efforts are achieved by EPN, WGC and WG. It is not suprising that EPN uses target jerk measurements to minimize commanded acceleration requirements.

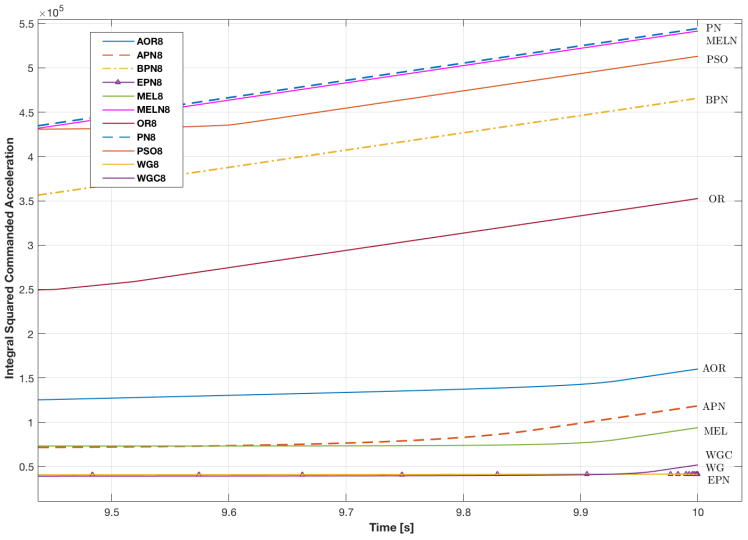

Figure 7.27 : Case 8 - control effort results.

7.2 Noise Filter Added Homing Loops

Scenarios from Case 9 to Case 17 belong to this section. Here, noise terms are added into homing loops. Target maneuvers, radome effects and guidance delays are considered. Firstly constant acceleration target maneuver with range independent noise added cases will be shown then barrel roll and vertical-s evasive maneuvers with glint, range dependent and independent noise added cases will be investigated.

7.2.1 Constant acceleration target maneuvers

Case 9 represents the first order lag noise filter added homing loop with 3g constant maneuver and 2MR range independent noise. Noise term is added into line of sight measurements. Kalman filter is used as an optimal noise filter in this case. Kalman filter gives an optimal estimates of target states: relative position, relative velocity and relative acceleration. Disturbances in this scenario are 3g constant maneuver, 2MR zero mean white gaussian noise ~ $N(0,4MR^2)$. Miss distance results can be seen in Figure 7.28 and 7.29 and corresponding standard deviations can be seen in Figure 7.30 and 7.31.

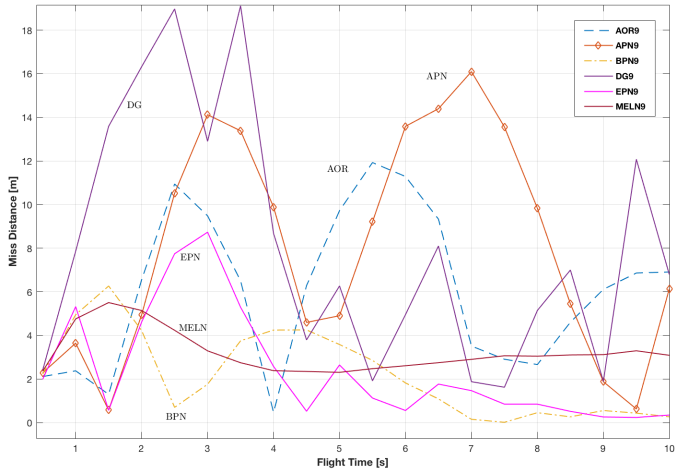

Figure 7.28 : Case 9 - miss distance results.

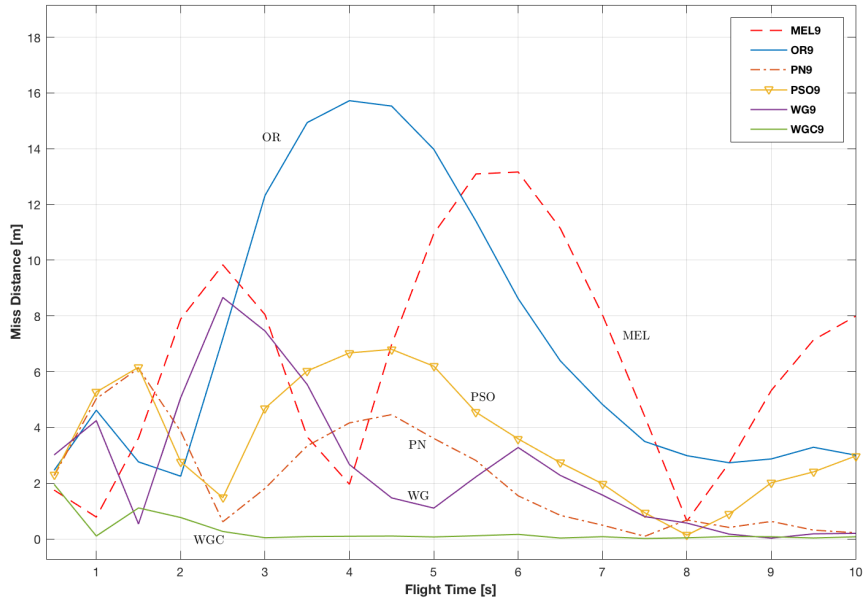

Figure 7.29 : Case 9 - miss distance results.

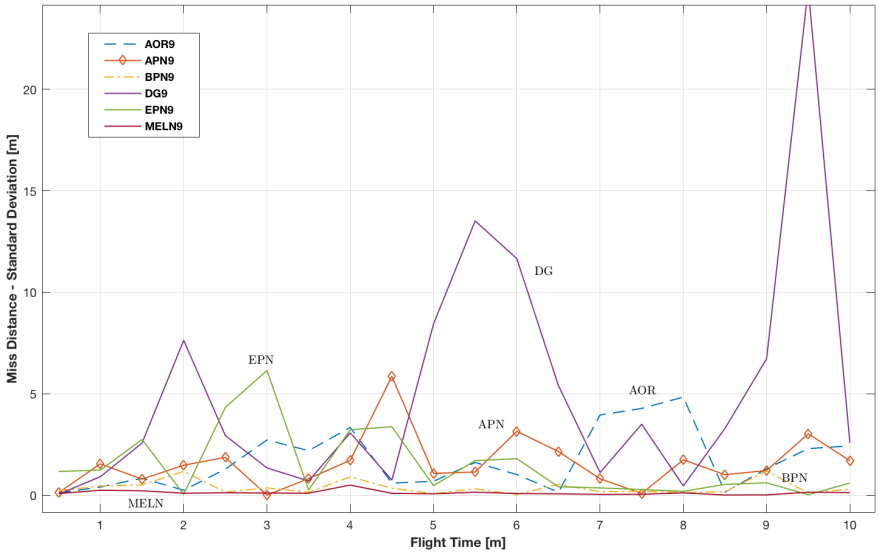

Figure 7.30 : Case 9 - standard deviation results.

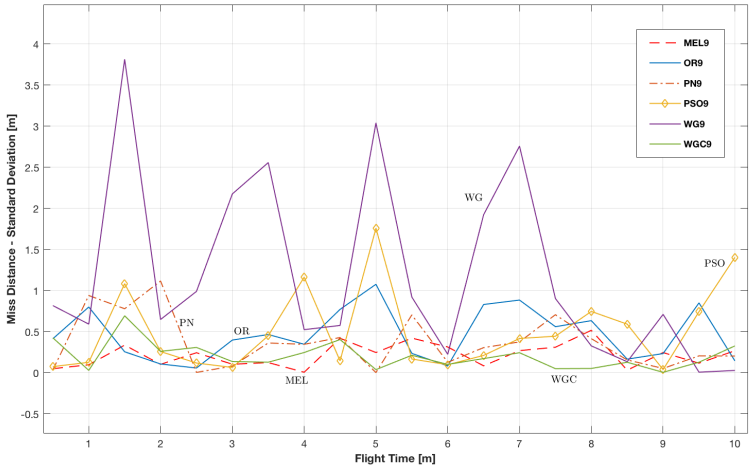

Figure 7.31 : Case 9 - standard deviation results.

It may be viewed that noise term effects the miss distance results significantly. No matter what kind a disturbance is added into guidance loop, WGC hits the target less than a meter at all the flight time. On the other hand, PN, PSO, MELN, BPN, EPN and WG gave acceptable results in this case. It is quite obvious that APN and AOR do not meet the requirements all the flight time. It may be observed that APN and AOR use unmatching target acceleration measurements. Hence fluctuations in acceleration measurements affect the miss distance quite a lot. Estimated and Actual values of target states in EPN and APN homing loop can be seen in Figure 7.32 and 7.33. All the guidance laws use the measured states in calculations.

Case 10 represents the first order lag noise filter added homing loop with 3g constant maneuver and 2MR range independent noise. Initial conditions are the different in this case. Initial relative separation and heading error are considered this time. Disturbances in this scenario are 3g constant maneuver, 2MR zero mean white gaussian noise ~ $N(0,4MR^2)$. Miss distance results can be seen in Figure 7.34 and 7.35 and corresponding standard deviations can be seen in Figure 7.36 and 7.37. Flight time between 4 to 10 seconds results are given in figures. Initial heading error and relative separations have an impact upon the miss distance results on APN, BPN, AOR, DC, OR and MEL. It takes around 7 secods to get into stable position in these guidance laws. On the other hand, four state filter used guidance laws such as EPN, WGC and WG are found to be well suited into this kind of scenario. Estimated and

actual values of target states in OR homing loop can be seen in Figure 7.38 as an example to this engagement.

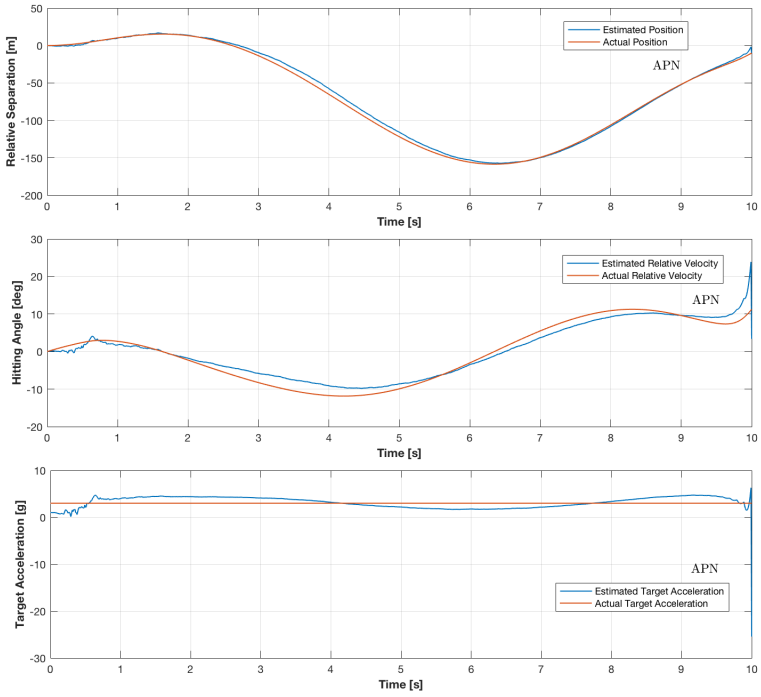

Figure 7.32 : Case 9 - APN target state estimations.

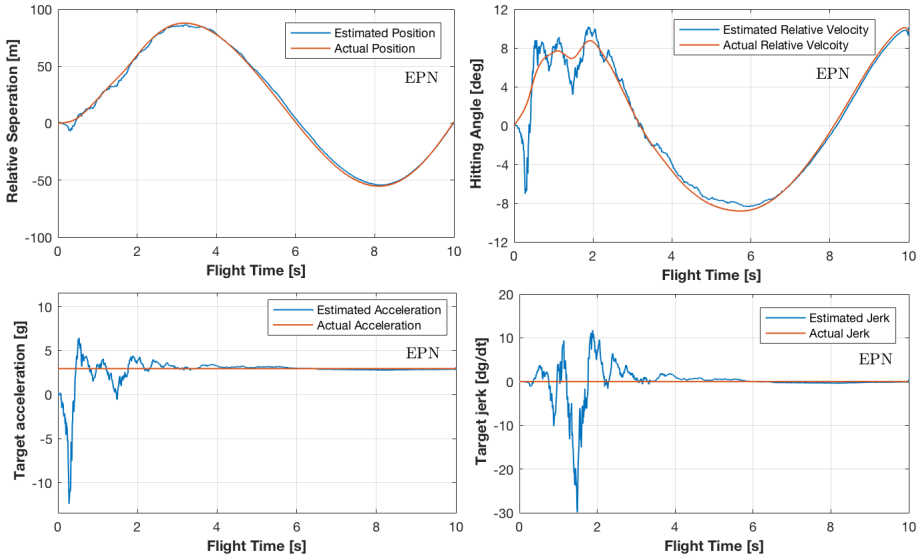

Figure 7.33 : Case 9 - EPN target state estimations.

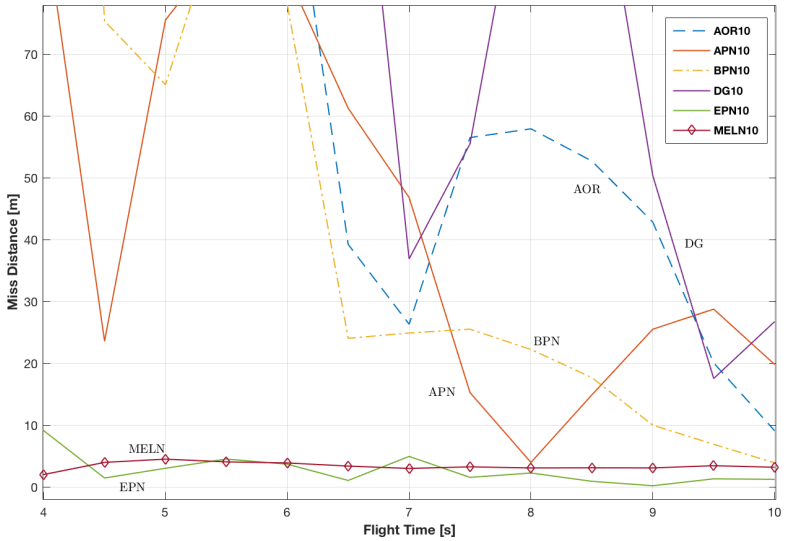

Figure 7.34 : Case 10 - miss distance results.

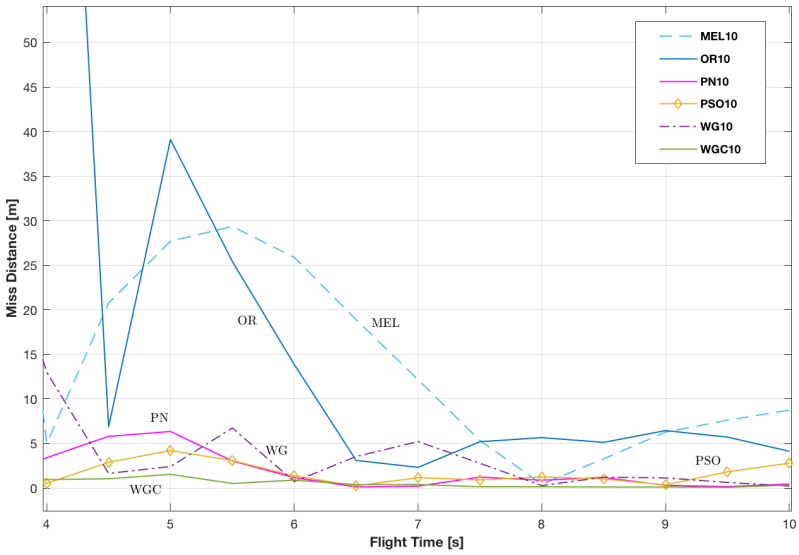

Figure 7.35 : Case 10 - miss distance results.

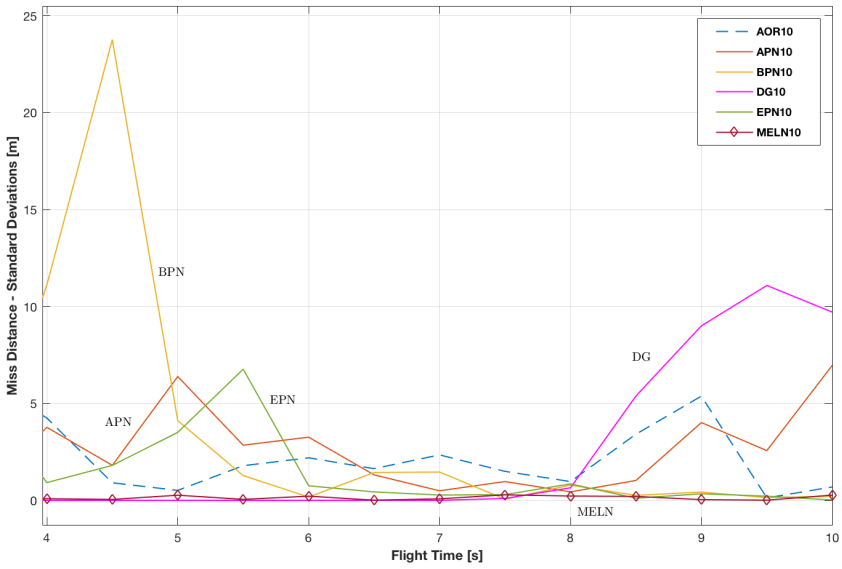

Figure 7.36 : Case 10 - standard deviation results.

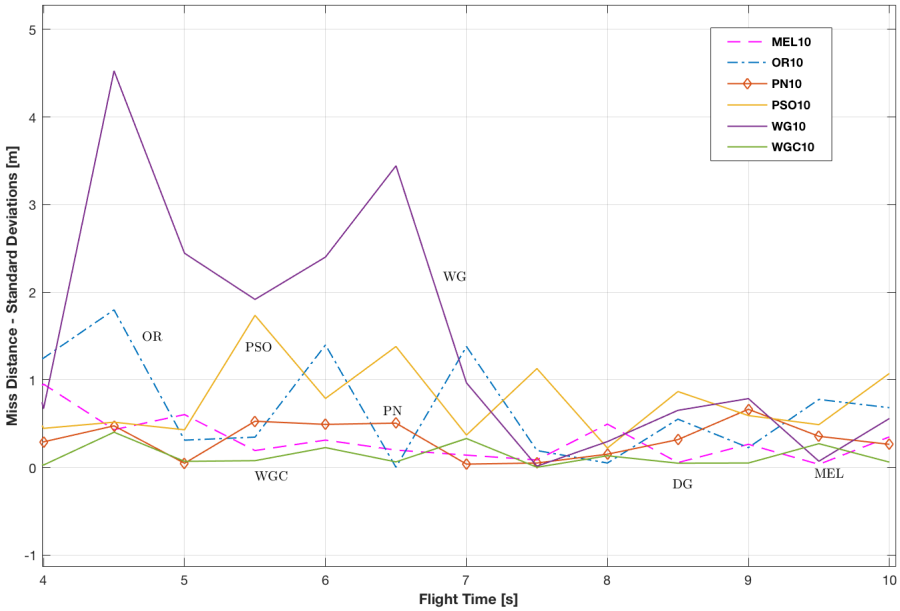

Figure 7.37 : Case 10 - standard deviation results.

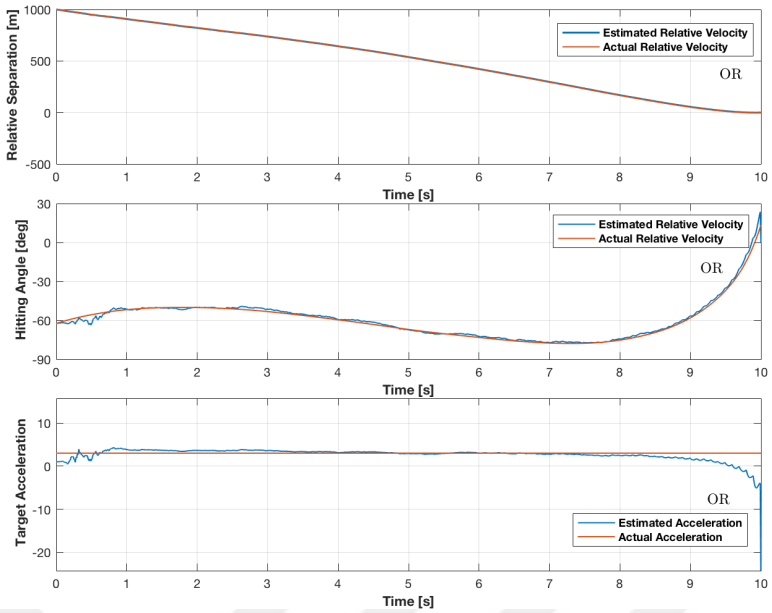

Figure 7.38 : Case 10 - OR target state estimations.

Case 11 represents the first order lag noise filter added homing loop with White Gaussian random maneuver $\sim N(0, \sigma^2 = 9g^2)$, 0.1 seconds sample rate, and 2MR range independent noise. Here target maneuvers randomly in $\pm 3g$ standard deviaton. Miss distance results can be seen in Figure 7.39, 7.40 and 7.41. It can be viewed that all guidance laws are effective against random target maneuver even if measurements are corrupted by noise.

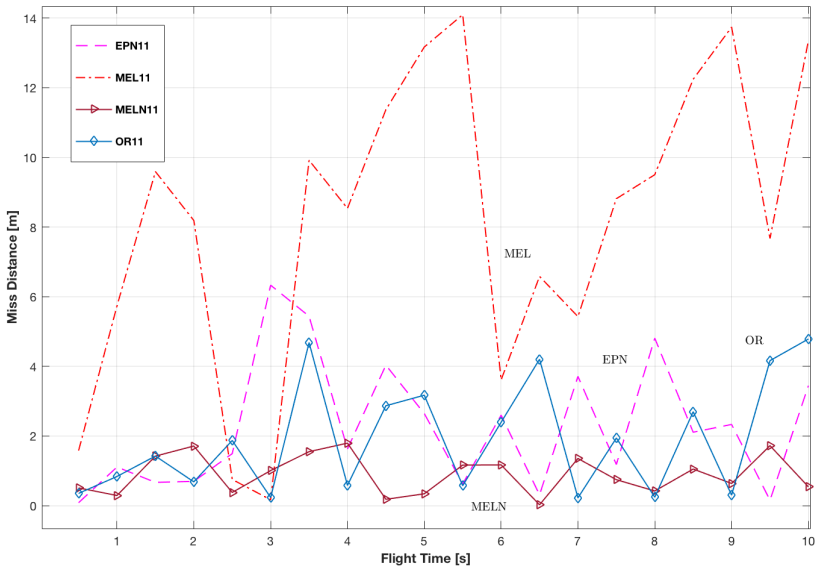

Figure 7.39 : Case 11 - miss distance results.

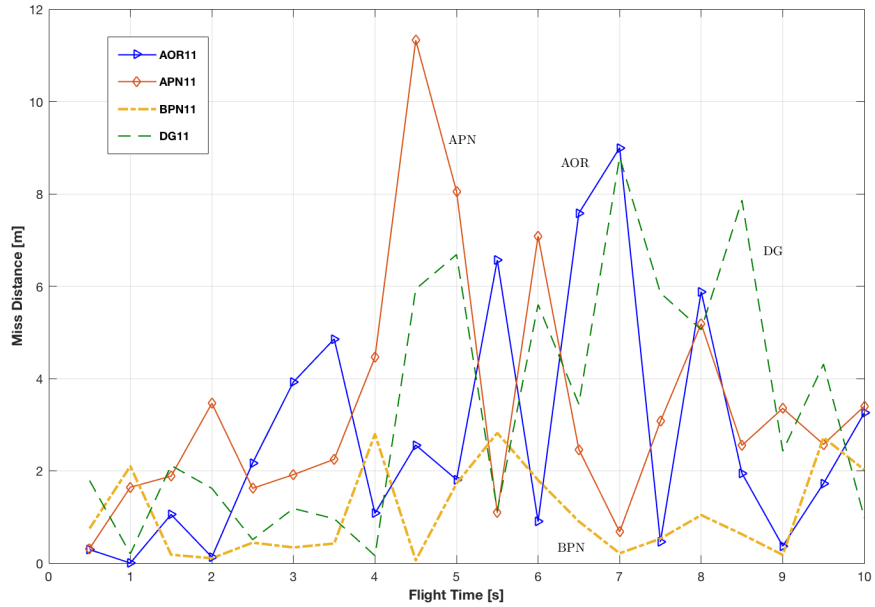

Figure 7.40 : Case 11 - miss distance results.

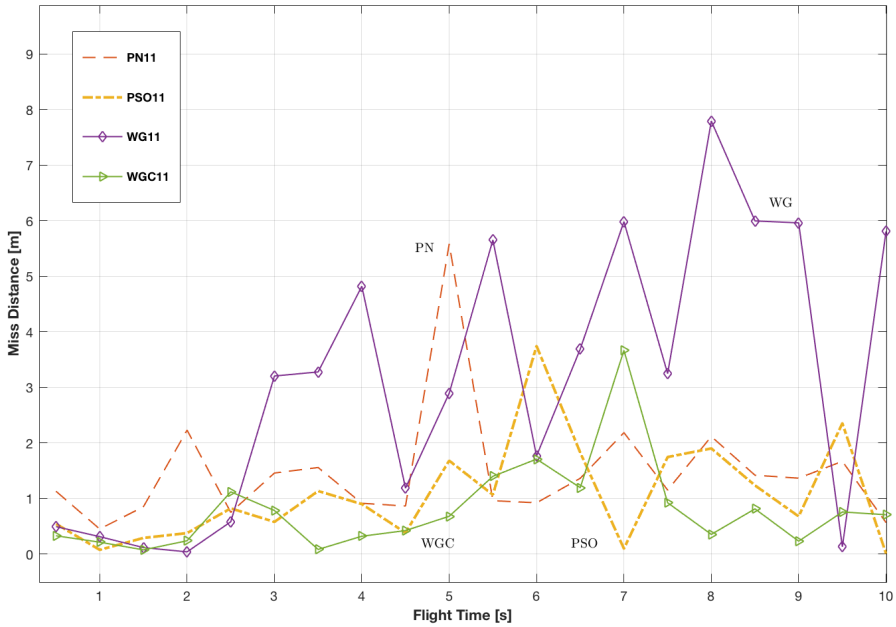

Figure 7.41 : Case 11 - miss distance results.

Control effort results of 10 seconds flight can be seen in Figure 7.42. Somehow PN has the minimum control effort and minimum miss distance achieved among all guidance law in this case. On the other hand, minimum control effort had been achieved by WGC almost all the cases up to now. It can be considered such that two

stated guidance laws, PN, MELN, PSO etc. are less sensitive to random target maneuver since target acceleration and jerk measurements are not taking into account in these guidance laws. Hence it can be said that response speeds are less than the others.

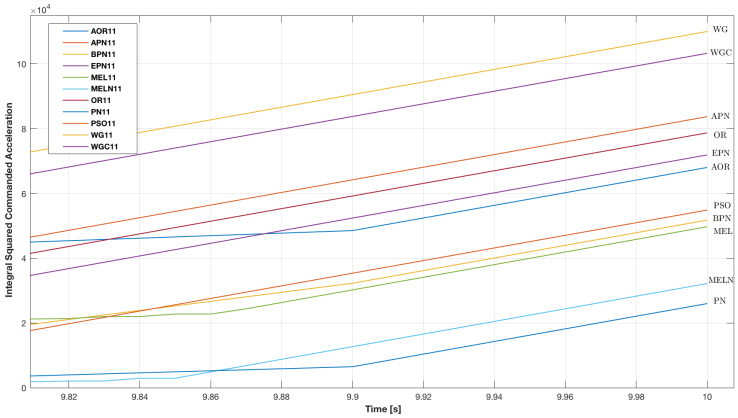

Figure 7.42 : Case 11 - control effort results.

Estimated and actual values of target states in MELN homing loop can be seen in Figure 7.43 as an example to random target maneuver homing loop.

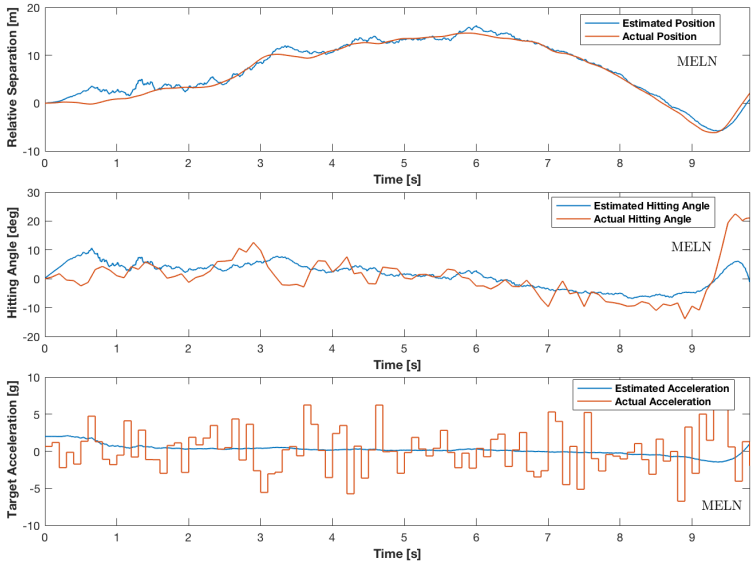

Figure 7.43 : Case 11 - MELN target state estimations.

Case 12 represents the first order lag noise filter added homing loop with 3g constant maneuver and 3m glint, 1MR range independent and 4MR range dependent noise.

Disturbances are target maneuver and noise terms in this case. Glint and range dependent noises are added in addition to Case 10. Miss distance results may be viewed in Figure 7.44 and 7.45 corresponding standard deviantions in Figure 7.46 and 7.47. Kalman filter in guidance loops is set up to 2MR noise. Actual values of noise level seem higher than the 2MR but range dependent noise level decreases by approach and at the end or interception noise vanishes. It was found reasonable to set filter to 2MR noise level.

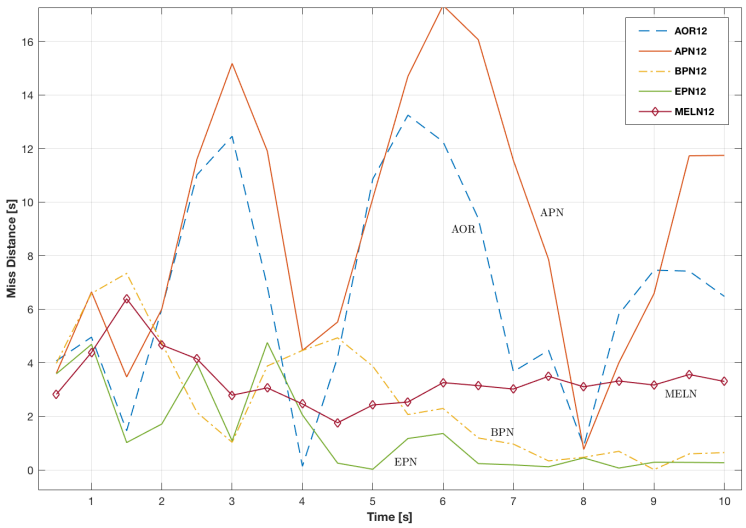

Figure 7.44 : Case 12 - miss distance results.

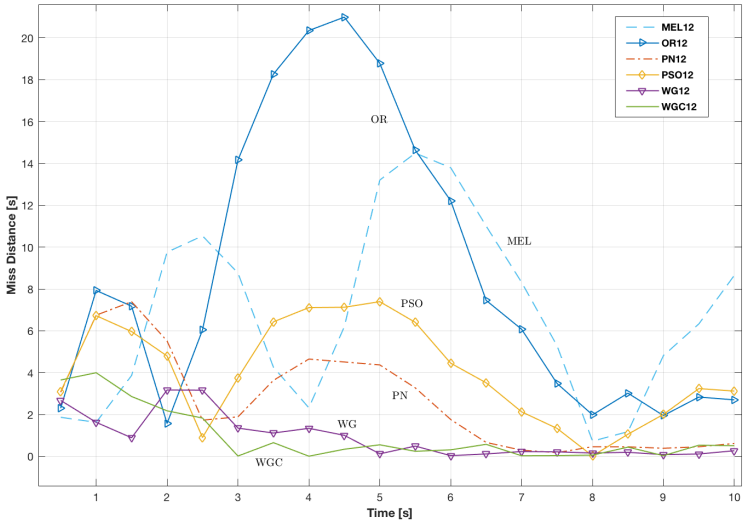

Figure 7.45 : Case 12 - miss distance results.

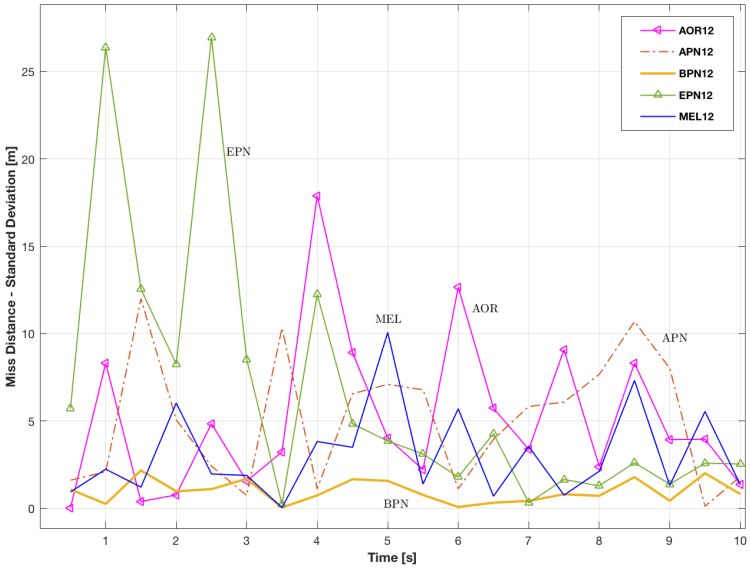

Figure 7.46 : Case 12 - standard deviation results.

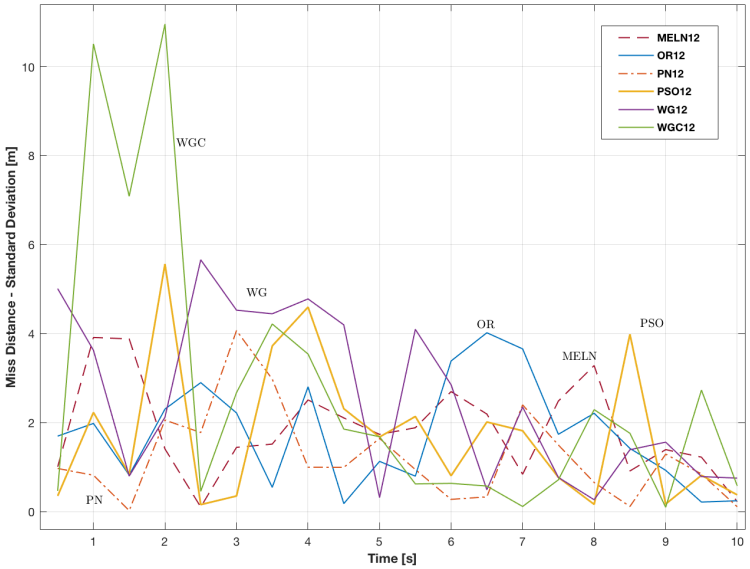

Figure 7.47 : Case 12 - standard deviation results.

It can be viewed in Figure 7.48 that four stated guidance laws such, EPN, WGC and WG laws require much more control effort than the others. Also even if there was noisy measurements, AOR and OR hit the target by zero angle in Figure 7.49.

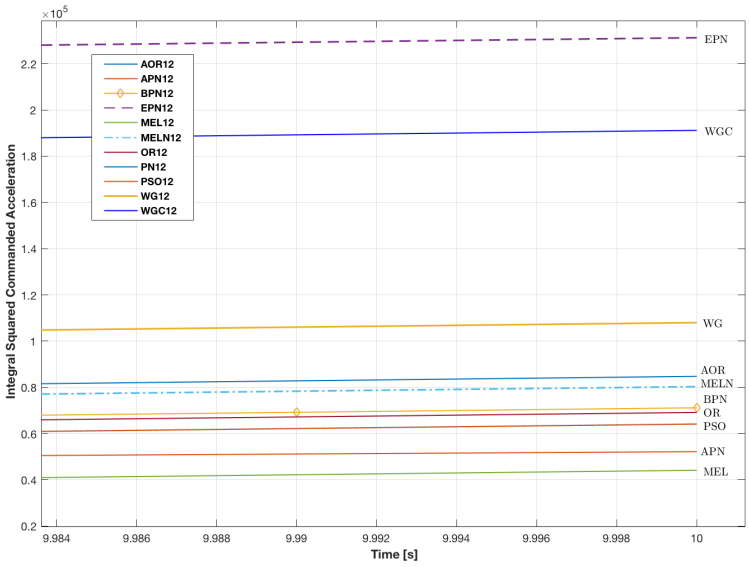

Figure 7.48 : Case 12 - control effort results.

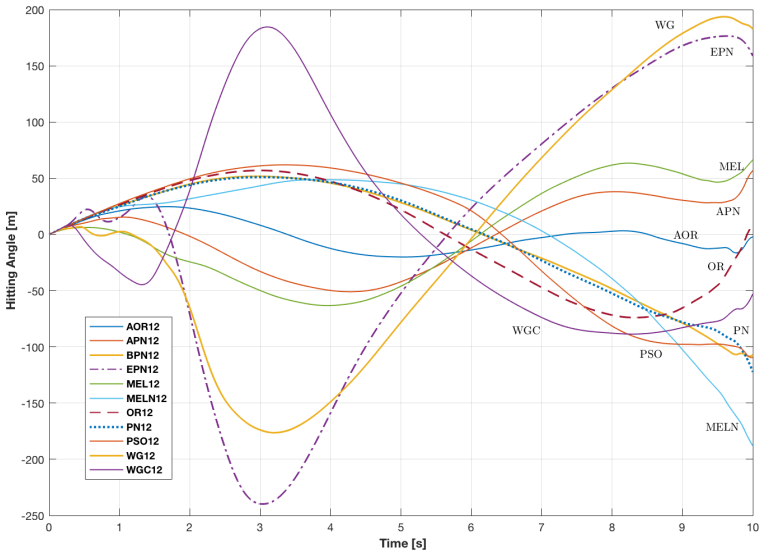

Figure 7.49 : Case 12 - hitting angle results.

Estimated and actual values of target states in AOR homing loop can be seen in Figure 7.50 as an example to multiple noise added homig loop.

Case 13 represents the third order lag noise filter added homing loop with 3g constant maneuver, given initial conditions and 3m glint, 1MR range independent and 4MR range dependent noises. Disturbances are target maneuver and noise terms in this case. First order transfer function is replaced by third order transfer function. 1000m initial relative separation and -20 deg initial heading errors are added in addition to Case 12. Miss distance results may be observed in Figure 7.51 and 7.52 corresponding standard deviations in Figure 7.53 and 7.54. PN, BPN, EPN,PSO,WG and WGC are found to be effective against multiple noise implemented scenarios.

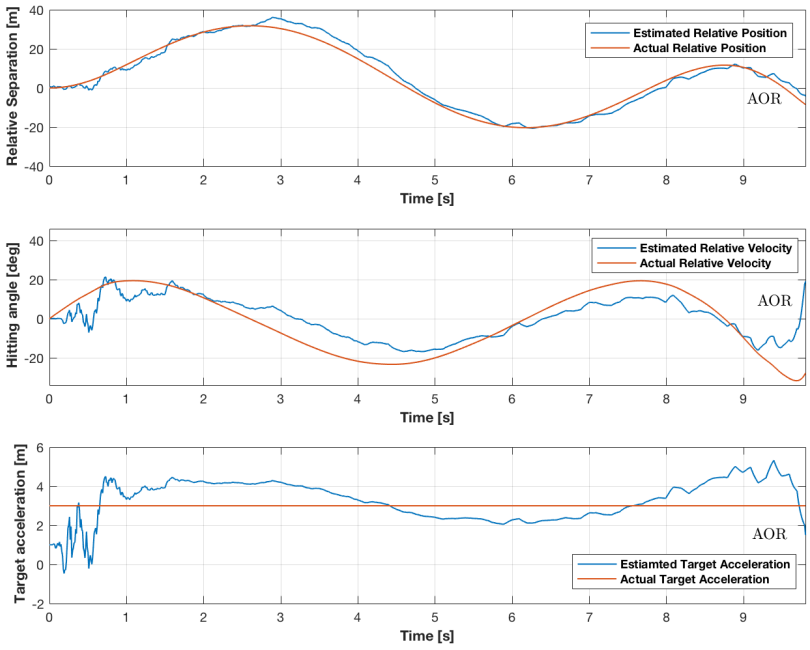

Figure 7.50 : Case 12 - AOR target state estimation.

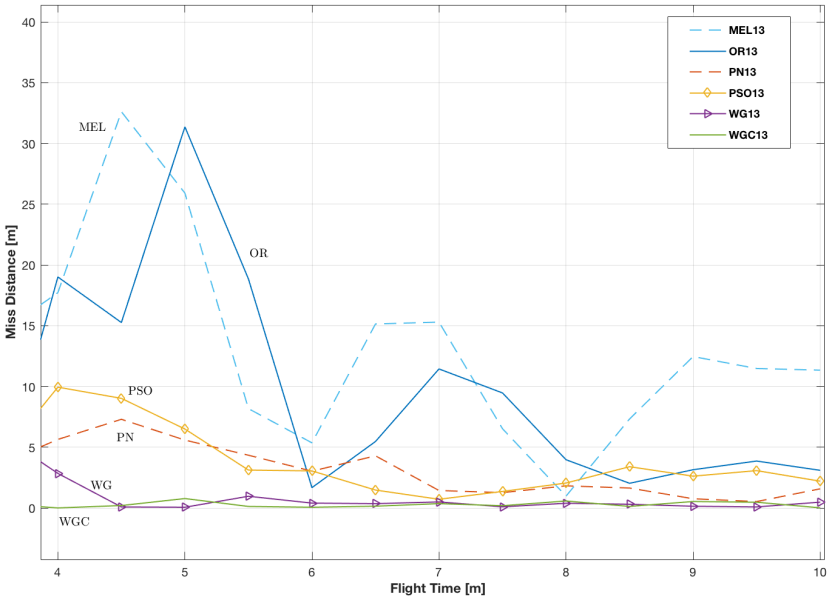

Figure 7.51 : Case 13 - miss distance results.

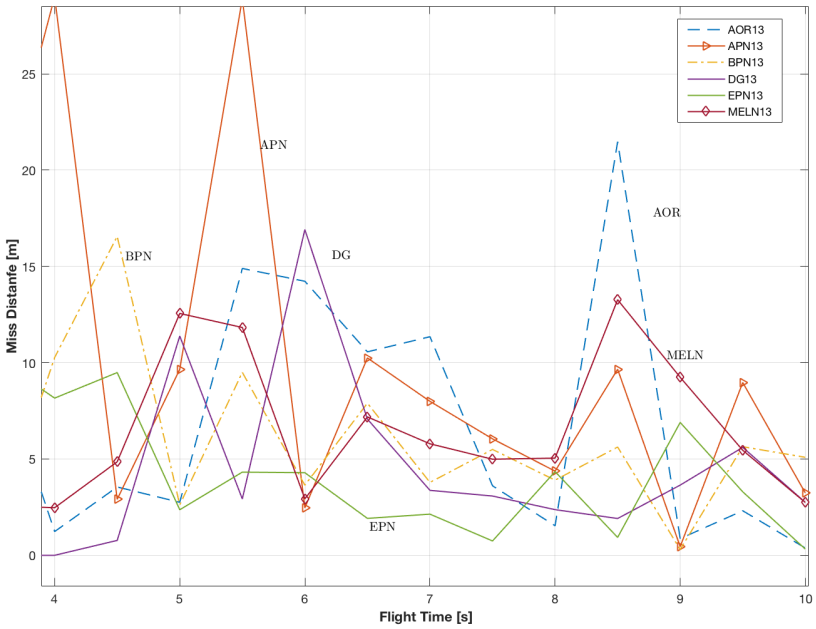

Figure 7.52 : Case 13 - miss distance results.

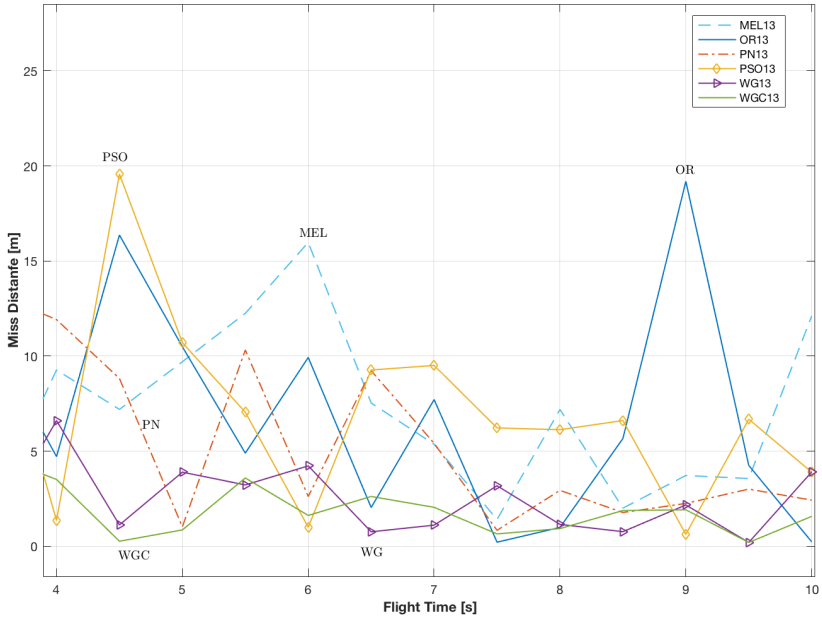

Figure 7.53 : Case 13 - standard deviation results.

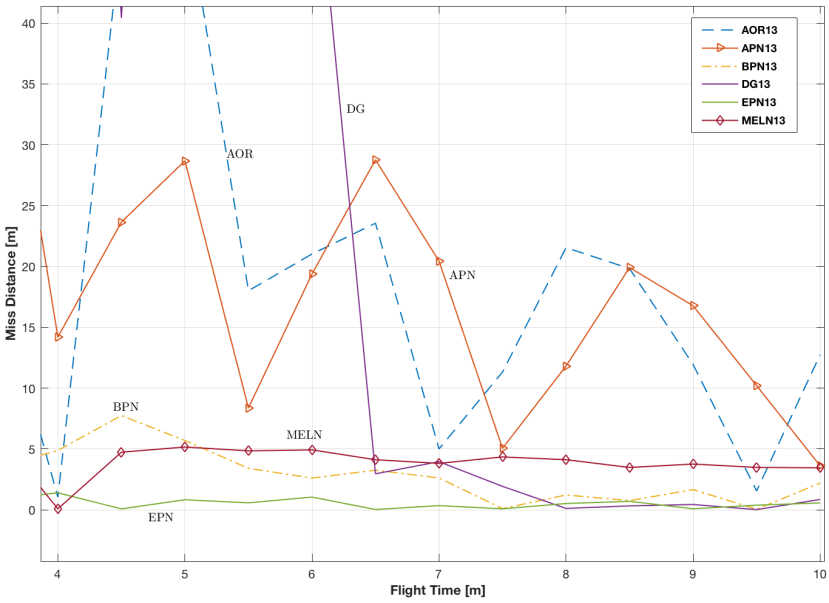

Figure 7.54 : Case 14 - standard deviation results.

Control effort results can be seen in Figure 7.55 corresponding commanded acceleration results in Figure 7.56 and 7.57. Even though target acceleration is 3g, all guidance laws reach the missile's physical limit $45g$ at the end of interception in 10 seconds of flight.

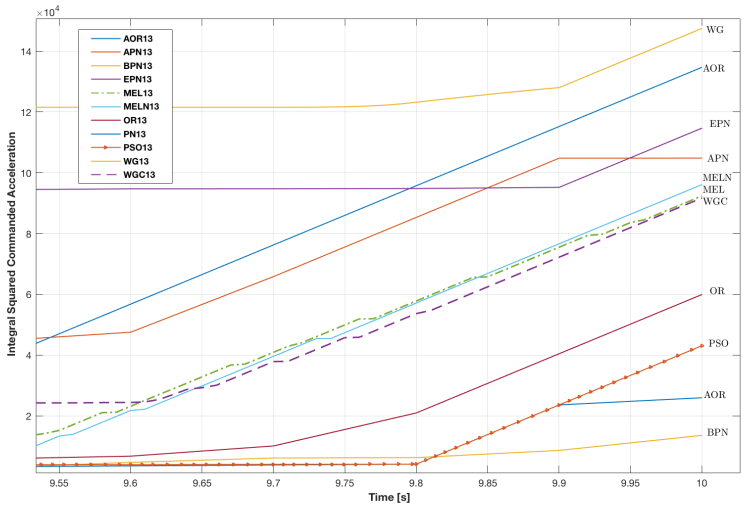

Figure 7.55 : Case 13 - control effort results.

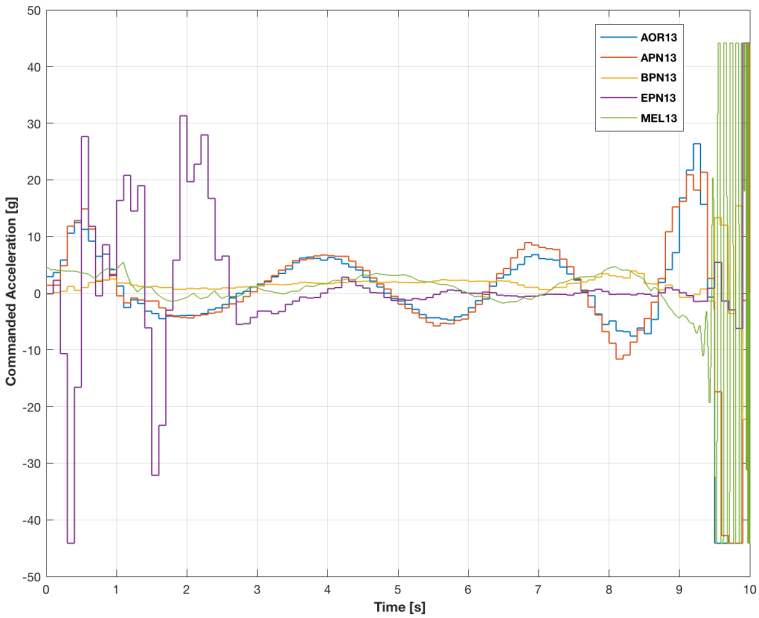

Figure 7.56 : Case 13 - commanded acceleration results.

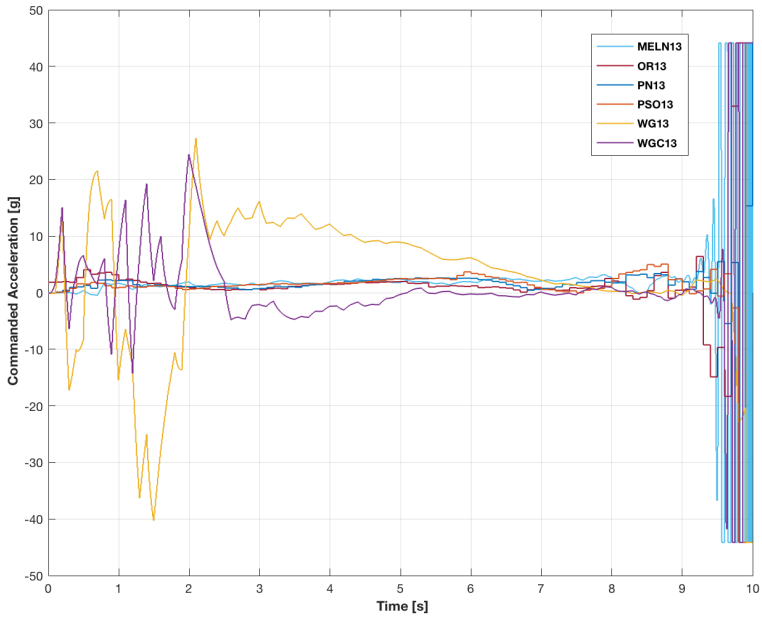

Figure 7.57 : Case 13 - commanded acceleration results.

Estimated and actual values of target states in BPN homing loop can be seen in Figure 7.58 : as an example to multiple noise added third order lag homing loop.

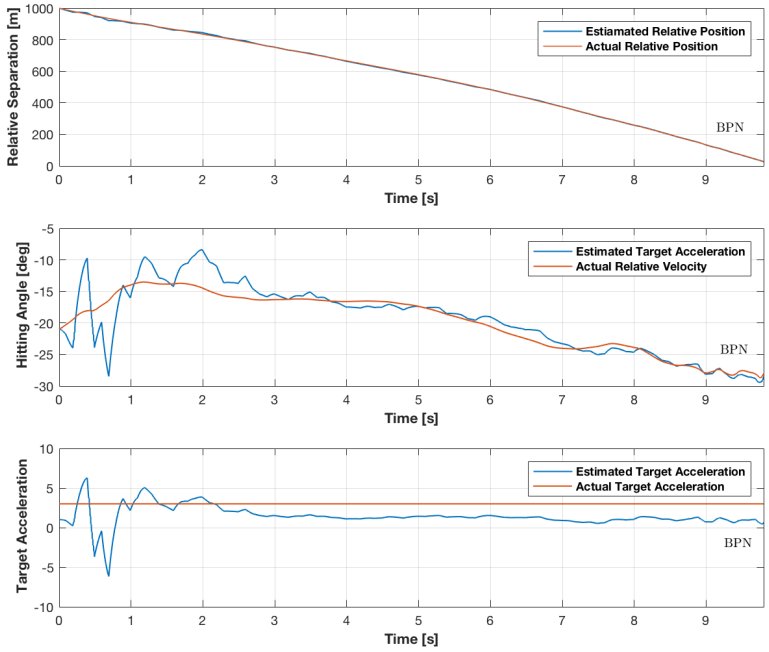

Figure 7.58 : Case 13 - BPN target state estimation.

7.2.2 Optimal evasive target maneuvers

Case 14 represents the third order lag noise filter added homing loop with 3g optimal evasive target maneuver and 3m glint, 1MR range independent and 4MR range dependent zero mean white gaussian noises. Disturbances are 3g Barrel-Roll target maneuver and noise terms in this case. Guidance delay was modeled as third order transfer function. Noise terms are added into actual values of line of sight and relative separation. Kalman filter is used as an optimal noise filter. Miss distance results can be seen in Figure 7.59 and 7.60 and corresponding standard deviations in Figure 7.61 and 7.62. EPN and WGC are seem to be superior to other guidance laws in this case. Other guidance law miss distance results are observed to tend to increase by flight time. It can be thought that it originated from range dependent noise level. In addition to that missile commanded acceleration limit is not enough to hit target in desired range due to target's weaving motion at long flight time. Hitting angle results can be viewed in Figure 7.63. AOR and OR trajectory shaped guidance laws gave poor performance against weaving target and multiple noise sources in this case.

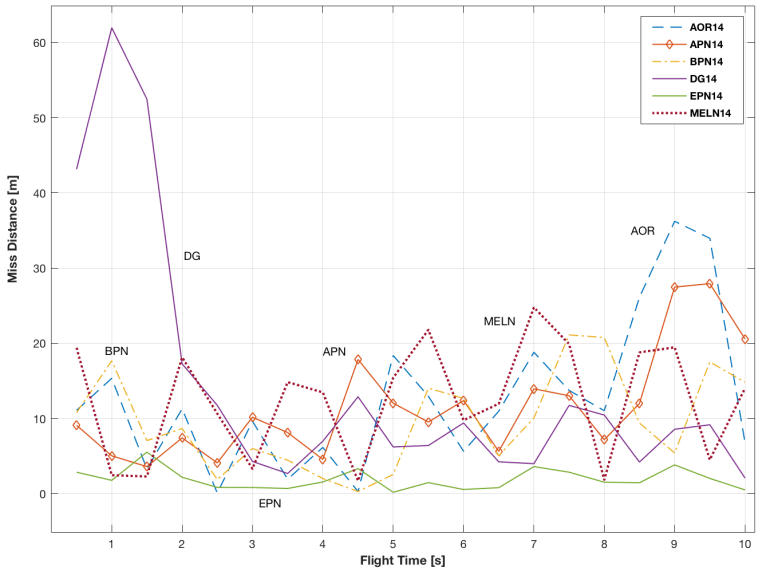

Figure 7.59 : Case 14 - miss distance results.

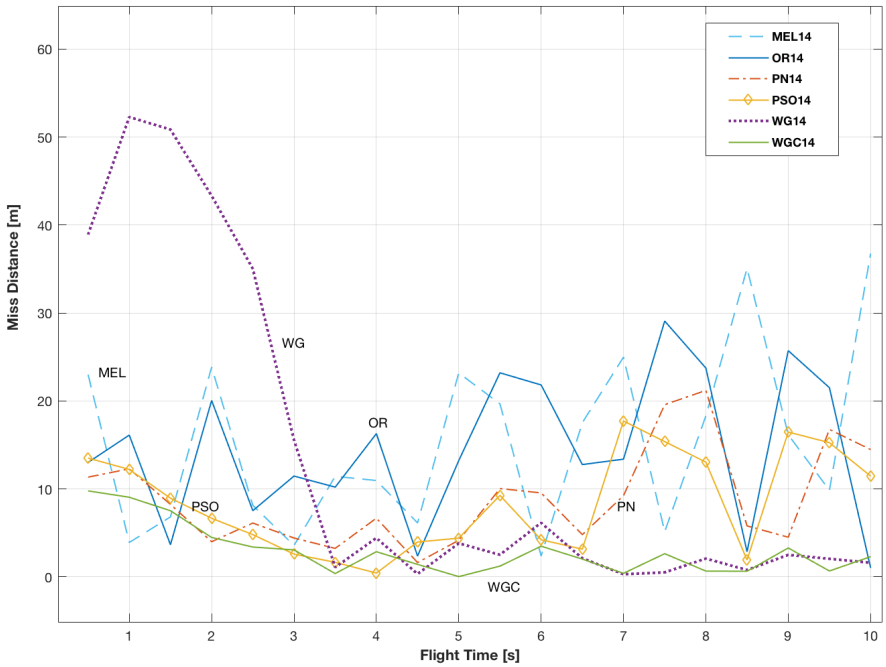

Figure 7.60 : Case 14 - miss distance results.

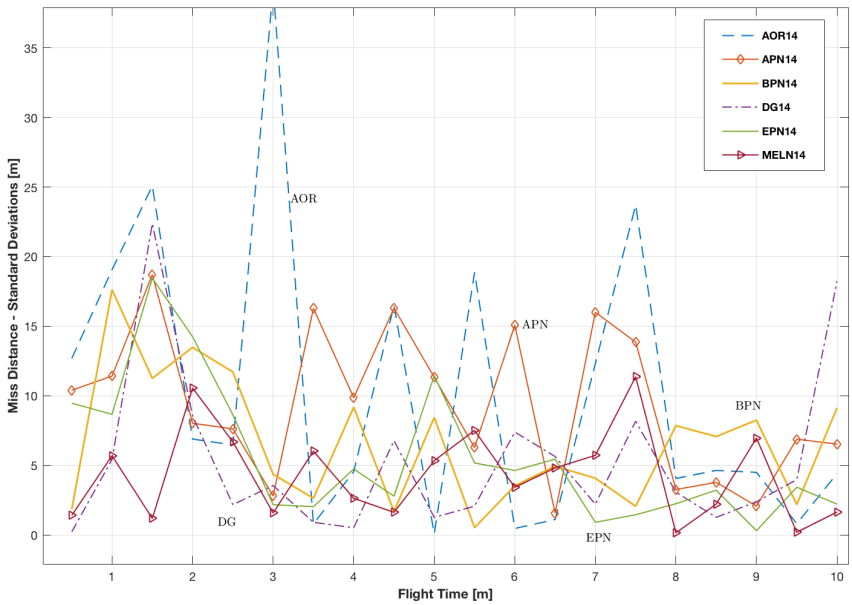

Figure 7.61 : Case 14 - standard deviation results.

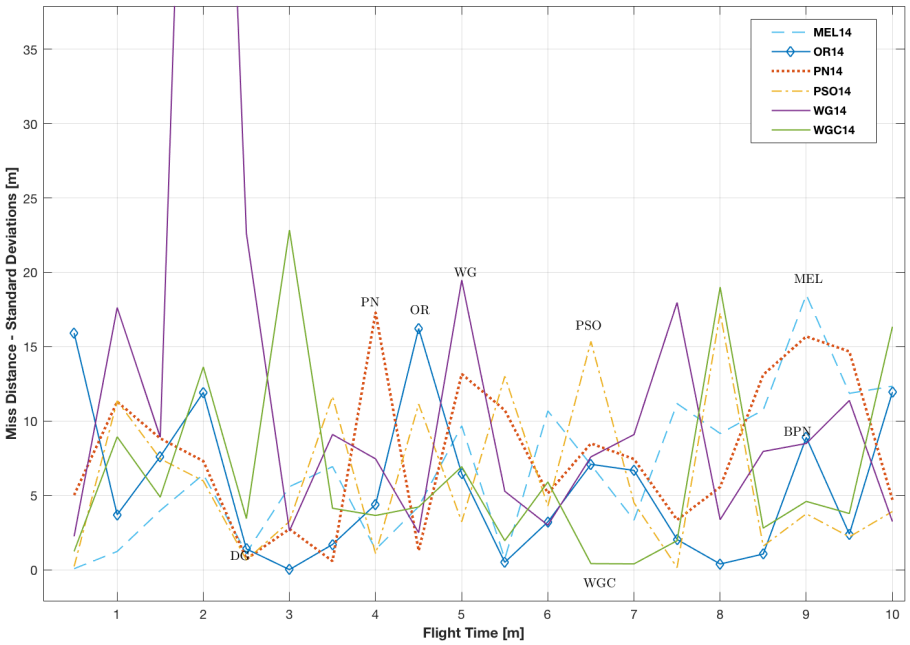

Figure 7.62 : Case 14 - standard deviation results.

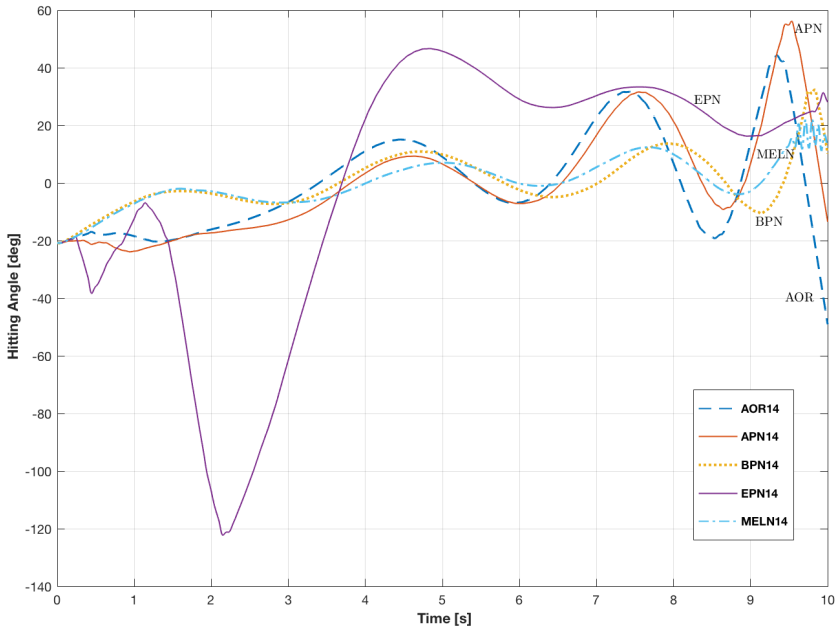

Figure 7.63 : Case 14 - hitting angle results.

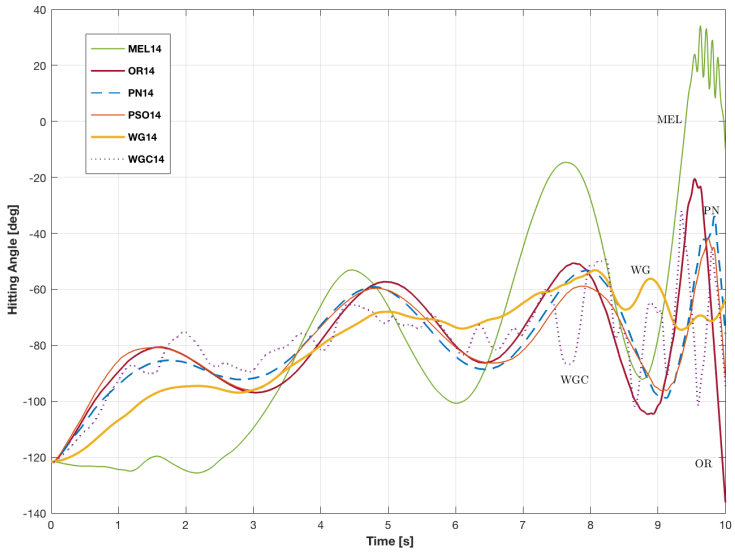

Figure 7.64 : Case 14 - hitting angle results.

Estimated and actual values of target states in PSO homing loop can be seen in Figure 7.65 as an example to multiple noise added weaving target homing loop. It may be observed that three state linear Kalman filter has difficulty in estimating the weaving target. Three state Kalman filter in this case is optimized for constant target maneuver and is not performed optimal for sinusoidal motion.

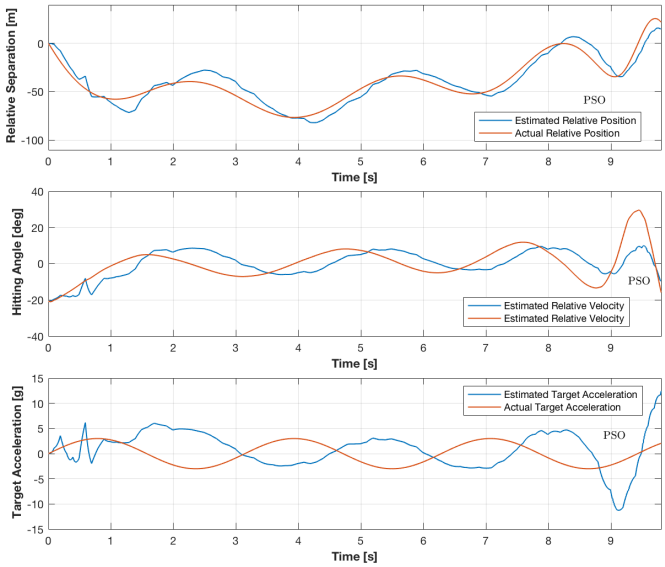

Figure 7.65 : Case 14 - PSO target state estimation.

Case 15 represents the third order lag noise filter added homing loop with 6g high evasive target maneuver and 3m glint, 1MR range independent and 4MR range dependent zero mean white gaussian noises. Disturbances are 6g high Barrel-Roll target maneuver and noise terms in this scneario. Miss distance results can be seen in Figure 7.66 and 7.67 and corresponding standard deviations in Figure 7.68 and 7.69. It is not suprising that four state Kalman filter used guidance laws, WGC, WG and EPN show superior performance.

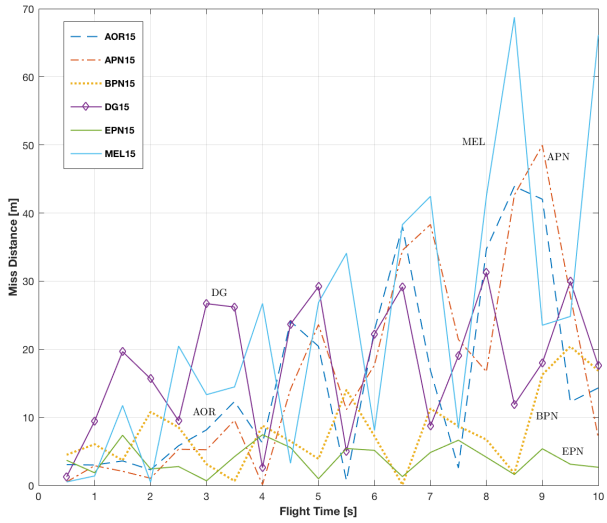

Figure 7.66 : Case 15 - miss distance results

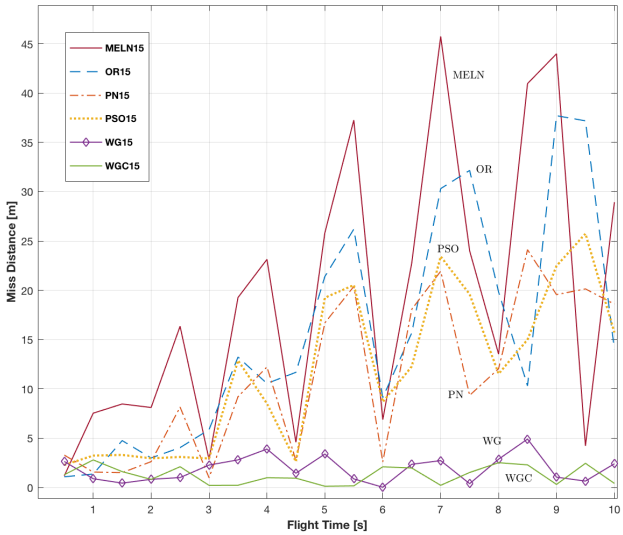

Figure 7.67 : Case 15 - miss distance results.

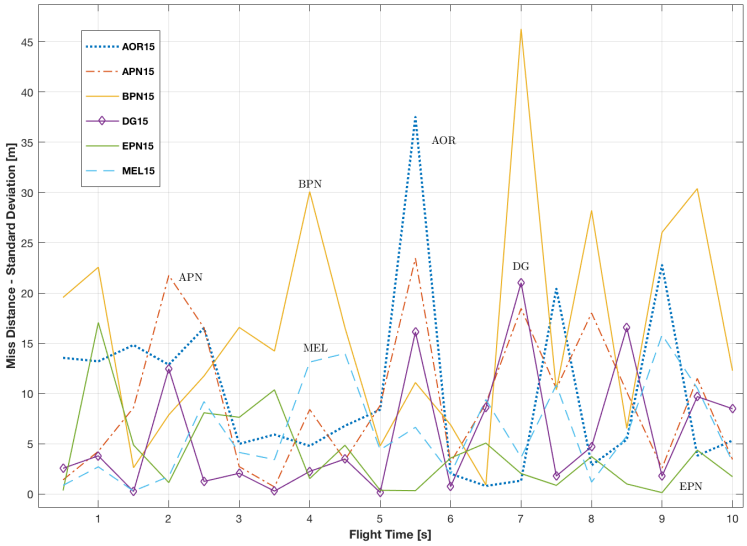

Figure 7.68 : Case 15 - standard deviation results.

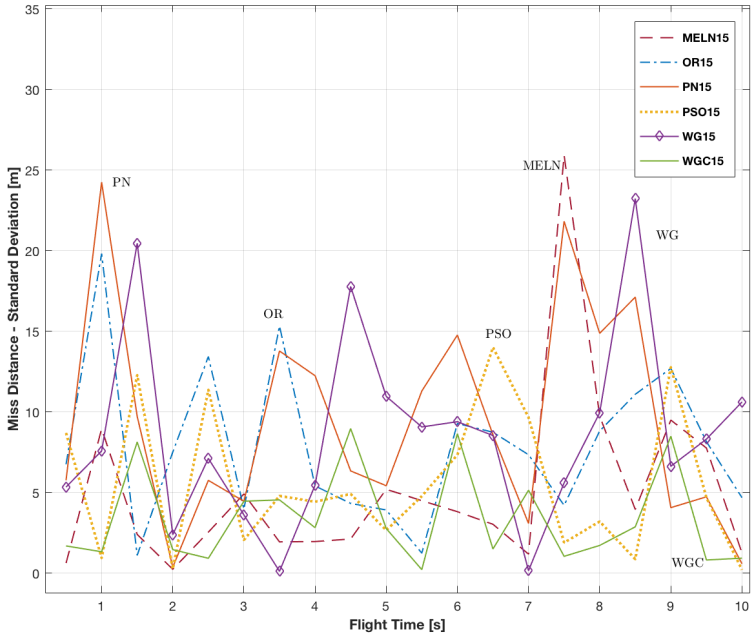

Figure 7.69 : Case 15 - standard deviation results.

Estimated and actual values of target states of case 15 in PN and WG homing loops can be seen in Figure 7.70 and 7.71. At the same time it may be observed that three state linear Kalman filter has difficulty in estimating the weaving target as similar result of Case 14. Three state Kalman filter in PN homing loop is optimized for

constant target maneuver and is not performed optimal for 6g sinusoidal maneuver. On the other hand four state Kalman filter in WG homing loop is optimized for weaving target and is carried out the scenario quiet good.

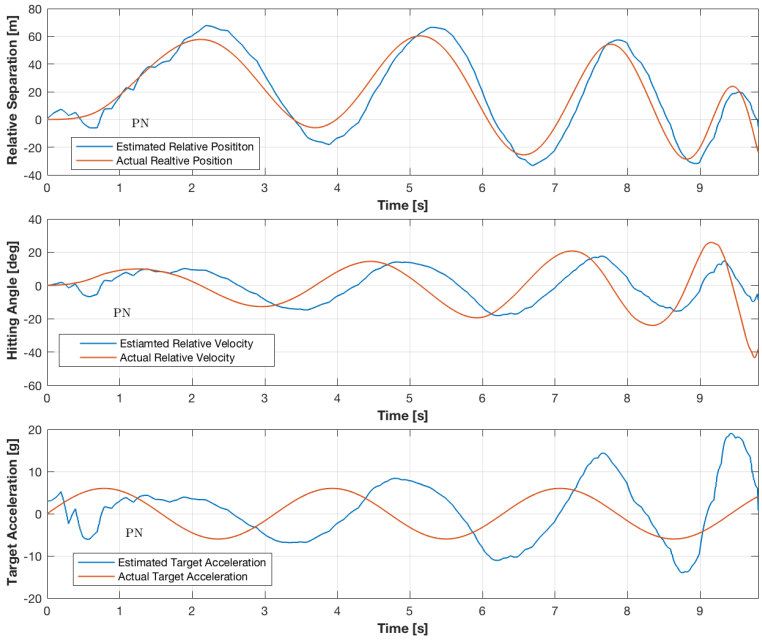

Figure 7.70 : Case 15 - PN target state estiamtion.

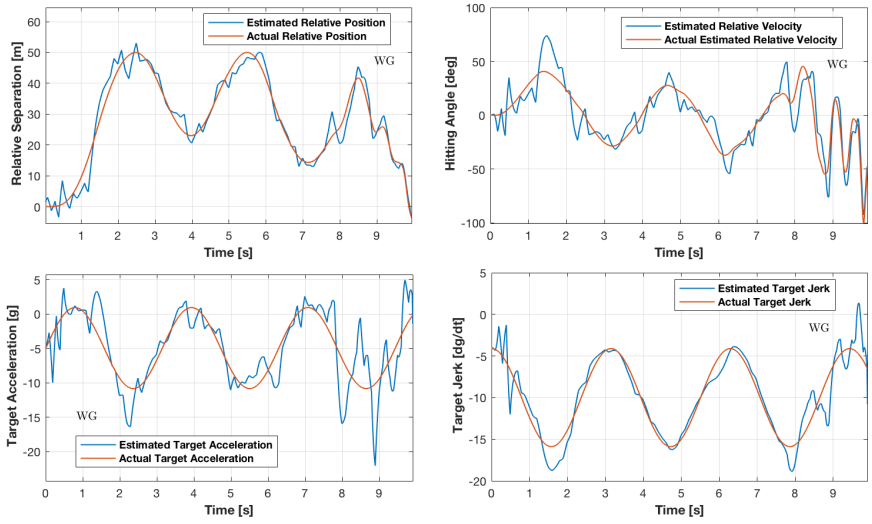

Figure 7.71 : Case 15 - WG target state estimation.

Case 16 represents the third order lag noise filter added homing loop with 6g high evasive, zero mean WG ~ $\boldsymbol{N(0, \sigma^2 = 1)}$ random target maneuver and 3m glint, 1MR

range independent and 4MR range dependent zero mean white gaussian noises. Disturbances are 6g high Barrel-Roll and WG $\sim N(0, \sigma^2 = 1)$ random target maneuver and noise terms in this scenario. In this case unknown smart target maneuver that pursuer can not predict is added into 6g barrel roll maneuver as white gaussian random noise. As previously stated that only WGC, WG and EPN are shown reasonable results for Case 15. Therefore only these guidance law results will be shown in here. Miss distance results can be seen in Figure 7.72, control efforts in Figure 7.73, flight paths in Figure 7.74 and hitting angles in Figure 7.75. Related to this case, WGC is found to be the best guidance law among others in control effort and miss distance point of view.

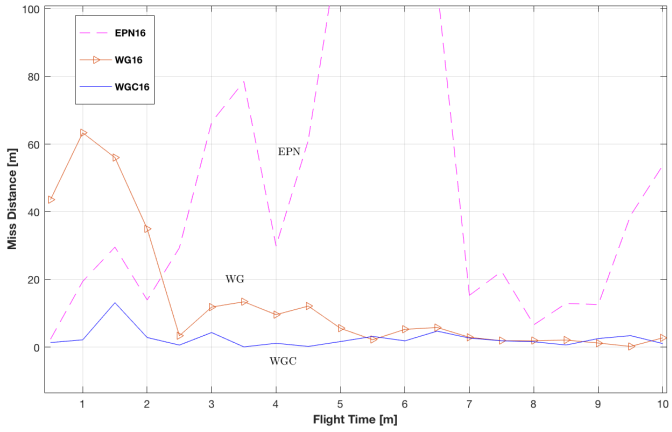

Figure 7.72 : Case 16 - miss distance results.

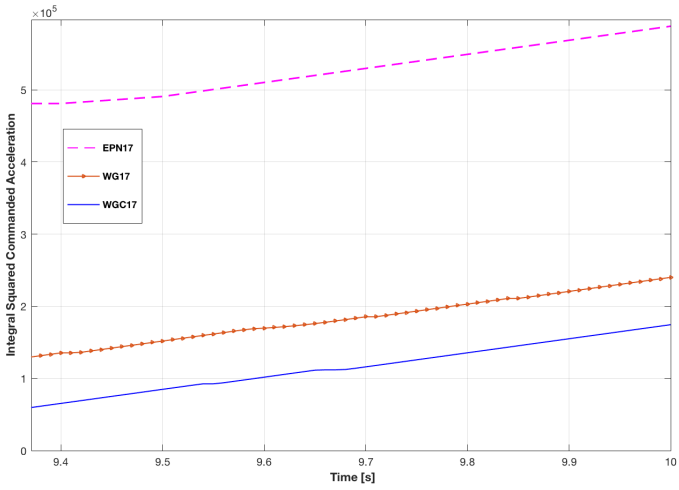

Figure 7.73 : Case 16 - control effort results.

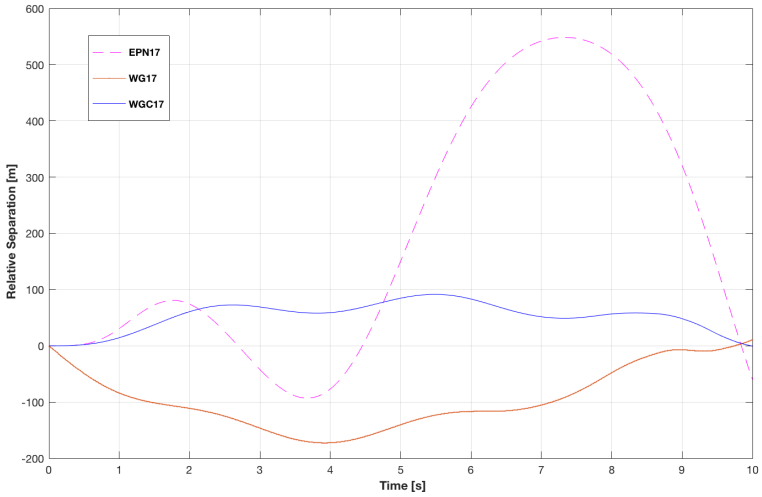

Figure 7.74 : Case 16 - flight path results.

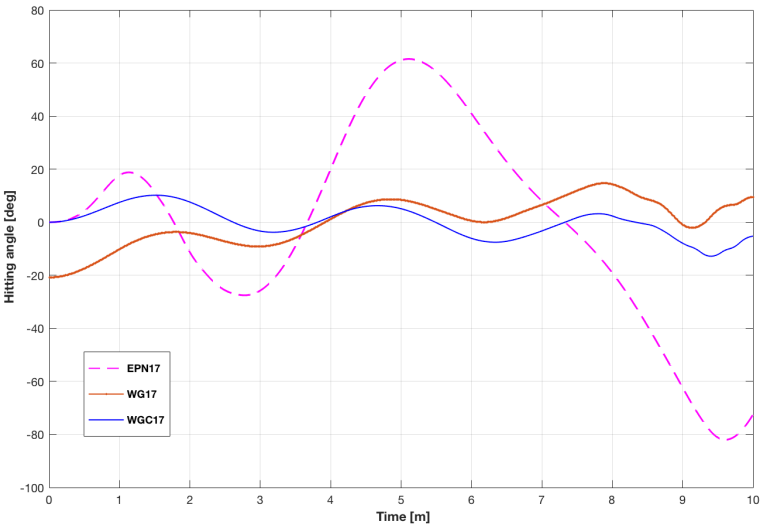

Figure 7.75 : Case 16 - hitting angle results.

7.3 Other Considerations

Multiple target issues are explained in previous sections. In homing loop analysis power centroid method is studied in different cases as relative separation or velocity initial conditions. The another approach was earliest intercept geometry (EIG). In Figure 7.76 four possible flight paths and initial EIG circle were shown as an example.

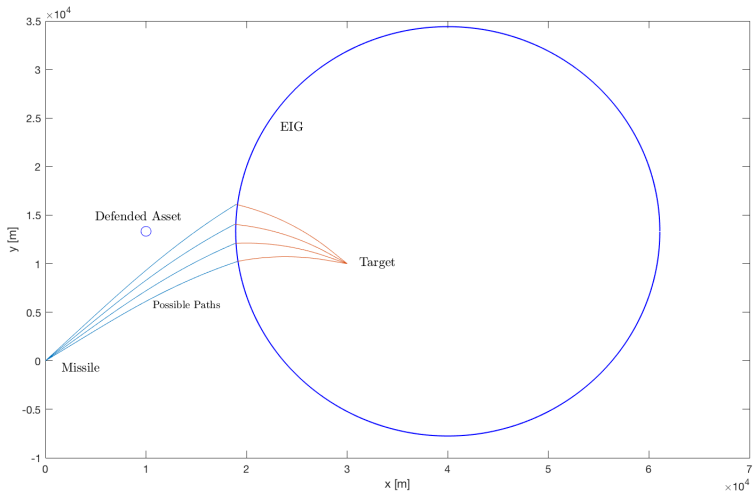

Figure 7.76 : EIG approach.

Nonlinear missile – multiple target engagement EIG scenario was performed in this study. In EIG case, two targets and one missile were assumed. One of the target directly flights to the defended asset and the other one makes complete turn maneuver. First target's velocity is assumed 500m/s and the other one 100m/s. Missile's velocity is adjusted as 600m/s at beginning of the flight. Initial positions of target and missile can be seen in EIG case Figure 7.77. In this multiple target approach, finding the closest target and approaching to the corresponding target is expected from the missile. The closest target can be considered as the riskiest target among them. At the beginning missile calculates the earliest intercept geometry circle EIG-0. Then during engagement EIGs are calculated from the missile at each second as in Figure 7.78.

As it can be seen in Figure 7.78, the missile is decided on the Target-1, 2 seconds after approach to the Target-2. If Target-2 decides to turn to the defended asset after a while, missile could be directed to Target-2 by EIG approach. In this case PN with effective navigation ratio 5 was used. Nonlinear analysis gave 0.07m miss distance and 7.6s time to go results. EIG approach is found to be useful against multiple target case.

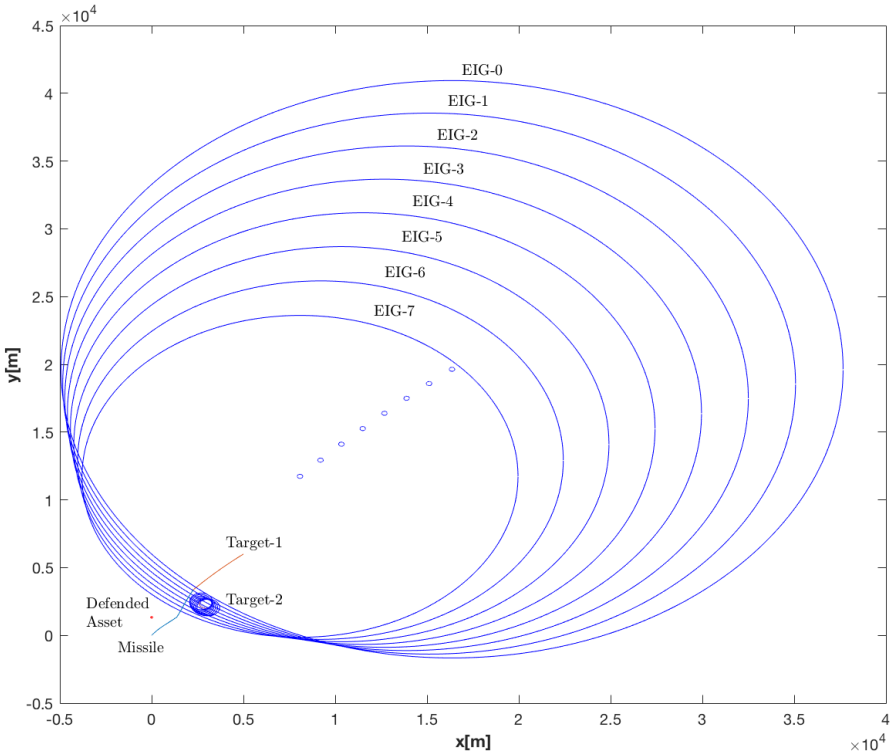

Figure 7.77 EIG case.

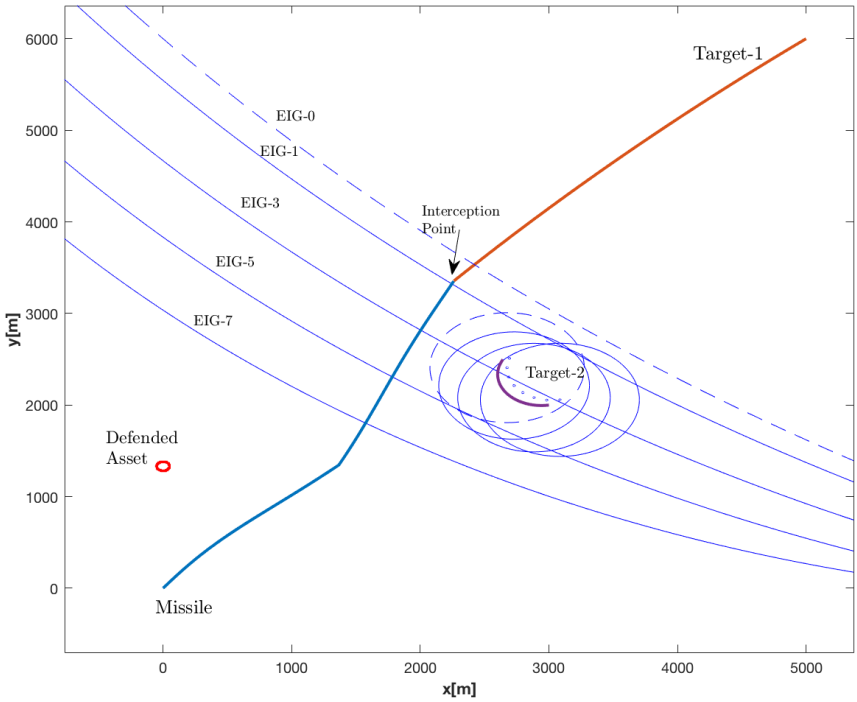

Figure 7.78 : EIG case result.

Bank filter approach is also studied in this thesis. In bank filter scenario, unknown target's weaving frequency was tried to be find. Four linear Kalman filter were performed in parallel. Each kalman filter was configurated to a different weaving frequency such as 0.1 rad/s, 1 rad/s, 2 rad/s and 4 rad/s. In here, target's actual weaving frequency was set as 1 rad/s. 10 seconds of flight time and 3g barrel roll maneuver were assumed. Corresponding state estimate results can be seen in Figure 7.79. In Figure 7.80 and 7.81, estimation of target weaving frequency takes 3s to be certain and finds that the correct filter is most likely the filter was set to 1 rad/s. Estimation was seen quite close to the actual target's weaing frequency.

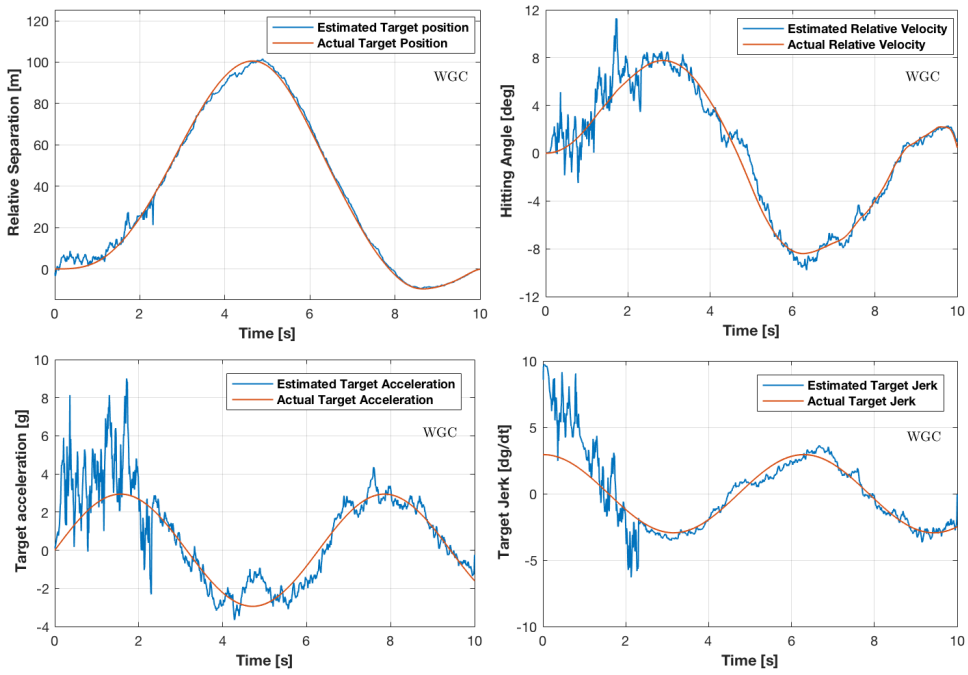

Figure 7.79 : MMAE approach target state estimation.

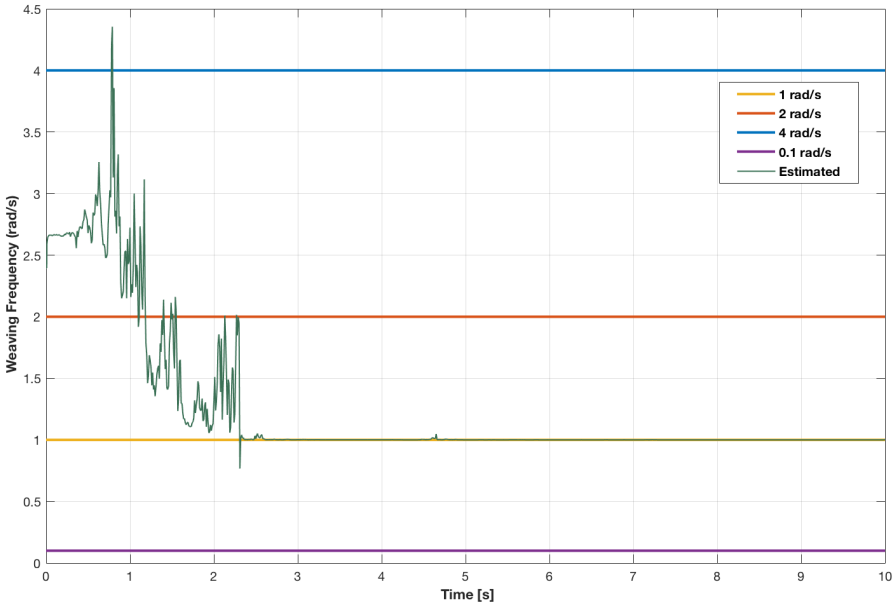

Figure 7.80 : Estimated target weaving frequency.

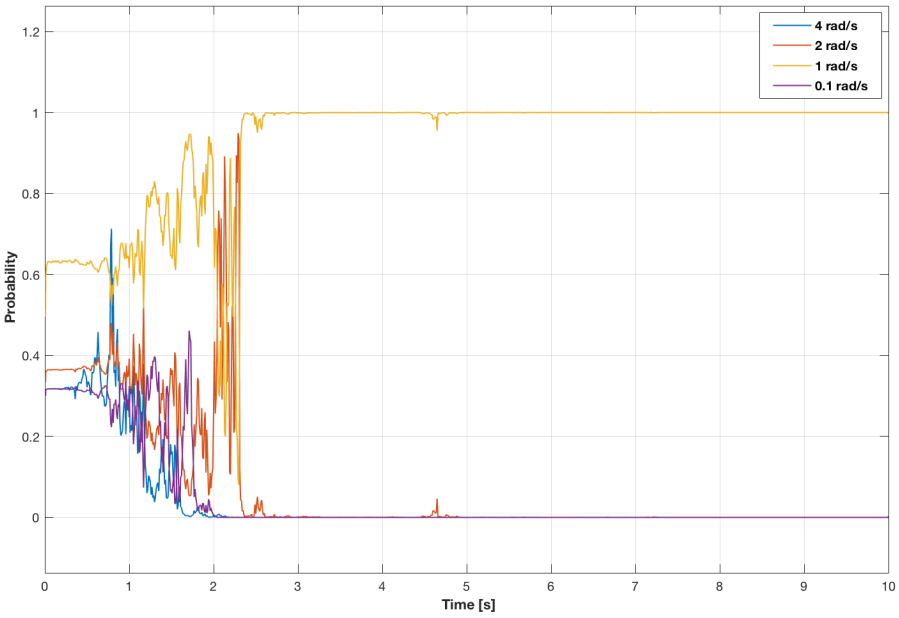

Figure 7.81 : Probability of which filter is correct.

8. CONCLUSION AND FUTURE WORKS

In this study, the guidance laws used in the terminal phase of active homing missiles were investigated. In the first chapter the general concepts in missile guidance, a literature survey of homing missiles and scope of the thesis were presented. In chapter 2, the missile – target engagement geometry was defined and linearized around collision triangle. Then the corresponding differential equations of motions were derived. The missile and target characteristics were explained in chapter 3. Possible disturbance sources in the homing loop were given in the same chapter. The classical and modern guidance laws were derived in chapter 4. Linear Kalman filter models were shown in chapter 5. In order to estimate target's weaving frequency, MMAE approach in missile guidance was shown. In the next chapter, the idea of multiple target scenarios and related solution methods were given. Homing guidance algorithms were simulated through 16 different case configurations shown in chapter-7.

In these studies, guidance laws were performed in the Matlab Simulink enviroment. Here, PN, OR, APN, EPN, AOR, MEL, MELN, BPN, WG, WGC, DG and PSO are considered. In each test case, homing loops were constituted based on target acceleration, initial relative separation, heading error, radome slope, and glint, range dependent, independent noises. Miss distance, control effort, commanded acceleration and hitting angle criterias were selected for comparison. Since the flight times were not known in advance, flights between 1 and 10 seconds were applied. In each 0.5s time step, up to 50 run Monte-Carlo simulations were performed. Miss distance statistical results were also investigated.

WGC was found to be the best guidance law in terms of miss distance results in all cases. Also, WGC was appeared the best in terms of control effort in all noise free cases. In noise added scenarios, WGC was found to be the best when only range dependent noise was considered. WGC's control effort results were poor in glint noise added cases. These findings are not surprising since WGC uses target jerk measurements in addition. Other guidance laws using target jerk measurements such

as WG and EPN gave similar results in terms of miss distance and control effort. WGC was never reached the physical limits of missile. Maximum acceleration of WGC was remained in between 45g. On the other hand WG and EPN were reached up to 45g. Compensation term was found to be necessary in order to minimize terminal miss distance and acceleration requirements. In order to estimate target's weaving frequency, MMAE was proved the effectiveness of the method.

AOR was found to be optimal in terms of hitting angle constraint against a constant accelerated target. Even if in noisy cases AOR gave applicable results. AOR only failed against weaving target. Another rendezvous guidance law was OR where was optimal against stationary targets. According to the hitting angle results of noise-free cases, OR was observed to be feasible against a constant accelerated target. OR also failed against weaving target.

It was appeared that MEL was optimal against any type of maneuver in noise-free cases. Therefore MEL was found to be the best guidance law without using target jerk measurements in terms of miss distance and control effort. In noise added cases, MEL's performance was decreased due to fluctuations in target's measured acceleration. Another variety of MEL was MELN which not uses target acceleration. It was seemed like compansation term added variation of PN. MELN gave quite good miss distance results in noise-free cases. On the other hand, in noise added cases, it turned out that MELN was shown better results than MEL in terms of miss distance. It is reasonable since MELN does not require fluctuated target acceleration measurements. However, MEL and MELN were not shown applicable results against weaving targets in noise added cases. Three state Kalman filter used in MEL and MELN was optimized for constant target maneuver not for weaving target.

MEL was the compensated variation of APN. In zero order homing loops, APN and MEL were shown the same results. Due to same reasons, APN's performance was degraded.

PN, OR, BPN, MELN, PSO may be used when target's acceleration measurements cannot be obtained. Those guidance laws were found to ineffective against high g target maneuvers. It was observed that in order to approach high g maneuvers, target acceleration measurements were needed to be estimated. PN and PSO were appeared to be useful against all type of maneuver in terms of miss distance except long

duration high g optimal evasive maneuvers. Two state guidance laws did not effected by estimated acceleration fluctuations. In order to reduce commanded acceleration requirements, PSO was seemed to be the better choice then PN. It can be clearly said that higher effective navigation ratio yields less acceleration capability. More importantly, compansetion term was found to be required to eliminate the guidance delays.

BPN's desired hitting angle control capability was seen ineffective against moving target. Still BPN which do not need to time to go and closing velocity measurements gave realistic results against contant accelerated targets in terms of miss distance.

DG's high acceleration requirements were made this guidance law unpractical. It was considered that DG could be applied at the near collision such as a couple of seconds before the interception. This brings us to investigate hybrid guidance laws as future work.

The guidance laws obtained in this study are dependent on the time to go. In real life applications, this parameter contains inaccuracies. As future work, disturbances can be implemented into time to go measurements and the impact on miss distance may be investigated. Another thought on future work, WGC can be extended to able hitting angle control. These guidance laws may be studied for multiple target cases.

REFERENCES

[1] **Locke, A.S.** (1955). *Guidance*, D.Van Nostrand.

[2] **Garnell, P. , and East D.J.** (1977). *Guided Weapon Control System*, Pergamon Press.

[3] **Dornberger, W**. (1954). *V-2*, The Viking Press, New York, NY, 1954.

[4] **Siouris, G. M.** (2004). *Missile guidance and control systems*. New York: Springer.

[5] **Pitman, G.R.** (1962). *Inertial Guidance,* JohnWiley&Sons, Inc., NewYork, NY.

[6] **Zarchan, P.** (1990). *Tactical and Strategic Missile Guidance*, Vol. 124, Progress in Astronautics and Aeronautics, AIAA, Washinton DC.

[7] **Lin, C.** (1991). *Modern navigation, guidance, and control processing*. Englewood Cliffs: Prentice-Hall.

[8] **Wildbergear, M. and Hunt M.W.** (1986). *"A Generic Missile Weapon System Model for Wargaming"* Proc.Conferance on Aerospace Simulation II, vol. 16, no.2 pp.64-75.

[9] **Jim, J., Null, R., and Wallace, J. (n.d.).** (1996) *GUNNER'S MATE M 3 & 2 Naval Training Command* Naval Education and Training Professional Development and Technology Center.

[10] **Pelegrini, M.** (1987) *"Homing of Aerospace Vehicles," Systems G.Control Encyclopedia, ed.* M.G.Singh, vol. 3, Oxford, Great Britain: Pergamon Press, p.2164.

[11] **Fossierm, W.** (1984) *"The Development of Radar Homing Missiles,"* J.Guidance, Control and Dynamics, vol.7, no.6, November-December pp.641-651.

[12] **Berglund, E.** (2000) *"Guidance and Control Technology",* RTO SCI Lecture Series on Technologies for Future Precision Strike Missile Systems, Atlanta, USA, pp. 1-10

[13] **Lin, C.L. and Chen, Y.Y.,** (1999) *"Design of Advanced Guidance Law against High Speed Attacking Target",* Proceeding of National Science Council, ROC(A), Vol. 23, No.1, pp.60-74

[14] **Zarchan, P.** (1998) *"Ballistic Missile Defense Guidance and Control Issues",* Science and Global Security, Vol. 8, pp.99-124

[15] **Babu, K.R., Sarma,I.G. and Swamy, K.N.** (1994) *"Two Mode Control Theory",* IEEE Proceedings, pp.540-547

[16] **Zarchan, P.** (1979) *"Complete Statistical Anaylsis of Nonliner Missile Guidance Systems – SLAM,"* Journal of Guidance and Control, Vol. 2, pp.71-78.

[17] **Zarchan, P.** (1995) *"Proportional Navigation and Weaving Targets,"* Journal of Guidance, Control and Dynamics, Vol.18, No.5, pp. 969-974

[18] **Hough, M.E.** (1995) *"Optimal Guidance and Nonlinear Estimation for Interception of Accelerating Targets",* Journal of Guidance, Control and Dynamics, Vol.18,No.5,959-968

[19] **Yaesh, I. and Ben-Asher, J.Z.** (1995) *"Optimum Guidance with a Single Uncertain Time Lag",* Journal of Guidance, Control, and Dynamics, Vol.18, No.5 pp.981-988

[20] **Nesline, F.W. and Zarchan, P.** (1981) *"A New Look at Classical vs. Modern Homing Missile Guidance",* Journal of Guidance, Control and Dynamics, Vol.4,No.1 pp.78-85

[21] **Ben-Asher, J. Z. and Yeash, I.** (1998) *Advances in Missile Guidance Theory. Reston,* VA:American Inst. of Aeronautics and Astronautics.

[22] **Cotrell., R. G.** (1971) "*Optimal Intercept Guidance for Short-Range Tactical Missiles",* AIAA Journal, Vol.9,No.7 (1971), pp.1414-1415

[23] **Ben-Asher, J. Z. and Yeash, I.** (1997) "*Optimal Guidance with Reduced Sensiticity to Time to Go Estimation Errors*", Journal of Guidance, Control, and Dynamics, Vol.20, No.1, pp.158-163

[24] **Ben-Asher, J. Z. and Yeash, I.** (1996) "*Linear Quadratic Pursuit-Evasion Games with Terminal Velocity Constraints"*, Journal of Guidance, Control, and Dynamics, Vol.19, No.2, pp.499-501

[25] **Gitizadeh, R., Yaesh, I. and Ben-Asher, J. Z.** (1999) "*Discrete-Time Optimal Guidance*", Journal of Guidance, Control, and Dynamics, Vol.22, No.1 pp.171-175

[26] **Zarchan, P.** (2000) "*Tracking and Intercepting Spiraling Ballistic Missiles"* IEEE 2000. Position Location and Navigation Symposium, San Diego, CA, USA, pp.277-284

[27] **Zarchan, P. and Alpert, J.** (2006) "*Using Filter Banks to Improce Interceptor Performance Against Weaving Targets",* AIAA Guidiance, Navigation, and Control Conference and Exhibit, Guidance, Navigation and Control and Co-located Conferences.

[28] **Gutman, O. and Palmor, J. Z.** (2011) "*Proportional Navigation Against Multiple Targets"*, Journal of Guidance, Control and Dynamics, Vol.34, No.6 pp.1728-1733

[29] **Shin, H. S., Tsourdos, A., White, B. A. and Tahk, M.J.** (2009) "*Earliest Intercept Geometry Guidance to Improve Mid-Course Guidance in Area Air-Defence"* 17th Mediterranean Conference on Control and Automation, Thessaloniki, pp. 1557-1562.

[30] **Kung, C. C., and Chen, K. Y.** (2013). "*Missile Guidance Algorithm Using Particle Swarm Optimization"* Applied Mechanics and Materials, pp. 284-287

[31] **Chen, K., Lee, Y., Liao, S., & Kung, C.** (2016) "*The Design of Particle Swarm Optimization Guidance Using a Line of Sight Evaluation Method"* Computers and Electrical Engineering,54,169-169

[32] **Lee, Y., Chen, K., Chen, Y., Chen, Y., & Liao, S.** (2016). "*The Design of a Modified PSO Guidance Law Using Predictor and LOS Rate Evaluation"* MATEC Web of Conferences, 71, 02001.

[33] **Shin, H.** (2012). "*Study on Cooperative Missile Guidance for Area Air Defence PhD Thesis, Cranfield University.*

[34] **Uhrmeister, B.** (1994). "*Kalman Filters for a Missile With Radar and/or Imaging Sensor"* Journal of Guidance Control and Dynamics, 17, 1339-1344.

[35] **Kim, Y. and Seo, J. H.** (1996). "*The Realization of The Three Dimensional Guidance Law Using Modified Augmented Proportional Navigation"* Proceedings of 35th IEEE Conference on Decision and Control, Kobe, Japan,pp.2707-2712 vol3.

[36] **Vergez, P.L. and Liefer R. K.** (1984). "*Target Acceleration modeling for Tactical Missile Guidance",* Journal of Guidance, Control and Dynamics, Vol.7, No.3 pp.315-321

[37] **Blakelock, J. H.** (1991). *Automatic Control of Aircraft and Missiles*, John Wiley & Sons.

[38] **Leboucher, C., Shin, H., Ménec, S. L., Tsourdos, A., and Kotenkoff, A.** (2013). "*Optimal Weapon Target Assignment Based on an Geometric Approach*" IFAC Proceedings Volumes, 46(19), pp. 341-346.

[39] **Brochu, R., Lestage, R.** (2003). "*Three Degree of Freedom (DOF) Missile Trajectory Simulation Model and Comparative Study with a High Fidelity 6DOF Model",* Defence Research and Development Canada, Technical Memorandum

[40] **Raghunathan, T., & Ghose, D** (2014). "*Differential Evolution based 3-D Guidance Law for a Realistic Interceptor Model"* Applied Soft Computing, 16, 20-33.

[41] **Imado, F., and Miwa, S.** (1986). "*Three Dimensional Study of Evasive Maneuvers of a Fighter Against a Missile"* Astroynamics Conference.

[42] **Imado, F., and Miwa, S.** (1983). "*The Optimal Evasive Maneuver of a Fighter Against Proportional Navigation Missiles*" 10th Atmospheric Flight Mechanics Conference.

[43] **Palumbo, N., Blauwkamp, A. R. And Lloyd, J.** (2010). "*Modern Homing Missile Guidance Theory and Techniques"* John Hopkins APL Technical Digest (Applied Physics Laboratory)

[44] **Mehrota, K. And Mahapatra, P. R.** (1997). "*A Jerk Model for Tracking Highly Maneuvering Targets*" in IEEE Transactions on Aerospace and Electronic Systems, vol 33,no.4,pp.1094-1105.

[45] **Zarchan, P.** (1970). "*Representation of Realistic Evasive Maneuvers by the Use of Shaping Filters",* Journal of Guidance, Control and Dynamics, Vol.2, No.4 pp.290-295

[46] **Akdağ, R. and Altilar, D. T.** (2005). "*A Comparative Study on Practical Evasive Maneuvers Against Proportional Navigation Missiles"*AIAA

Guidance, Navigation and Control Conference and Exhibit, San Francisco, California.

[47] **Imado, F., and Miwa, S.** (1994). "*Missile Guidance Algorithm Against High-g Barrel Roll Maneuvers"* Journal of Guidance, Control, and Dynamics Vol.17, No.1

[48] **Shaw, R. L.** (1985). *Fighter combat:Tactics and Maneuvering.* Annapolis, MD: Naval Inst.Press

[49] **Wang,Y., Dong, J., Liu, X., and Zhang, L.** (2015). "*Identification and standardization of Maneuvers Based Upon Operational Flight Data"* Chinese Journal of Aeronautics, 28(1), 133-140

[50] **Huang, H., Tong, Z., Li, T., Jia L. And Li, S.** (2017). "*Defense Strategy of Aircraft Confronted with IR Guided Missile"* Mathematical Problems in Engineering Volume 2017

[51] **Palumbo, N., Blauwkamp, A. R. And Lloyd, J.** (2010). "*Guidance Filter Fundamentals"* John Hopkins APL Technical Digest (Applied Physics Laboratory)

[52] **Chui,C.K. and Chen,G.** (1999). "*Kalman Filtering with Real-Time Applications"* 3rd Ed., Springer, New York.

[53] **Zarchan,P. and Musoff, H.** (2000). "*Fundamentals of Kalman Filtering: A Practical Approach"* American Institute of Aeronautics and Astronautics, Reston, VA.

[54] **Crassidis, J. and Yang, C.** (2006). "*Generalized Multiple-Model Adaptive Estimation Using an Autocorrelation Approach"* 9th International Conference on Information Fusion.

APPENDICES

APPENDIX A : Simulink Models.

APPENDIX A: Simulink models of guidance laws for simulated scenarios in this study were given below. All Simulink models were not given here. The models have been added for information purposes.

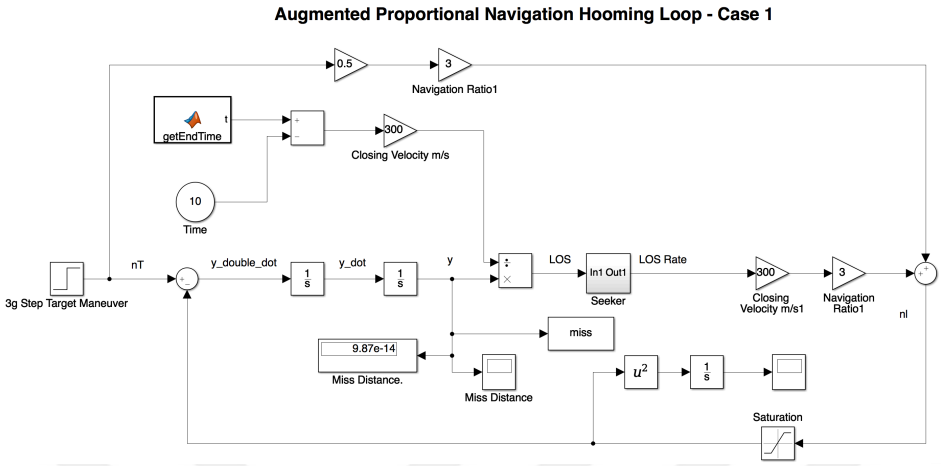

Figure A.1 : Augmented proportional navigation homing loop – case 1.

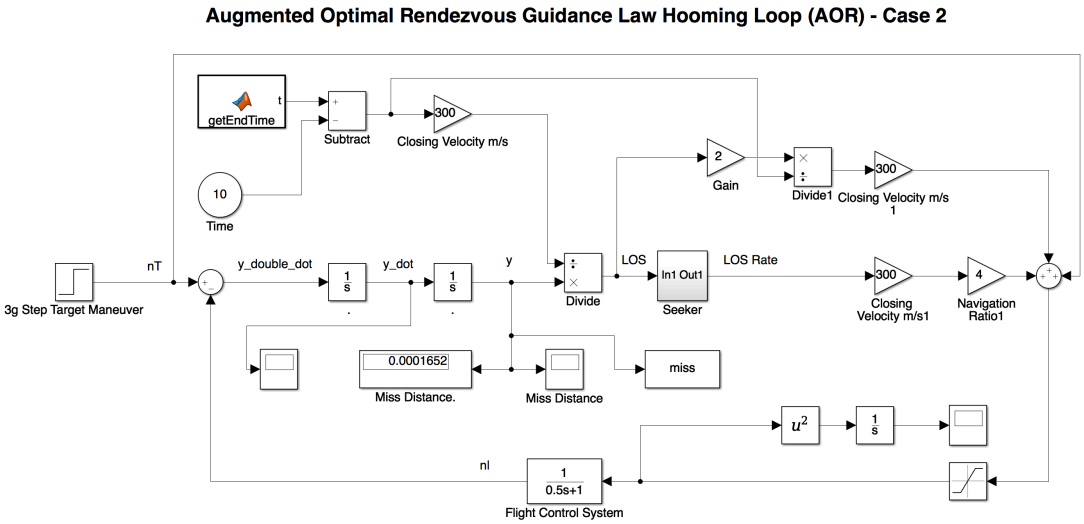

Figure A.2 : Augmented optimal rendezvous homing loop – case 2.

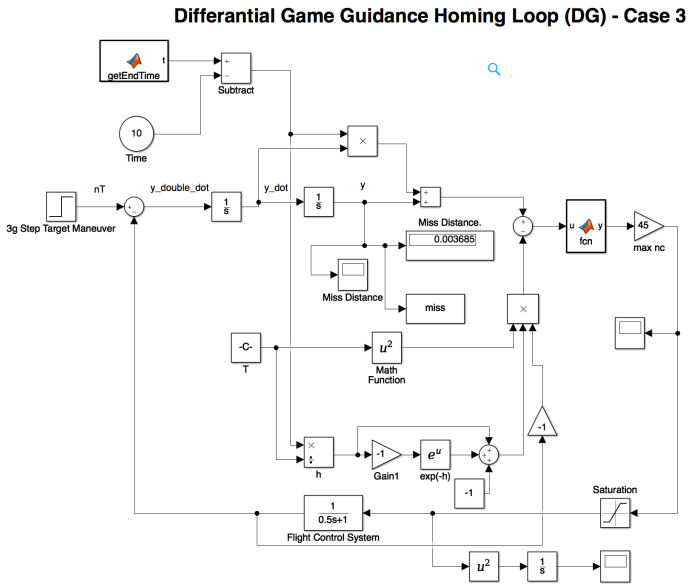

Figure A.3 : Differential game guidance homing loop – case 3.

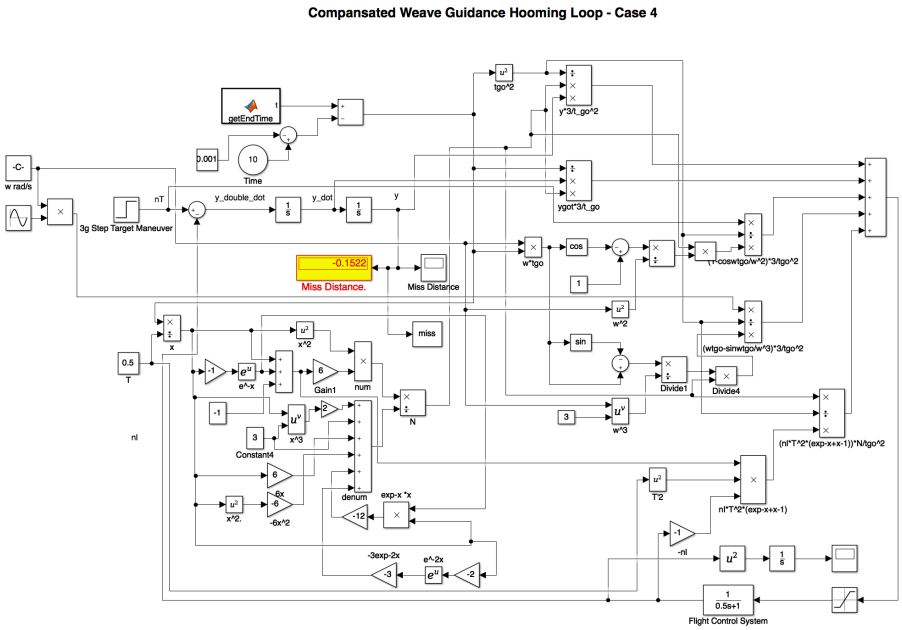

Figure A.4 : Compansated weave guidance law homing loop – case 4.

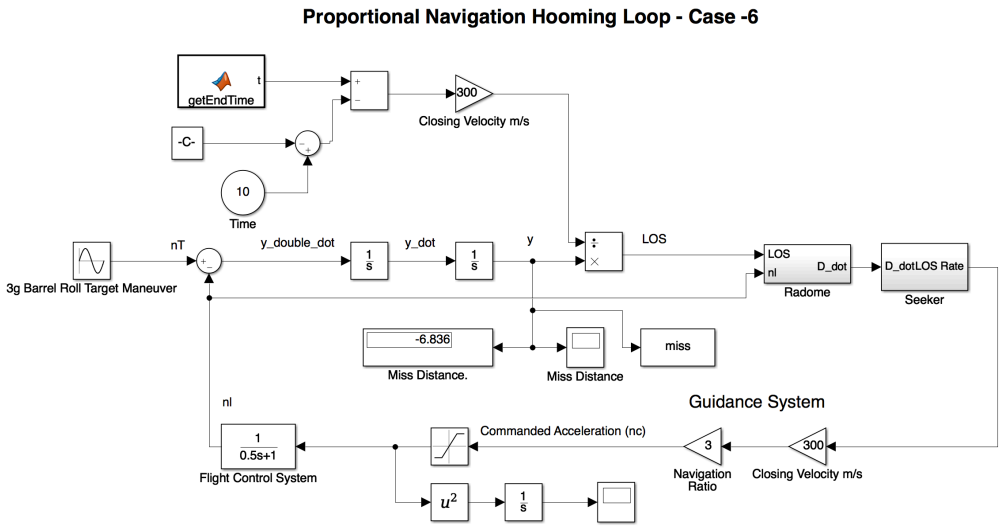

Figure A.5 : Proportinal navigation homing loop – case 6.

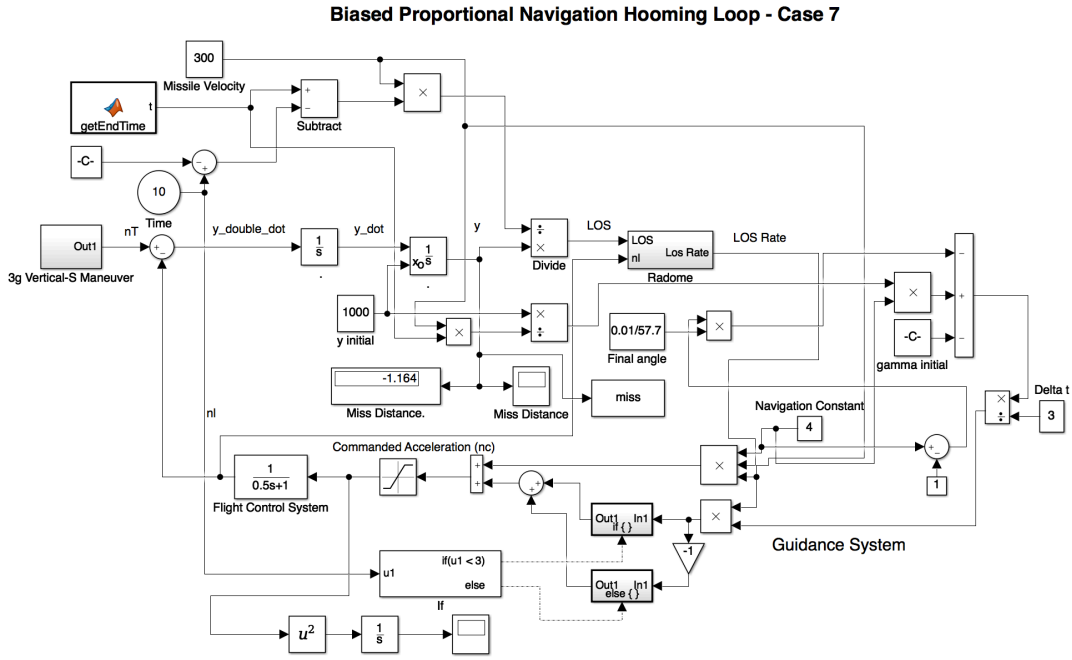

Figure A.6 : Biased proportional navigation – case 7.

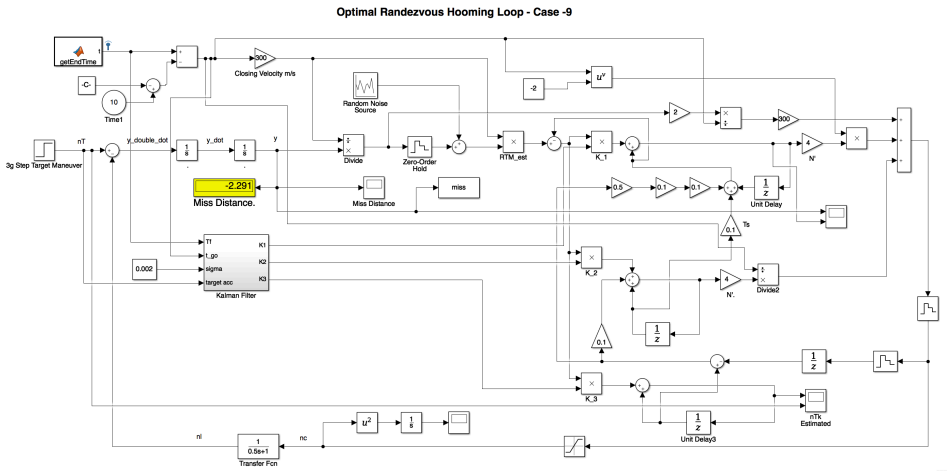

Figure A.7 : Optimal rendezvous homing loop – case 9.

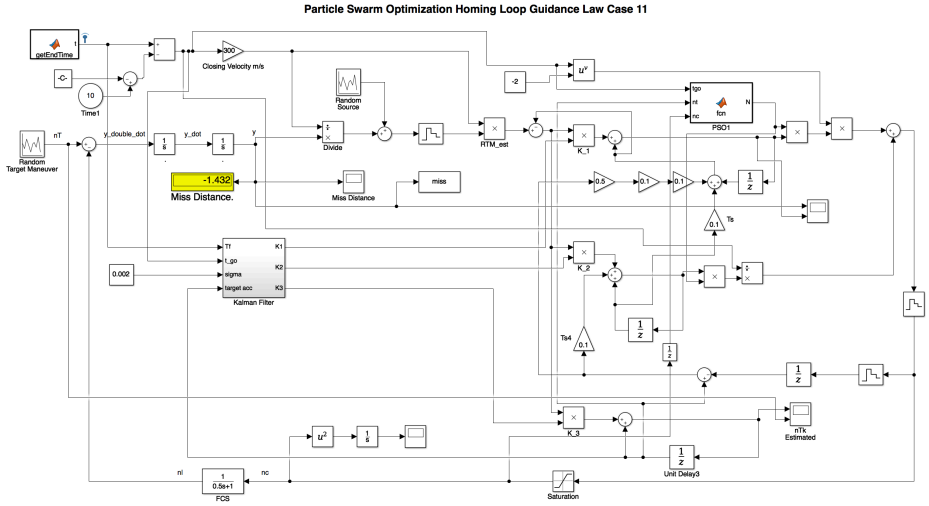

Figure A.8 : Particle swarm optimization homing loop – case 11.

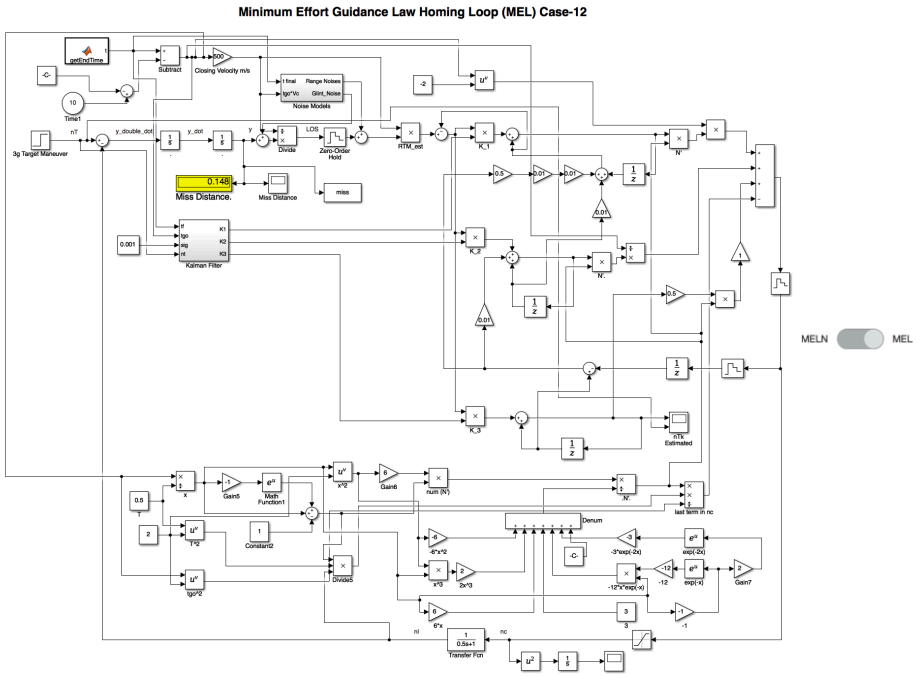

Figure A.9 : Minimum effort guidance law homing loop – case 12.

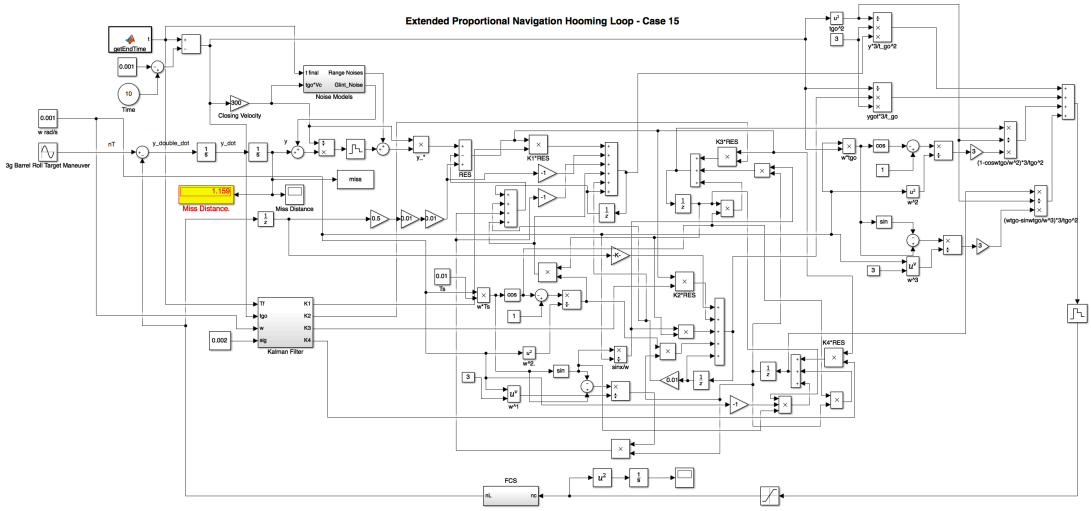

Figure A.10 : Extended proportional navigation homing loop – case 15.

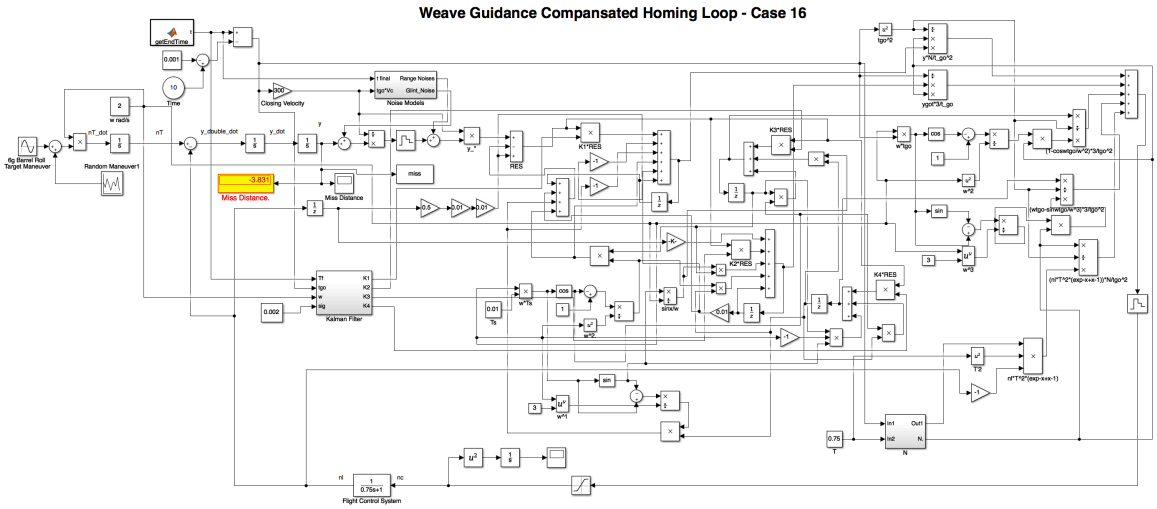

Figure A.11 : Compansated weave guidance homing loop – case 16.

CURRICULUM VITAE

Name Surname	**:**	Erdem TURAN
Place and Date of Birth	**:**	Tekirdağ / Çorlu 06.11.1989
E-Mail	**:**	erdemturan@outlook.com

EDUCATION **:**

- **B.Sc.** **:** 2017, University of Turkish Aeronautical Association, Faculty of Aeronautics and Astronautics, Astronautical Engineering Department, Astronautical Engineering.
- **M.Sc.** **:** 2019, Istanbul Technical University, Defence Technologies Program.